Contract No. DTRS-57-93-D-00027
TTD No. VA-3204

REPORT

Technical Report

Modeling and Linear Analysis of High-Speed Articulated Trainsets

To

Volpe National Transportation Systems Center

U.S. Department of Transportation

Cambridge, Massachusetts

May 22, 1995

Battelle
. . . Putting Technology To Work

Modeling and Linear Analysis of High Speed Articulated Trainsets

Imtiaz Haque

Chengyu Liu

Guang Zhu

Mechanical Engineering Department

Clemson University

Clemson, SC 29631

May 1995

EXECUTIVE SUMMARY

This report describes analytical activities that were performed for The Volpe Center as part of Technical Task Directive (TTD) No. VA-3204, Dynamic Analysis Support for Evaluation of HSGGT Systems, (Contract No. DTRS-57-93-D-00027, Multiple Contractor Resource Base: Vehicle, Guide way, and Terminal Systems). The overall scope of this TTD is to acquire, develop, maintain, and apply analytical models for predicting the safety-related dynamic performance of High Speed Guided Ground Transportation (HSGGT) systems, including High-Speed Rail (HSR) and magnetically-levitated (Maglev) configurations. This work supports the mission of the Federal Railroad Administration (FRA) to ensure the safety of such systems if deployed in the United States.

The activities in the study reported here-in focused on the safety-related dynamic performance of articulated HSR train sets, of which the French TGV and the Spanish Talgo are examples. With articulated train sets, adjacent car bodies share a common bogie, and the car body-to-car body connections are carefully designed for effective high-speed performance. Traditionally, single vehicle models of rail vehicles have been used to evaluate safety-related dynamic performance (e.g., lateral stability, curving performance and forced response). However, a single vehicle model may be an inaccurate representation of an articulated train set because of the relatively strong coupling between car bodies. The work presented in this report focused on developing a set of linear dynamic models of a generalized articulated train set. Computer codes were developed for predicting lateral stability and vertical/pitch dynamic response to track irregularities. The codes were exercised in limited parameter studies to investigate the influence of train set length, articulation joint characteristics and car-to-truck suspension characteristics on stability, forced response and ride quality. User's manuals for the codes are provided in companion documents.

A number of simulation models have been developed to compute the lateral stability and vertical pitch and bounce response of articulated train sets on tangent track. Simulation tools for the curving behavior of articulated train sets have also been developed but have not been reported in this

document. These models include the essential features of articulated train sets such as shared trucks and suspension characteristics such as car to car connections and car to truck yaw dampers. The modeling assumptions made simplify the analysis so that linear analysis tools can be applied. Outputs from the lateral stability models include critical speeds of the train sets, mode shapes, natural frequencies, and damping ratios. The bounce and pitch model outputs include transfer functions and power spectra for various classes of track as well as time histories of the response to discrete disturbances in the track.

In the course of this work, an effort has been made to put together a parameter set of a generic articulated train set. This has been done through an extensive literature review. Information on suspension parameters and inertial parameters of the conventional elements is readily available. However information about the articulation connections is hard to find as is information about center of mass locations of the various elements. Hence it has been necessary in some instances to assume certain values for them. Therefore the results of this study should be carefully used in extrapolating to actual candidate HSR vehicles.

For the lateral stability study, a set of parameters representing a baseline consist consisting of ten vehicles and giving a critical speed of approximately 310 km/hr were assembled. A limited set of parameter studies were then conducted to assess the influence of various parameters on consist stability. Mainly suspension parameters were chosen for the study. The studies show that consist stability is sensitive to the yaw damping between the trucks and the car body, the conicity of the wheel profile, and the primary suspension. Other parameters affect the stability but to a lesser degree. A decrease in yaw damping adversely affects the critical speed. A stiffer primary suspension increases the critical speed to a point past which the speed may begin to drop. The results were found to be fairly insensitive to the inter body yaw and roll connections. The model predict the presence of a low conicity instability for the articulated train set. The results show that an increase in wheelset conicity increases the critical speed of the train set until it reaches an optimum value. Past this optimum value, the critical speed begins to drop. The modal behavior of the consist suggests that the instability is in the form of whole consist modes, in some cases a wave-like

motion, especially at the low conceits. The influence of the number of car bodies in a consist was also explored. Dropping consist size from ten to five did not change the critical speed significantly.

For the case of bounce and pitch response, again a ten car consist on Class 6 track was studied. In this case the response was computed to vertical track alignment irregularities. Displacement and acceleration transfer functions, along with acceleration PSD's of the different elements of the consist were computed. The results showed the presence of a number of lightly damped modes with natural frequencies in the range of 1.2 to 2 Hz. These modes corresponded to the pitch and bounce motions of specific cars in the consist. The response of the individual cars was more pronounced at the rear of the train than at the front. This has implications for ride quality for this type of train set. The results were found to be parameter dependent. Hence before any specific decisions are made regarding this type of vehicular arrangement, it is important that accurate data be obtained for the particular design.

With the development of computer programs to analyze the vertical response of an articulated train set to both discrete and distributed rail disturbances, a new capability has been added to the FRA's ability to assess the dynamic performance of high speed rail vehicles. This is however a first step in developing a comprehensive tool kit to address the safety related issues that may arise with such train sets. It is recommended that non-linear simulation tools be developed to provide a more advanced capability for assessing safety related behavior of HSR articulated train sets.

ACKNOWLEDGEMENTS

This work was supported by the U.S. Department of Transportation through the Volpe National Transportation Center (VNTSC), Cambridge, MA.

The authors would like to thank Dr. Herbert Weinstock of The Volpe Center for his support and guidance during the course of this work. The contributions of Mr. Jeffrey Hadden, and Mr. Richard Rice of Battelle (Columbus, OH) and Dr. Mark Nagurka of CMRI (Pittsburgh, PA) are also acknowledged.

TABLE OF CONTENTS

LIST OF FIGURES

LIST OF FIGURES

NOMENCLATURE

a	Track Semi Gage, m.
a_t	Longitudinal Distance between Truck cg and Secondary Vertical Suspension, m.
b	Semi Distance Between Primary Suspension, m.
c	Longitudinal Distance Between Vertical Side Spring Suspension, and Car cg, m.
C_{cx}	Inter-Body Roll Damping, N.m.s/rad.
C_{cy}	Inter-Body Pitch Damping, N.m.s/rad.
C_{cz}	Inter-Body Yaw Damping, N.m.s/rad.
C_{JTF}	Yaw Damping for Female Joint-Truck Connection, N.m.s/rad.
C_{JTM}	Yaw Damping for Male Joint-Truck Connection, N.m.s/rad.
C_{px}	Primary Longitudinal Suspension Damping Coefficient, N.s/m.
C_{py}	Primary Lateral Suspension Damping Coefficient, N.s/m.
C_{pz}	Primary Vertical Suspension Damping Coefficient, N.s/m.
C_{sy}	Joint-to-Truck Lateral Suspension Damping Coefficient, N.s/m.
C_{sz}	Secondary Vertical Damping, N.s/m.
C_s	Joint-to-Truck Vertical Suspension Damping Coefficient, N.s/m.
d_f, d_r	Distance Between Truck Cg And Front And Rear Wheelsets Respect., m.
f_{11}	Lateral Creep Coefficient, N/wheel.
f_{12}	Lateral-Spin Creep Coefficient, N.m/wheel.
f_{22}	Spin Creep Coefficient, $N.m^2$/wheel.
f_{33}	Longitudinal Creep Coefficient, N/wheel.
F_{xl}, F_{xr}	Longitudinal Creep Force, Left and Right Wheels Respectively.
F_{yl}, F_{yr}	Lateral Creep Force, Left and Right Wheels Respectively.
F_{sy}	Joint Suspension Lateral Force on Truck.
F_{py}	Primary Suspension Lateral Force on Truck.

h_3	Vertical Distance of Joint Lateral Suspension to Truck cg, m.
h_4	Vertical Distance of Primary Lateral Suspension to Truck cg, m.
I_{cx}	Car Body Roll Moment of Inertia, kg. m^2.
I_{cz}	Car Body Yaw Moment of Inertia, kg. m^2.
I_{cx}	Car Body Pitch Moment of Inertia, kg. m^2.
I_{tz}	Truck Frame Yaw Moment of Inertia, kg. m^2.
I_{tx}	Truck Frame Roll Moment of Inertia, kg. m^2.
I_{wy}	Wheelset Pitch Moment of Inertia, kg. m^2.
I_{wz}	Wheelset Yaw Moment of Inertia, kg. m^2
I_{wx}	Wheelset Roll Moment of Inertia, kg. m^2
k_{cx}	Inter-Body Roll Stiffness, N.m/rad.
k_{cy}	Inter-Body Pitch Stiffness, N.m/rad.
k_{cz}	Yaw Stiffness of Car-to-Car Connection, N-m/rad.
k_{jtm}	Male Joint-to-Truck Yaw Suspension Stiffness Coefficient, N/m.
k_{jtf}	Female Joint-to-Truck Yaw Suspension Stiffness Coefficient, N/m.
k_{px}	Primary Longitudinal Suspension Stiffness Coefficient, N/m.
k_{py}	Primary Lateral Suspension Stiffness Coefficient, N/m.
k_{pz}	Primary Vertical Suspension,N/m.
k_{sy}	Joint-to-Truck Lateral Suspension Stiffness Coefficient, N/m.
k_{sz}	Inter-Car Yaw Stiffness, N/m.
k_s	Vertical Stiffness between Articulation Joint and Truck, N/m.
m_c	Mass of Car Body, kg.
m_J	Mass of Joint, kg.
m_t	Mass of Truck Frame, kg.
m_w	Wheelset Mass, kg.
M_{zl} ,M_{zr}	Creep Moment, Left and Right wheels Respectively..
$M_{p\psi w}$	Primary Suspension Yaw Moment on Wheelset.

$M_{p\phi w}$	Primary Suspension Roll Moment on Wheelset.
$M_{p\psi}$	Primary Suspension Yaw Moment on Truck.
$M_{p\phi}$	Primary Suspension Roll Moment on Truck.
$M_{sj\psi}$	Joint Suspension Yaw Moment on Truck.
$M_{s\phi}$	Secondary Suspension Roll Moment on Truck.
N_y	Lateral Component of Normal Force.
p	Semi distance between Secondary Suspension, m.
r_l, r_r	Rolling Radii, Left and Right Wheels Respectively, m.
S_f	Distance from Car cg to Male Joint, m.
S_r	Distance from Car cg to Female Joint, m.
V	Forward Speed, m/sec.
W_{app}	Applied Load, N/wheel.
λ	Conicity.
Γ	Roll Angle Coefficient.
Δ	Contact Angle Coefficient.
δ_0	Contact Angle Offset.
δ_l, δ_l	Contact Angles , left and right wheels respectively, rads.
ω	Angular Velocity, rads/s.
ξx, ξ_y	Longitudinal and Lateral Creepages Respectively.
ξ_{sp}	Spin Creepage.

1. INTRODUCTION

1.1 Background

High Speed Guided Ground Transportation (HSGGT) vehicle/guideway systems - high speed rail (HSR) and magnetically levitated (Maglev) - are being considered for deployment in the United States. The Federal Railroad Administration (FRA) has the mission of ensuring the safety of such systems. In support of this mission, it is necessary that credible models and analytical procedures be developed that can be used to predict safety-related behavior. The purpose of this document is to present the first phase of the development of such models for a special class of systems being considered for deployment, namely high-speed articulated trains. An example of such a system is the French TGV. Details of the configurations of such systems are given in [1].

High-speed articulated trains differ from conventional trains in a number of ways, the most significant being the presence of an articulation connection between two adjacent cars. In addition, trucks are shared by two consecutive car bodies except at the ends of the train. The kinematics of the articulation and the associated car-to-car and car-to-truck connections produce dynamic interaction between adjacent vehicles that cannot be accurately accounted for by considering single vehicle models, which has been the practice in the past. Hence, a multi-vehicle model is needed in the analysis and simulation of articulated trains to describe and evaluate their dynamic performance.

Dynamic performance of articulated vehicles can be grouped into three regimes:

1. Stability,
2. Curving Performance, and
3. Dynamic Forced Response.

Stability of rail vehicles usually refers to lateral stability and identification of speeds above which the 'hunting' phenomena occurs in rail vehicles. Hunting is a self-excited lateral-yaw oscillation that is produced at a specific forward speed by the wheel-rail forces. The speed at which this oscillation is initiated is called the 'critical speed'. It is characterized by the violent oscillation of

the wheelset and truck assemblies. Severe hunting is detrimental to good dynamic performance of the vehicle and poses significant safety problems. It can lead to track damage and derailment. Thus, the study of lateral stability is of particular importance for a high speed passenger train. The purpose of a lateral stability analysis is to determine the safe operating speed of the vehicle for a given set of parameters and to delineate safe and unsafe regions of behavior.

The curving behavior of rail vehicles has been studied quite extensively in the past [2-4]. The purpose of these studies has been to assess the ability of vehicles to successfully negotiate curves without derailing or adversely affecting the structural integrity of the track structure as well as the vehicle components themselves. Both steady state and dynamic models have been constructed. The steady state models predict component positions, wheel/rail forces, energy dissipation at the wheel-rail interface, and flange boundaries for vehicles traversing constant radius curves. The dynamic models predict vehicle response due to changing track conditions such as transitions from tangent to curved track and vice-versa. These models can also predict vehicle overturning, wheel-climb, as well as the vehicle states and forces. Typically the requirement of good lateral stability and good curving performance are in conflict thereby requiring trade-offs to obtain acceptable performance in both areas.

Forcing in a rail vehicle system occurs through vehicle-track structure interaction as well as due to external sources such as wind. Severe forced response can produce degraded ride quality, severe loading of vehicle components, and even derailment. Forced response can occur in the lateral plane and the vertical plane where the two motions are uncoupled or it can occur such that the motions are coupled. Lateral forced response occurs because of track irregularities or perturbation of the track. Vertical response occurs because of vertical track irregularities or track perturbations with coupling between the motions occurring because of cross-level misalignments. Wind loading can produce forced behaviors in both the lateral and vertical plane. Pitch and bounce models predict dynamic behaviors of vehicles due to vertical track irregularities. It is possible to assess the vertical dynamic performance in the frequency domain when the system is simplified as a linear mathematical model.

1.2 Scope of Work

This reports presents the development of linear models of articulated train sets in the lateral stability and forced response regimes. Stability is restricted to the development of linear eigenvalue-eigenvector analyses for determining a 'critical speed' of the train set for a given set of parameters. The forced response model is a linear model restricted to predicting pitch and bounce behavior in response to vertical track irregularities. A limited set of simulation studies have been conducted. A curving model also has been developed [5] and is available for use but is not discussed in this report.

The organization of the report is as follows: In Chapter 2, the development of a lateral stability model of an articulated train is discussed, as well as some parameter studies conducted to determine the behavior of such systems for a given set of parameters. Chapter 3 presents the development of mathematical models for pitch and bounce behavior as well as results of parameter studies. Finally, Chapter 4 summarizes the work presented in this research and suggests future developmental efforts.

2. LATERAL STABILITY OF ARTICULATED VEHICLES

2.1 Introduction

This section describes the lateral stability models developed for a high speed articulated train. Descriptions of the associated computer programs are given in [6]. A set of representative baseline parameters are also presented. These were developed to give a critical speed of approximately 300 km/h for a ten car consist. The data were assembled from a number of different sources (see for example [1]). The computer models developed were used to assess the influence of several vehicle parameters on the critical speed and shape of the least damped mode for lateral stability of the consist.

2.2 Model Development

For an articulated train, the key element of focus is the articulation design for support and stability of two consecutive vehicles. The purpose of the articulation is to couple consecutive vehicles together more tightly than is typically the case for conventional arrangements. Typical articulated train sets contain conventional components such as wheelsets, truck frames and car bodies as well as primary and secondary suspensions which are modeled in much the same way as with conventional trains. For the models developed in this report, a typical car body/truck/vehicle assembly is shown in Figure 2-1 through Figure 2-4. The assembly consists of conventionally attached trucks in the front and rear, and shared trucks in-between. The conventional trucks are connected to the car body through lateral, yaw and roll suspension elements. The shared trucks are connected directly to the car body through roll suspension elements and through the articulation joints. A key element of articulated train modeling is the modeling of the articulation connections between the cars bodies and the interconnections with the trucks. In the model developed here the articulation joint model has been made as generic as possible to allow the analyst to model different

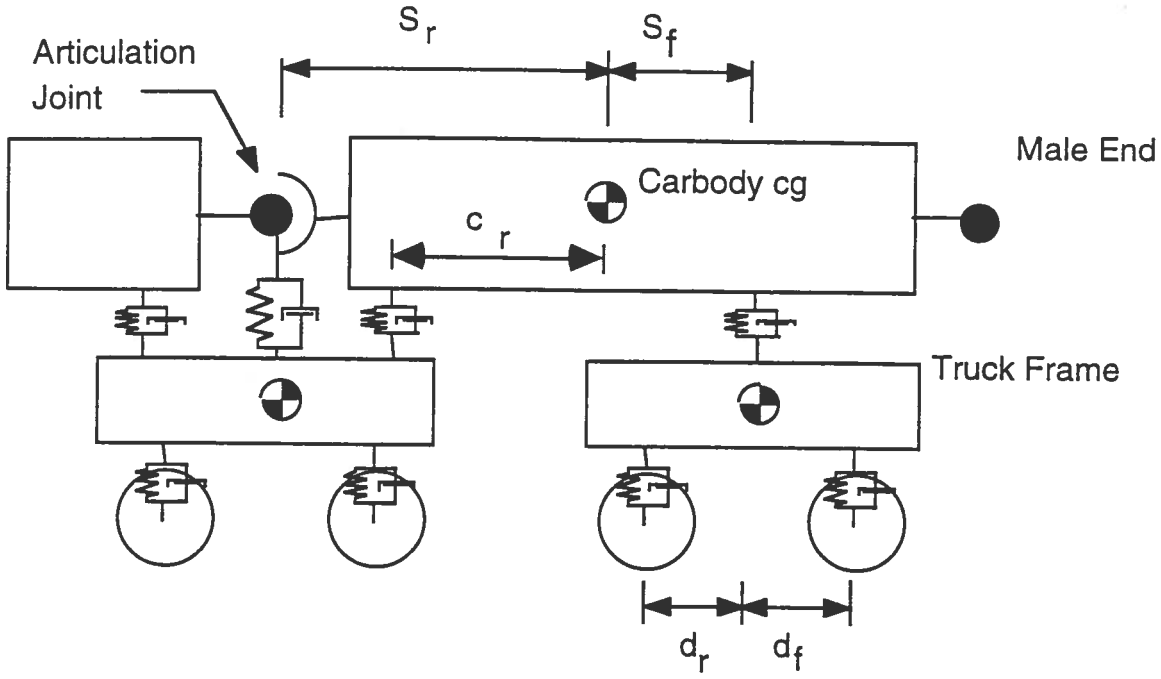

Figure 2-1. Schematic Showing The Truck Arrangement At Front Of Train set.

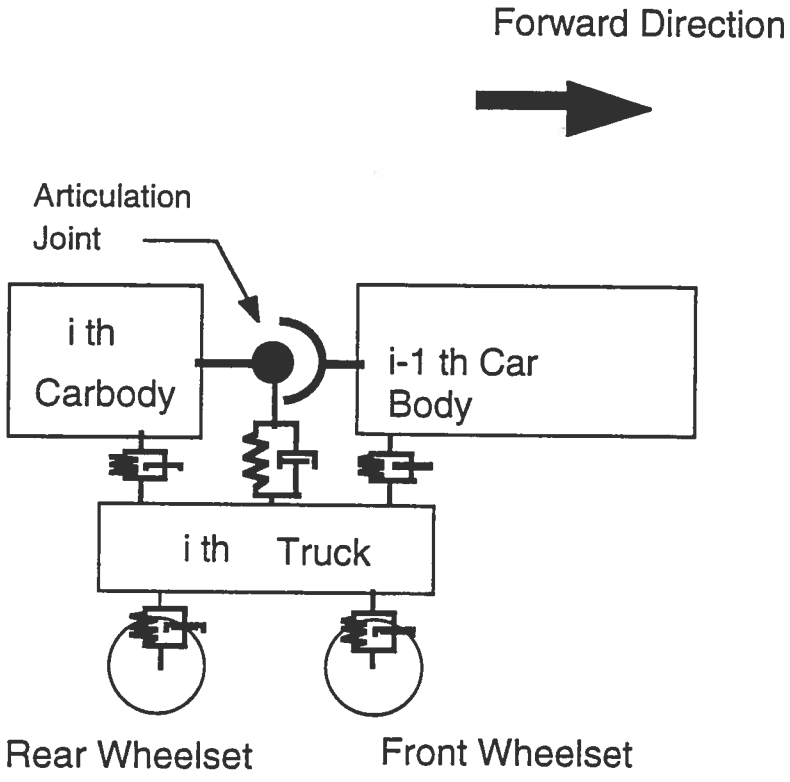

Figure 2-2. Schematic Showing Arrangement Of Components Of Train Set.

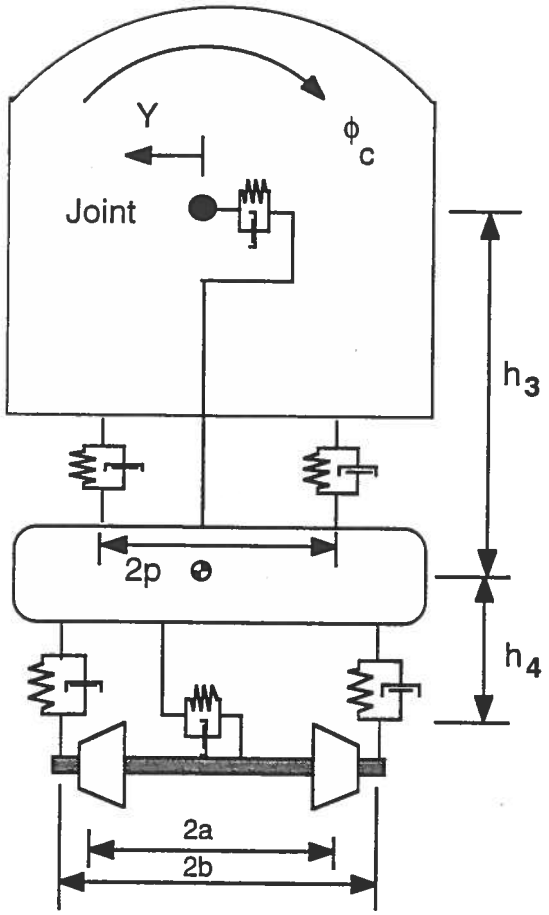

Figure 2-3. Schematic of Model in Rear View.

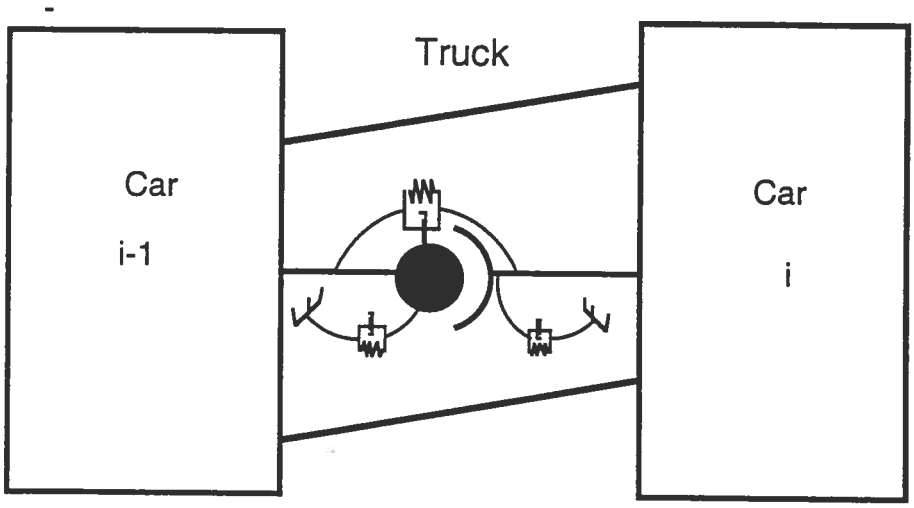

Figure 2-4. Plan View of Truck/Articulation Joint Connections.

designs by picking the suspension elements appropriately. It consists of yaw and roll suspension connections between the male and female ends of the joint, and yaw suspension elements between the female and male ends and the trucks individually. These elements represent the car to truck yaw dampers that are normally seen in high speed vehicles. A lateral and vertical suspension also exists between the joint and the truck frame.

The equations of motion for the articulated train set are derived using the Principle of Virtual Work also known as Lagrange's form of D'Alembert's Principle[7]. The principle has the advantage of retaining the vector approach to deriving equations of motion as per Newton's 2nd Law but at the same time eliminating the non working forces from the equations directly. This approach is especially suited to this particular problem due to the presence of the articulation constraints between two adjacent car bodies. The principle can be stated as follows:

$$\sum_{i=1}^{n}(\vec{F}_i - m_i\vec{a}_i)\bullet\frac{\partial\vec{R}_i}{\partial q_j} + \sum_{i=1}^{m}(\vec{M}_i - \dot{\vec{H}}_i)\bullet\frac{\partial\vec{\omega}_i}{\partial\dot{q}_j} = 0 \qquad (2\text{-}1)$$
$$j = 1..k$$

where n is the total number of particles and bodies, m is the number of bodies, k is the number of generalized coordinates, $\vec{F}_i$ is the externally applied force, $\vec{a}_i$ is the acceleration of the particle or body, $\vec{M}_i$ is the torque applied to the body, and $\vec{H}_i$ is the angular momentum. $\vec{R}_i$ and $\vec{\omega}_i$ are the position vector and the body angular velocity respectively. The coordinate systems used for this development are shown in Figure 2-5. The $i_T, j_T k_T$ coordinate system is fixed in the track. The i",j",k"system represents an intermediate system that yaws with the body, and the i',j',k' system represents a body fixed axis. These coordinate systems have been commonly used by many researchers to write the equations of motion of rail vehicles [9].

2.2.1 Wheelset Equations

The derivation of the equations of motion for a wheelset follows previous efforts [9]. The models derived consist of two degrees of freedom, *i.e.* lateral y_w and yaw ψ_w, linear wheel-rail

geometry, and linear creep force characteristics based on Kalker's linear creep theory [9]. The angular motions associated with the wheelset are assumed to be small as are the angles of contact between the wheel and the rail. The contact forces, *i.e.* normal forces, creep forces, and moments on the wheel-rail contact patches are illustrated in Figure 2-6. Also shown in the figure are the suspension forces between the wheelset and the truck frame.

The wheel profile consists of a tread with a constant conicity λ. The flange is not modeled. The contact angles at the left and right patch are respectively δ_l and δ_r. The roll angle ϕ_w depends only on the wheelset lateral displacement y_w. The wheel-rail geometric parameters are linearized as follows:

$$\begin{aligned} \frac{r_l - r_r}{2a} &= \frac{\lambda y_w}{a} \\ \frac{\delta_l - \delta_r}{2} &= \frac{\Delta y_w}{a} \\ \phi &= \frac{\Gamma\ y_w}{a} \end{aligned} \tag{2-2}$$

The friction forces between the wheel and the rail are dependent on the slip velocities or creepages in the wheel-rail interface. The creepage is defined as the relative velocity between the wheel and the rail normalized by the forward velocity of the wheelset. The creep forces on the left (l) and right (r) wheels are related to the creepages through Kalker's linear creep theory as follows:

$$\begin{aligned} F_{xr} &= -f_{33}\xi_{xr} \\ F_{yr} &= -f_{11}\xi_{yr} - f_{12}\xi_{spr} \\ M_{zr} &= f_{12}\xi_{yr} - f_{22}\xi_{spr} \\ F_{xl} &= -f_{33}\xi_{xl} \\ F_{yl} &= -f_{11}\xi_{yl} - f_{12}\xi_{spl} \\ M_{zl} &= f_{12}\xi_{yl} - f_{22}\xi_{spl} \end{aligned} \tag{2-3}$$

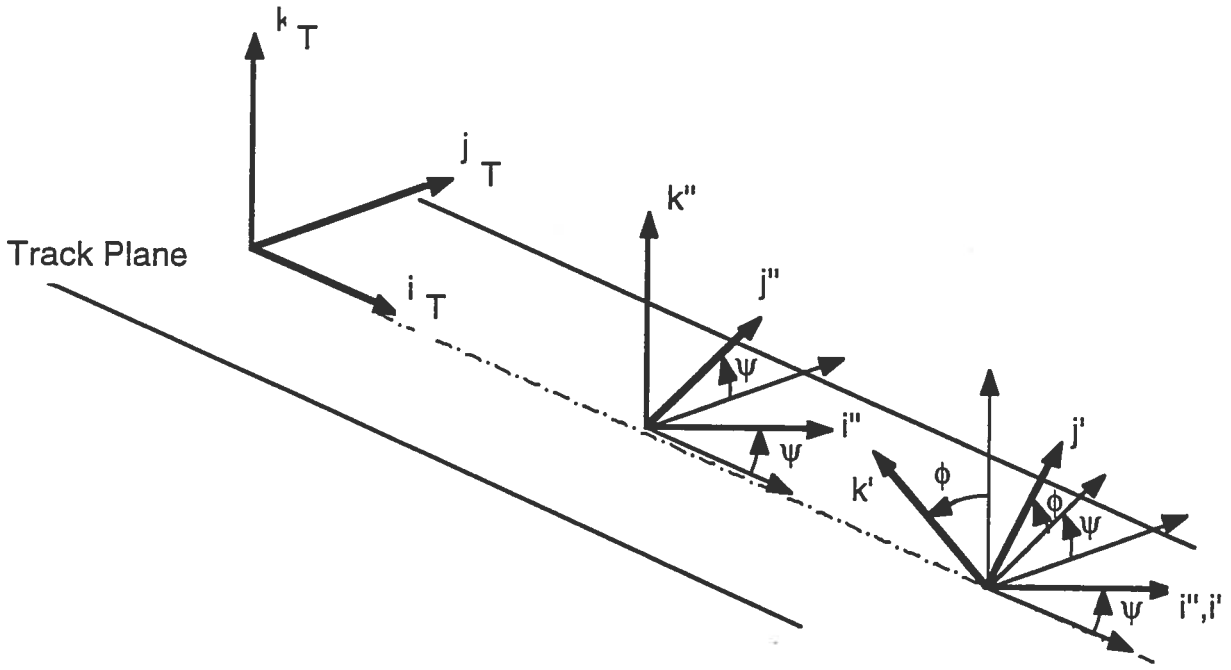

Figure 2-5. Coordinate Systems.

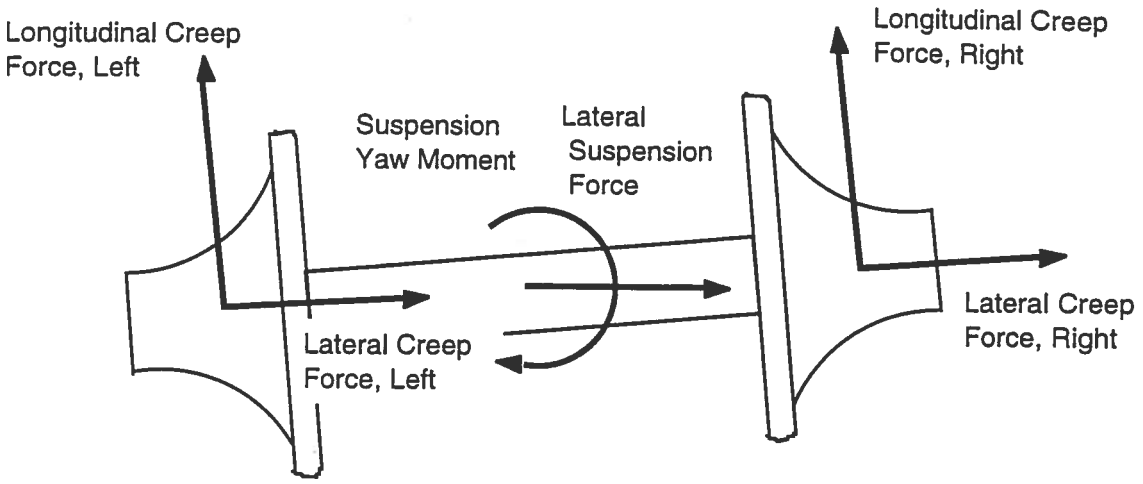

a) Plan View.

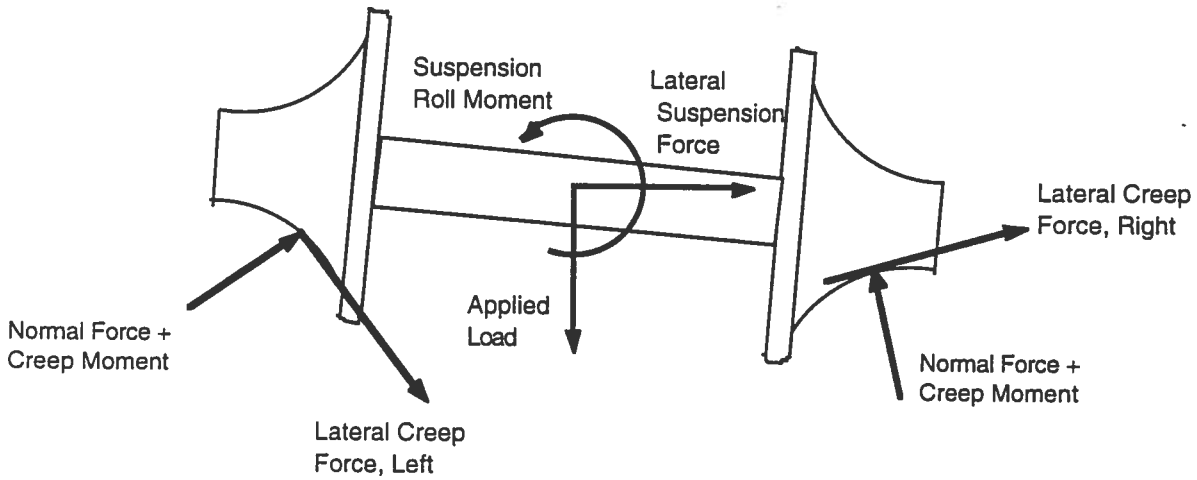

b) End View

Figure 2.6. Free-Body Diagram of Wheelset

Here the creep coefficients f_{ij} depend on the normal load on the wheel, the geometry of the wheel and rail profiles, and the material properties of the contacting bodies. The creepage expressions are derived for rigid wheel and rail and depend on the wheelset states. These expressions pertain to lateral slip, longitudinal slip, and relative spin. The linearized expressions for the creepages are:

$$\begin{aligned}
\xi_{xr} &= +a\frac{\dot{\psi}_w}{V} - \frac{r_r}{r_0} + 1 \\
\xi_{yr} &= \frac{\dot{y}_w + r_o\dot{\phi}_w - V\psi_w}{V} \\
\xi_{spr} &= \frac{\dot{\psi}_w}{V} + \frac{\Omega\delta_r}{V} \\
\xi_{xl} &= -a\frac{\dot{\psi}_w}{V} - \frac{r_l}{r_0} + 1 \\
\xi_{yl} &= \frac{\dot{y}_w + r_o\dot{\phi}_w - V\psi_w}{V} \\
\xi_{spl} &= \frac{\dot{\psi}_w}{V} - \frac{\Omega\delta_l}{V}
\end{aligned} \tag{2-4}$$

where $\Omega = \frac{V}{r_0}$ is the nominal angular velocity of the wheelset, V is the forward speed of the wheelset, and r_0 is the mean rolling radius. These creepage expressions are the same on the front and rear wheelsets of the truck. The gravitational stiffness force, which is the lateral resultant of the normal forces N_l and N_r is described by:

$$N_{yl} + N_{yr} = -W_{app}[(\delta_l - \delta_r)/2 + \phi_w] \tag{2-5}$$

Assuming linear suspension elements, the lateral suspension forces and yaw moments on the front and rear wheelsets of the ith truck can then be written as:

Forces

$$F_{py_{wfi}} = k_{pyfi}(y_{ti} + d_{pi}\psi_{ti} + h_{4i}\phi_{ti} - y_{wfi}) + C_{pyfi}(\dot{y}_{ti} + d_{pi}\dot{\psi}_{ti} + h_{4i}\dot{\phi}_{ti} - \dot{y}_{wfi})$$

$$F_{py_{wri}} = k_{pyri}(y_{ti} - d_{pi}\psi_{ti} + h_{4i}\phi_{ti} - y_{wri}) + C_{pyri}(\dot{y}_{ti} - d_{pi}\dot{\psi}_{ti} + h_{4i}\dot{\phi}_{ti} - \dot{y}_{wri})$$

Moments

$$M_{p\psi_{wfi}} = -2k_{pxfi}b_i^2(\psi_{wfi} - \psi_{ti}) - 2C_{pxfi}b_i^2(\dot{\psi}_{wfi} - \dot{\psi}_{ti})$$

$$M_{p\psi_{wri}} = -2k_{pxri}b_i^2(\psi_{wri} - \psi_{ti}) - 2C_{pxri}b^2(\dot{\psi}_{wri} - \dot{\psi}_{ti})$$

$$M_{p\phi i_{front}} = -2k_{zpfi}b_i^2(\phi_{wfi} - \phi_{Ti}) - 2C_{zpfi}b_i^2(\dot{\phi}_{wfi} - \dot{\phi}_{Ti}) \qquad (2\text{-}6)$$

$$M_{p\phi i_{rear}} = -2k_{zpri}b_i^2(\phi_{wri} - \phi_{ti}) - 2C_{zpri}b_i^2(\dot{\phi}_{wri} - \dot{\phi}_{ti})$$

The subscripts wf and wr represent the front and rear wheelsets in a truck respectively. The equations of motion for a wheelset are written using the Principle of Virtual Work. The equations of motion for a wheelset in the ith truck are:

Lateral Equation

$$m_w\ddot{y}_w = -2\frac{f_{11}}{V}(\dot{y}_w + r_o\dot{\phi} - V\psi_w) - 2\frac{f_{12}}{V}(\dot{\psi}_w - \Omega\frac{\Delta y_w}{a}) - W_{app}(\Delta + \Gamma)\frac{y_w}{a}$$
$$+k_{py}(y_{ti} \pm d_{f,ri}\psi_{ti} + h_{4i}\phi_{ti} - y_w) + C_{py}(\dot{y}_{ti} \pm d_{f,ri}\dot{\psi}_{ti} + h_{4i}\dot{\phi}_{ti} - \dot{y}_w)$$

Yaw Equation (2-7)

$$I_{wz}\ddot{\psi}_w = -2a^2\frac{f_{33}}{V}\dot{\psi}_w - 2a\frac{f_{33}}{V}(\Omega\frac{\lambda y_w}{a}) + 2\frac{f_{12}}{V}(\dot{y}_w + r_o\dot{\phi}_w - V\psi_w) - 2\frac{f_{22}}{V}\dot{\psi}_w$$
$$+2\frac{f_{22}}{V}(\Omega\frac{\Delta y_w}{a}) + aW_{app}\delta_o\psi_w - I_{wy}V\Gamma\frac{\dot{y}_w}{ar_o} - 2k_{px}b_i^2(\psi_w - \psi_{ti})$$
$$-2C_{px}b_i^2(\dot{\psi}_w - \dot{\psi}_{ti})$$

The subscripts wf and wr have been removed for conciseness.

2.2.2 Truck Equations

As shown in Figures 2-2 and 2-3, each truck consists of two wheelsets, a truck frame and certain primary and secondary suspension components. A truck frame is considered to have lateral, yaw, and roll degrees of freedom. The primary suspensions contain longitudinal, lateral, and vertical stiffness elements as well as damping. The secondary suspension components include connections between the truck frame and car body and with connections between the truck frame and the articulation joint. These connections are illustrated in a schematic in Figure 2-4.

The presence of the articulation joint between two adjacent car bodies and the connections between the car bodies and the shared truck preclude the necessity of having lateral and longitudinal suspensions between the car body and the trucks. The vertical suspension characteristics between truck and car body consist of linear stiffnesses and damping. The lateral and yaw suspensions between the car bodies and the trucks are accounted for through suspension elements that connect the articulation joint to the truck.

The truck equations consist of three equations for the truck frame with linear suspension elements connecting the wheelsets, the car bodies, and the articulation joint. These equations pertain to a truck lateral displacement y_t, a truck yaw displacement ψ_t, and a truck roll displacement ϕ_t. The forces and moments acting on the truck in the lateral plane are shown in Figure 2-7. The generalized inertia force of the i^{th} truck corresponding to the jth generalized coordinate is:

$$Q_{ij}^{*} = m_i \bar{a}_i \bullet \frac{\partial \bar{R}_i}{\partial q_j} + \dot{\bar{H}}_i \bullet \frac{\partial \bar{\omega}_i}{\partial \dot{q}_j} \tag{2-8}$$

where

$$\bar{R}_i = y_{ti} \bar{j}_T$$

and

$$\vec{\omega}_{ti} = \dot{\psi}_{ti}\vec{k}_T + \dot{\phi}_{ti}\vec{i}_T$$

i_T, j_T, k_T represent coordinate axes fixed in the track and the above equations are valid for small motions. The generalized coordinates are $y_{ti}, \psi_{ti}, \phi_{ti}$. Then for the ith truck frame, the generalized inertia force becomes:

$$\begin{aligned} Q_{iy} &= m_{ti}\ddot{y}_{ti} \\ Q_{i\psi} &= I_{tzi}\ddot{\psi}_{ti} \\ Q_{i\phi} &= \frac{1}{2} I_{txi}\ddot{\phi}_{ti} \end{aligned} \tag{2-9}$$

The generalized force associated with the i^{th} body and the j^{th} coordinate is:

$$Q_{ij} = \vec{F}_{ti} \bullet \frac{\partial \vec{R}_i}{\partial q_j} + \vec{M}_{ti} \bullet \frac{\partial \vec{w}_i}{\partial \dot{q}_j} \tag{2-10}$$

where

$$\vec{F}_{ti} = (F_{pyi} + F_{syi})_{stiff}\, j_T + Damping\ Terms$$
$$\vec{M}_{ti} = (M_{p\psi i} + M_{sj\psi i})_{stiff}\, \vec{k}_T + (M_{p\phi i} + M_{s\phi i})_{stiff}\, \vec{i}_T + Damping\ Terms$$

These forces and moments arise from the suspension elements between the wheelsets and the truck frame and between the articulation joint and the car body and the truck frame.

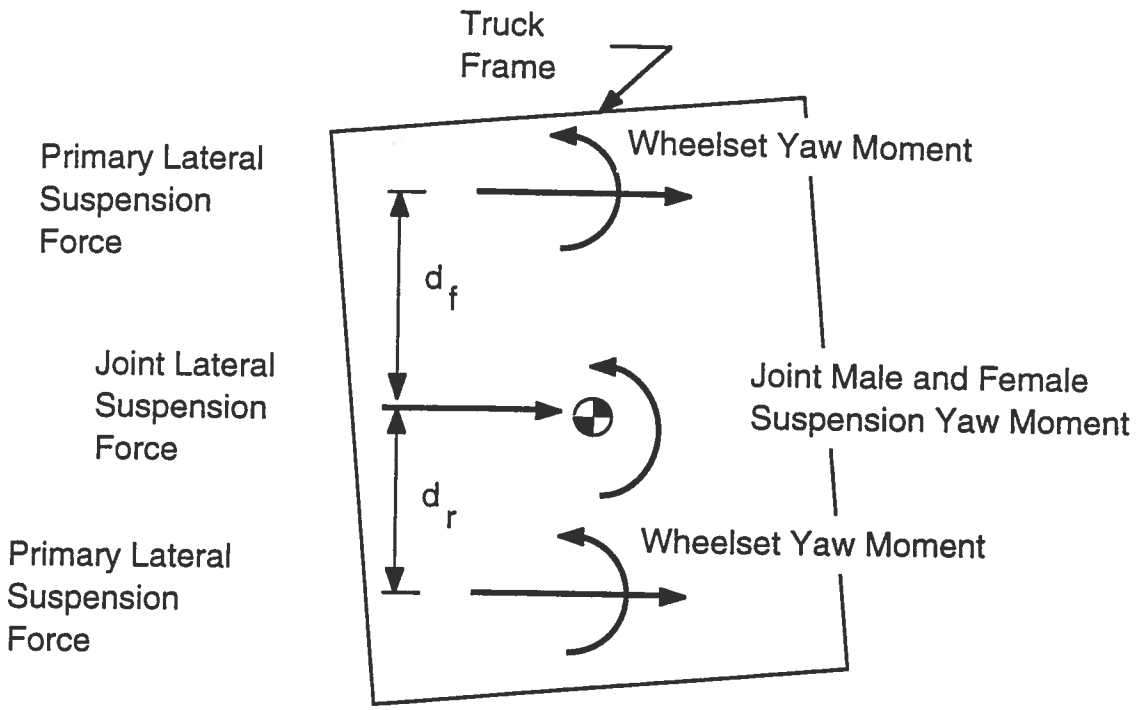

a) Plan View

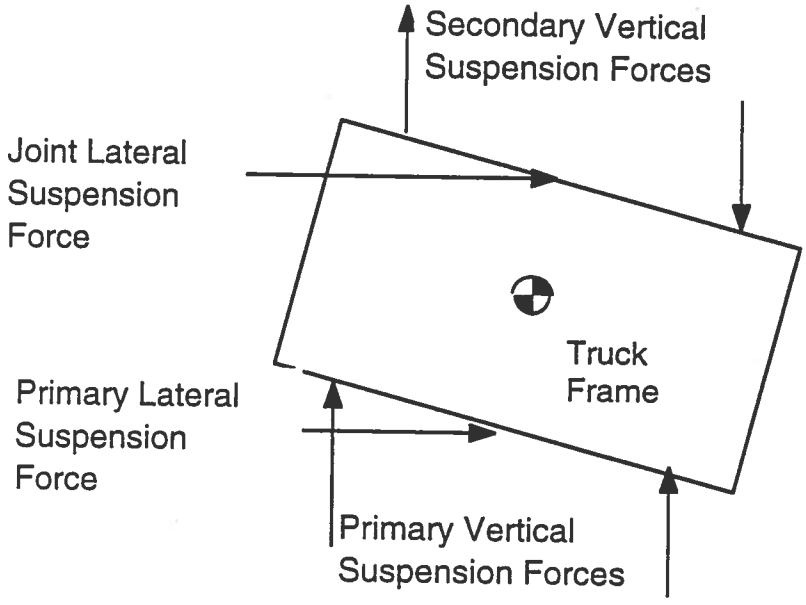

b) End View

Figure 2-7. Free-body Diagram of Shared Truck.

The suspension stiffness terms are:

Forces

$$F_{syi} = -k_{syi}(y_{ti} - h_{3i}\phi_{ti} - Y_i)$$

$$F_{pyi} = -2k_{pyfi}(y_{ti} + d_{fi}\psi_{ti} + h_{4i}\phi_{ti} - y_{wfi}) - 2k_{pyri}(y_{ti} - d_{ri}\psi_{ti} + h_{4i}\phi_{ti} - y_{wri})$$

Moments

$$\begin{aligned}
M_{p\psi ti} &= 2k_{pxfi}b_i^2(\psi_{wfi} - \psi_{ti}) + 2k_{pxri}b_i^2(\psi_{wri} - \psi_{ti}) \\
&\quad -2k_{pyfi}d_{fi}(y_{ti} + d_{fi}\psi_{ti} + h_{4i}\phi_{ti} - y_{wfi}) \\
&\quad +2k_{pyri}d_{ri}(y_{ti} - d_{ri}\psi_{ti} + h_{4i}\phi_{ti} - y_{wri}) \\
M_{sj\psi ti} &= k_{jif_{i-1}}(\psi_{c_{i-1}} - \psi_{ti}) + k_{jtmi}(\psi_{ci} - \psi_{ti}) \\
M_{p\phi ti} &= -2k_{pyi}h_{4i}(y_{ti} + d_{pi}\psi_{ti} + h_{4i}\phi_{ti} - y_{wfi}) \\
&\quad -2k_{pyri}h_{4i}(y_{ti} - d_{pi}\psi_{ti} + h_{4i}\phi_{ti} - y_{wri}) \\
&\quad +2k_{zpfi}b_i^2(\phi_{wfi} - \phi_{ti}) + 2k_{zpri}b_i^2(\phi_{wri} - \phi_{ti}) \\
M_{s\phi ti} &= -2k_{sz_{i-1}}p_i^2(\phi_{c_{i-1}} - \phi_{ti}) - 2k_{szi}p_i^2(\phi_{ci} - \phi_{ti})
\end{aligned} \tag{2-11}$$

Similar terms are obtained due dampers in the suspensions, the only difference being that the stiffness coefficients are changed to the damping coefficients and the displacements are changed to velocities. The equations of motion for the ith truck are:

Lateral Equation

$$\begin{aligned}
m_t\ddot{y}_{ti} &= -k_{syi}(y_{ti} - h_{3i}\phi_{ti} - Y_i) - 2k_{pyfi}(y_{ti} + d_{fi}\psi_{ti} + h_{4i}\phi_{ti} - y_{wfi}) \\
&\quad -2k_{pyri}(y_{ti} - d_{ri}\psi_{ti} + h_{4i}\phi_{ti} - y_{wri}) - 2C_{syi}(\dot{y}_{ti} - h_{3i}\dot{\phi}_{ti} - \dot{Y}_i) \\
&\quad -2C_{pyfi}(\dot{y}_{ti} + d_{fi}\dot{\psi}_{ti} + h_{4i}\dot{\phi}_{ti} - \dot{y}_{wfi}) - 2C_{pyri}(\dot{y}_{ti} - d_{ri}\dot{\psi}_{ti} + h_{4i}\dot{\phi}_{ti} - \dot{y}_{wri})
\end{aligned}$$

Yaw Equation

$$\begin{aligned}
I_{tz}\ddot{\psi}_{ti} &= 2k_{pxfi}b^2(\psi_{wfi} - \psi_{ti}) + 2k_{pxri}b_i^2(\psi_{wri} - \psi_{ti}) \\
&\quad -2k_{pyfi}d_{fi}(y_{ti} + d_{fi}\psi_{ti} + h_{4i}\phi_{ti} - y_{wfi}) + 2k_{pyi}d_{ri}(y_{ti} - d_{ri}\psi_{ti} + h_{4i}\phi_{ti} - y_{wri}) \\
&\quad +k_{jtf_{i-1}}(\psi_{c_{i-1}} - \psi_{ti}) + k_{jtmi}(\psi_{ci} - \psi_{ti}) \\
&\quad -2C_{pyfi}d_{fi}(\dot{y}_{ti} + d_{fi}\dot{\psi}_{ti} + h_{4i}\dot{\phi}_{ti} - \dot{y}_{wfi}) + 2C_{pyri}d_{ri}(\dot{y}_{ti} - d_{ri}\dot{\psi}_{ti} + h_{4i}\dot{\phi}_{ti} - \dot{y}_{wri}) \\
&\quad +C_{jtf_{i-1}}(\dot{\psi}_{c_{i-1}} - \dot{\psi}_{ti}) + C_{jtmi}(\dot{\psi}_{ci} - \dot{\psi}_{ti})
\end{aligned}$$

Roll Equation

$$
\begin{aligned}
I_{tx}\ddot{\phi}_{ti} = & -2k_{pyfi}h_{4i}(y_{ti} + d_{fi}\psi_{ti} + h_{4i}\phi_{ti} - y_{wfi}) \\
& -2k_{pyri}h_{4i}(y_{ti} - d_{ri}\psi_{ti} + h_{4i}\phi_{ti} - y_{wri}) \\
& +2k_{zpfi}b_i^2(\phi_{wfi} - \phi_{ti}) + 2k_{zpri}b_i^2(\phi_{wri} - \phi_{ti}) - 2k_{sz_{i-1}}p_{i-1}^2(\phi_{c_{i-1}} - \phi_{ti}) \\
& -2k_{szi}p_i^2(\phi_{ci} - \phi_{ti}) - 2C_{pyfi}h_{4i}(\dot{y}_{ti} + d_{fi}\dot{\psi}_{ti} + h_{4i}\dot{\phi}_{ti} - \dot{y}_{wfi}) \\
& -2C_{pyri}h_{4i}(\dot{y}_{ti} - d_{ri}\dot{\psi}_{ti} + h_{4i}\dot{\phi}_{ti} - \dot{y}_{wri}) + 2C_{zpfi}b_i^2(\dot{\phi}_{wfi} - \dot{\phi}_{ti}) \\
& +2C_{zpri}b_i^2(\dot{\phi}_{wri} - \dot{\phi}_{ti}) - 2C_{sz_{i-1}}p_{i-1}^2(\dot{\phi}_{c_{i-1}} - \dot{\phi}_{ti}) - 2C_{szi}p_i^2(\dot{\phi}_{ci} - \dot{\phi}_{ti})
\end{aligned}
\tag{2-12}
$$

2.2.3 Articulation Joint

The modeling of the articulation joint is done to accommodate a variety of possible designs. The articulation joint is assumed to have a mass even though this mass may be small compared to the car body mass. The articulation joint is modeled as kinematically constraining adjacent car bodies in the lateral and vertical planes. Connections between a joint and a truck is through suspension elements. The joint has a female end and a male end. The male end is fixed in front of car body, and the female one at the rear of the car body. The articulation joint allows relative yaw and roll motions between the bodies. The suspension characteristics consist of:

1. Yaw and roll stiffness and damping between the male and female ends;
2. Yaw stiffness and damping between the male end and the truck frame as well as between the female end and the truck frame; and
3. Lateral stiffness and damping between the whole joint and truck frame.

2.2.4 Car Body Equations

Typical models of rail vehicles that assess lateral stability assign three degrees of freedom to the car body. These are lateral displacement (Y_{cg}) and yaw (ψ) and roll (ϕ) rotations. In the case of articulated trains, the presence of the articulation joint provides a constraint between the adjacent bodies of the consist thereby reducing the degrees of freedom of the system. The constraint is that the lateral motion of the points of interconnection of two adjacent bodies move

equally in the lateral plane. The generalized coordinates chosen here to represent the motion of the bodies consist of the lateral displacements of the articulated joints and the roll angles of each of the bodies. The lateral translations of ith and $(i+1)^{th}$ articulation joint are sufficient to represent the i^{th} car body yaw around its cg and the lateral translation of the i^{th} car body's cg. Figure 2-8 shows the coordinates chosen. The generalized coordinate Y_i appears in the accelerations of the i-1 and i^{th} car body as well as the acceleration of the i^{th} articulation joint. The relationship between the joint accelerations and the i^{th} car body accelerations is as follows:

$$\ddot{Y}_{cgi} = \frac{S_{ri}}{S_{ri} + S_{fi}}(\ddot{Y}_i - \ddot{Y}_{i+1}) + \ddot{Y}_{i+1}$$
$$\ddot{\psi}_i = \frac{\ddot{Y}_i - \ddot{Y}_{i+1}}{S_{ri} + S_{fi}} \qquad (2\text{-}13)$$

Similar accelerations can be written for the i-1 car body. These are:

$$\ddot{Y}_{cgi-1} = \frac{S_{ri-1}}{S_{ri-1} + S_{fi-1}}(\ddot{Y}_{i-1} - \ddot{Y}_i) + \ddot{Y}_i$$
$$\ddot{\psi}_{i-1} = \frac{\ddot{Y}_{i-1} - \ddot{Y}_i}{S_{ri-1} + S_{fi-1}} \qquad (2\text{-}14)$$

The equations for the i+1 car body do not contain the coordinate Y_i. They are:

$$\ddot{Y}_{cgi+1} = \frac{S_{ri+1}}{S_{ri+1} + S_{fi+1}}(\ddot{Y}_{i+1} - \ddot{Y}_{i+2}) + \ddot{Y}_{i+2}$$
$$\ddot{\psi}_{i+1} = \frac{\ddot{Y}_{i+1} - \ddot{Y}_{i+2}}{S_{ri+1} + S_{fi+1}} \qquad (2\text{-}15)$$

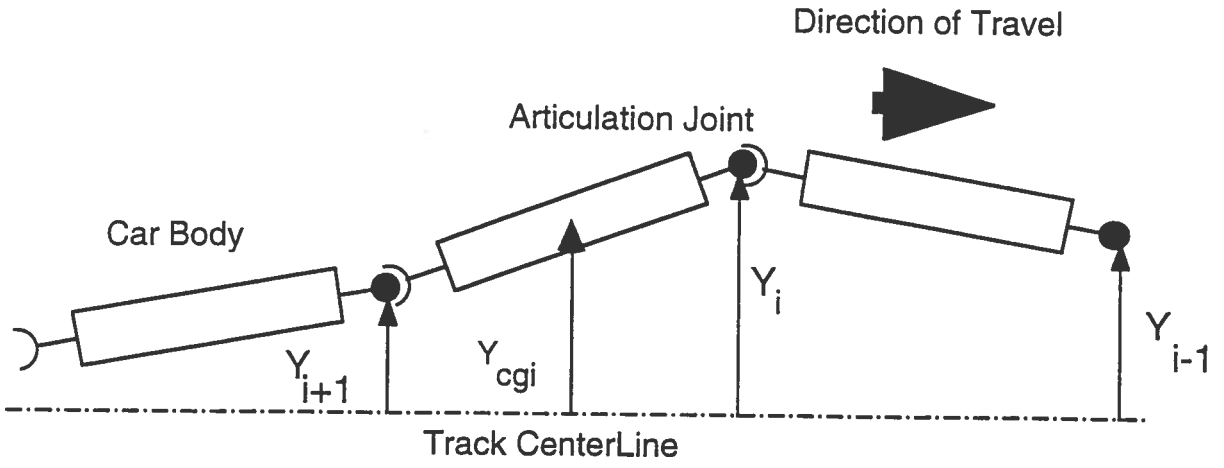

Figure 2-8. Articulation Joint Generalized Coordinates in Track Plane.

The generalized coordinate Y_i appears in the acceleration terms of bodies i-1 and i, as well as in the acceleration term for the articulation joint i. Therefore in determining the generalized inertia and applied forces, the accelerations of all three must be considered. The generalized inertial force corresponding to the ith body and the jth generalized coordinate Y_i is:

$$Q_{Y_i}{}^{*} = \frac{S_{ri} m_C}{S_{ri} + S_{fi}} \left[\frac{S_{ri}}{S_{ri} + S_{fi}} (\ddot{Y}_i - \ddot{Y}_{i+1}) + \ddot{Y}_{i+1} \right] - \frac{I_{CZi}}{(S_{ri} + S_{fi})^2} (\ddot{Y}_i - \ddot{Y}_{i+1}) \qquad (2\text{-}16)$$

The generalized inertial force corresponding to the i-1th body and the jth generalized coordinate Y_i is:

$$Q_{Y_{i-1}}{}^{*} = \frac{S_{fi-1} m_{Ci-1}}{S_{ri-1} + S_{fi-1}} \left[\frac{S_{ri-1}}{S_{ri-1} + S_{fi-1}} (\ddot{Y}_{i-1} - \ddot{Y}_i) + \ddot{Y}_i \right] - \frac{I_{CZi-1}}{(S_{ri-1} + S_{fi-1})^2} (\ddot{Y}_{i-1} - \ddot{Y}_i) \qquad (2\text{-}17)$$

and for the ith articulation joint is:

$$Q^{*}{}_{j_{Y_i}} = m_{ji} \ddot{Y}_i \qquad (2\text{-}18)$$

Hence the total generalized inertia force associated with the generalized coordinate Y_i is:

$$Q^*_{ToT_{Y_i}} = Q^*_{Y_i} + Q^*_{Y_{i-1}} + Q^*_{j_{Y_i}} \tag{2-19}$$

Figure 2-9 shows the free-body diagram of the ith car body in plan view. The internal reactions are not shown. Using these forces, the generalized force associated with the coordinate Y_i can be calculated. The generalized force associated with the i^{th} body and the generalized coordinate Y_i is:

$$\begin{aligned} Q_{Y_i} = & -\frac{k_{jtmi}}{S_{ri}+S_{fi}}\left(\frac{Y_i - Y_{i+1}}{S_{ri}+S_{fi}} - \psi_{ti}\right) - \frac{k_{jtfi+1}}{S_{ri}+S_{fi}}\left(\frac{Y_i - Y_{i+1}}{S_{ri}+S_{fi}} - \psi_{ti+1}\right) \\ & + \frac{k_{czi}}{S_{ri}+S_{fi}}\left(\frac{Y_{i-1} - Y_i}{S_{ri-1}+S_{fi-1}} - \frac{Y_i - Y_{i+1}}{S_{ri}+S_{fi}}\right) + \frac{k_{czi+1}}{S_{ri}+S_{fi}}\left(\frac{Y_{i+1} - Y_{i+2}}{S_{ri+1}+S_{fi+1}} - \frac{Y_i - Y_{i+1}}{S_{ri}+S_{fi}}\right) \\ & - \frac{C_{jtmi}}{S_{ri}+S_{fi}}\left(\frac{\dot{Y}_i - \dot{Y}_{i+1}}{S_{ri}+S_{fi}} - \dot{\psi}_{ti}\right) - \frac{C_{jtfi+1}}{S_{ri}+S_{fi}}\left(\frac{\dot{Y}_i - \dot{Y}_{i+1}}{S_{ri}+S_{fi}} - \dot{\psi}_{ti+1}\right) \\ & + \frac{C_{czi}}{S_{ri}+S_{fi}}\left(\frac{\dot{Y}_{i-1} - \dot{Y}_i}{S_{ri-1}+S_{fi-1}} - \frac{\dot{Y}_i - \dot{Y}_{i+1}}{S_{ri}+S_{fi}}\right) + \frac{C_{czi+1}}{S_{ri}+S_{fi}}\left(\frac{\dot{Y}_{i+1} - \dot{Y}_{i+2}}{S_{ri+1}+S_{fi+1}} - \frac{\dot{Y}_i - \dot{Y}_{i+1}}{S_{ri}+S_{fi}}\right) \end{aligned} \tag{2-20}$$

and that for the i-1 body is:

$$\begin{aligned} Q_{y_{i-1}} = & \frac{k_{jtmi-1}}{S_{ri-1}+S_{fi-1}}\left(\frac{Y_{i-1} - Y_i}{S_{ri-1}+S_{fi-1}} - \psi_{ti-1}\right) - \frac{k_{jtfi}}{S_{ri-1}+S_{fi-1}}\left(\frac{Y_{i-1} - Y_i}{S_{ri-1}+S_{fi-1}} - \psi_{ti}\right) \\ & + \frac{k_{czi}}{S_{ri-1}+S_{fi-1}}\left(\frac{Y_{i-1} - Y_i}{S_{ri-1}+S_{fi-1}} - \frac{Y_i - Y_{i+1}}{S_{ri}+S_{fi}}\right) + \frac{k_{czi-1}}{S_{ri-1}+S_{fi-1}}\left(\frac{Y_{i-1} - Y_i}{S_{ri-1}+S_{fi-1}}\right. \\ & \left. - \frac{Y_{i-2} - Y_{i-1}}{S_{ri-2}+S_{fi-2}}\right) + \frac{C_{jtmi}}{S_{ri-1}+S_{fi-1}}\left(\frac{\dot{Y}_{i-1} - \dot{Y}_i}{S_{ri-1}+S_{fi-1}} - \dot{\psi}_{ti-1}\right) \\ & + \frac{C_{jtfi}}{S_{ri-1}+S_{fi-1}}\left(\frac{\dot{Y}_{i-1} - \dot{Y}_i}{S_{ri-1}+S_{fi-1}} - \dot{\psi}_{ti}\right) + \frac{C_{czi}}{S_{ri-1}+S_{fi-1}}\left(\frac{\dot{Y}_{i-1} - \dot{Y}_i}{S_{ri-1}+S_{fi-1}}\right. \\ & \left. - \frac{\dot{Y}_i - \dot{Y}_{i+1}}{S_{ri}+S_{fi}}\right) + \frac{C_{czi-1}}{S_{ri-1}+S_{fi-1}}\left(\frac{\dot{Y}_{i-1} - \dot{Y}_i}{S_{ri-1}+S_{fi-1}} - \frac{\dot{Y}_{i-2} - \dot{Y}_{i-1}}{S_{ri-2}+S_{fi-2}}\right) \end{aligned} \tag{2-21}$$

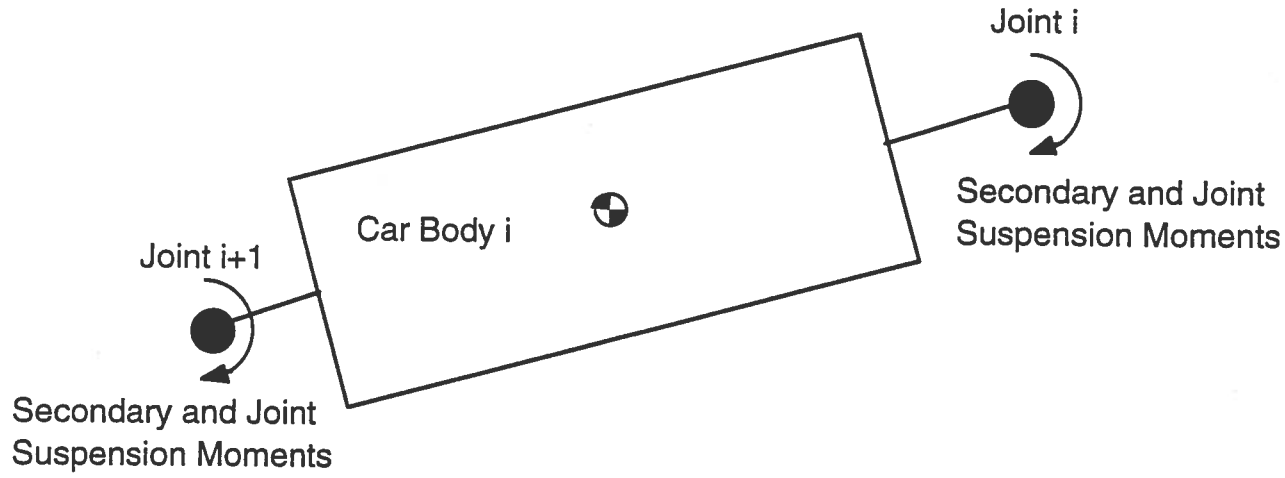

Figure 2-9. Free-body Diagram of ith Car Body in Plan View Showing Non-Working Moments.

The generalized external force for the i[th] joint is:

$$Q_{j_{Y_i}} = k_{sy}(y_{ti} - h_{3i}\phi_{ti} - Y_i) \tag{2-22}$$

The total generalized external force associated with the generalized coordinate Y_i is then:

$$Q_{ToT_{Y_i}} = Q_{Y_i} + Q_{Y_{i-1}} + Q_{j_{Y_i}} \tag{2-23}$$

and the corresponding equations are:

$$Q_{ToT_{Y_i}} - Q^*_{ToT_{Y_i}} = 0 \tag{2-24}$$

Similarly, the roll equations of the ith car body can be found. The equations of motion for the coordinate ϕ_{ci} are:

Roll Equation

$$\begin{aligned} I_{xci}\ddot{\phi}_{ci} = &-2k_{sz_{2i-1}}p_i^2(\phi_{ci} - \phi_{ti}) - 2k_{sz_{2i}}p_{i+1}^2(\phi_{ci} - \phi_{ti+1}) - 2k_{cx_i}(\phi_{ci} - \phi_{ci-1}) \\ &-2k_{cx_{i+1}}(\phi_{ci} - \phi_{ci+1}) - 2C_{sz_{2i-1}}p_i^2(\phi_{ci} - \phi_{ti}) - 2C_{sz_{2i}}p_{i+1}^2(\phi_{ci} - \phi_{ti+1}) \\ &-2C_{cx_i}(\phi_{ci} - \phi_{ci-1}) - 2C_{cx_{i+1}}(\phi_{ci} - \phi_{ci+1}) \end{aligned} \tag{2-25}$$

The full equations of motion are derived using the above recursive equations.

2.3 Method of Solution

The equations of motion can be written in matrix form as:

$$\mathbf{M}\ddot{y} + \mathbf{C}\dot{y} + \mathbf{K}y = \mathbf{0} \tag{2-26}$$

Where M, C, and K are the mass, damping, and stiffness matrices respectively, and $y^T = [y_1, y_2, \ldots, y_{n-1}, y_n]$ is the general displacement vector. The equations can be written in state variable form as:

$$\begin{Bmatrix} \dot{y} \\ \ddot{y} \end{Bmatrix} = A \begin{Bmatrix} y \\ \dot{y} \end{Bmatrix} \tag{2-27}$$

where $\mathbf{A} = \begin{bmatrix} 0 & I \\ M^{-1}K & M^{-1}C \end{bmatrix}$. If we assume a solution $\{y\} = \{\Psi\}e^{\lambda t}$, where $\{\Psi\}$ is a complex modal vector, the eigenvalues can be found by solving the characteristic equation $|A - \lambda I| = 0$. The roots λ_i of the characteristic equation represent 2n eigenvalues which may contain complex conjugates. By substituting the eigenvalues into the original equations we can find the corresponding eigenvectors.

The critical speed for hunting stability is found by running the program sequentially through a number of forward speeds until the real part of any eigenvalue becomes a positive number and the corresponding damping ratio becomes zero or negative. This means that the system is unstable. The least damped hunting mode is then obtained from the corresponding eigenvector.

In analyzing the results, it is useful to know the frequency of wheelset kinematic motions as well as those for a free rigid truck. The wheelset frequency equation is:

$$f_w = \frac{V}{2\pi}\sqrt{\frac{\lambda}{ar_o}} \tag{2-28}$$

and that for the truck is:

$$f_t = \frac{V}{2\pi}\sqrt{\frac{\lambda}{ar_o}}\sqrt{\frac{1}{1+(\frac{d_f + d_r}{2a})^2}} \tag{2-29}$$

Figure 2-10 shows the kinematic frequency of a free wheelset as a function of forward speed with the conicity as a parameter on the plot. Figure 2-11 shows an equivalent plot for a rigid truck. For the same conicity, the truck always has a lower kinematic frequency than the wheelset.

2.4 Computer Program Development

The models presented contain many components connected together and therefore a large number of degrees of freedom. This results in large systems of equations to solve and large amounts of data to interpret. To enable the analyst to consider a subset of a consist and thereby reduce the number of degrees of freedom in the model, a number of different computer programs have been developed [6]. These programs written in FORTRAN, are based on two different models. In Model I, the arrangement of the car bodies and trucks is such that it resembles a subset of a consist (The end connection is represented by that shown in Figure 2-2 without car body i-1). This subset contains a maximum of five bodies connected together and the end trucks are essentially the shared trucks between two adjacent bodies. In Model II (Figure 2-1), each truck is shared by contiguous vehicles except at the ends of the train, where the truck is placed under the car body and connected to it by conventional means. This is through a lateral yaw, and roll suspension connection located in the transverse plane of the cg of the truck frame. Table 2-1 shows typical degrees of freedom for a Model II-based 10 car articulated train set. The total DOFs for n articulated vehicles are 9n +8 *i.e.* 98 degrees of freedom (DOFs) for a 10 articulated-vehicle train set.

Table 2-1. DOFs of 10 Articulated Vehicle Model for the Lateral Stability.

Symbols	Definition of DOFs	Specification
$Y_{1+7(i-1)}$	1st wheelset lateral disp.	for i^{th} truck
$Y_{2+7(i-1)}$	1st wheelset yaw disp.	
$Y_{3+7(i-1)}$	2nd wheelset lateral disp.	
$Y_{4+7(i-1)}$	2nd wheelset yaw disp.	
$Y_{5+7(i-1)}$	i^{th} truck frame lateral disp.	
$Y_{6+7(i-1)}$	i^{th} truck frame yaw angle.	
$Y_{7+7(i-1)}$	i^{th} truck frame roll angle	i=1, 2, ..., 11
Y_{78} --Y_{88}	lateral disp. of 1st to 11^{th} joint	for articulated joints
Y_{89} --Y_{98}	roll disp. of 1st to 10^{th} car body	for car body motion

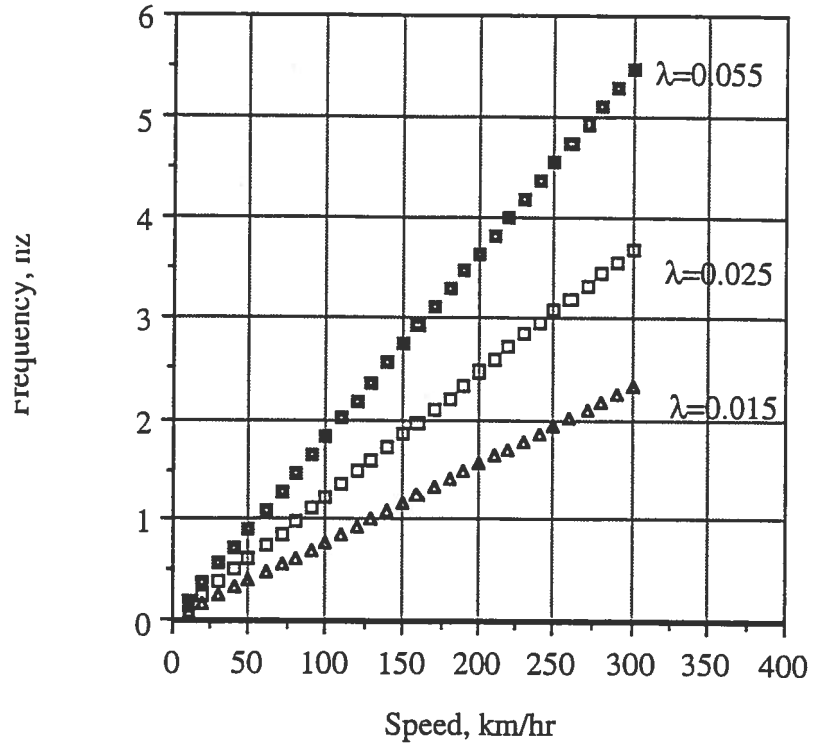

Figure 2-10. Kinematic Frequency of Wheelset Versus Forward Speed.

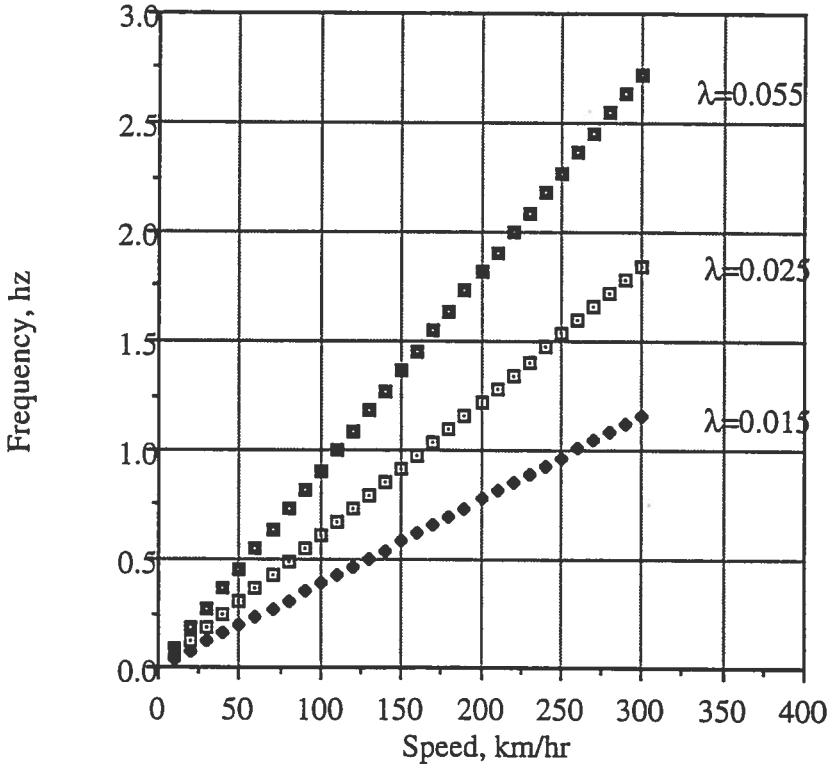

Figure 2-11. Kinematic Frequency of Free Truck Versus Forward Speed.

2.5 Results

To investigate the stability of an articulated train set, a typical set of representative parameters was developed. This parameter set represents a hypothetical train set and was chosen to provide a critical speed of approximately 300 km/hr for a ten car consist with conventional truck configurations at the ends. Some of the sources for these data are given in [1] and the data are presented in Table 2-2. Models such as those presented here require large quantities of input data, not all of which is readily available in the literature. Therefore a number of parameters had to be estimated or guessed.

The above parameter set was used as a baseline parameter set to investigate articulated vehicle stability behavior. All the vehicles in the consist were assumed to have identical suspension characteristics and were assumed to be perfectly symmetrical about the longitudinal axis. Only Model II was used in the study. The results shown in the figures and discussed in the text are for the ten car consist only.

The stability characteristics of an articulated train set differs considerably from that of a single vehicle. With the number of elements connected together through kinematic constraints, there is the possibility of numerous modes of instability. The presence and characteristics of these modes depends primarily on the suspension parameters, the wheel/rail geometry parameters, and the masses and inertia's of the interconnected elements. Hence, a different combination of data could give different results. An exhaustive study of the influence of all vehicle parameters on stability was beyond the scope of this study. Our parameter study focused on a select group of suspension, geometry, and inertial parameters.

The following aspects were investigated: a) Typical modes of instability or the nature of the eigen solution for the nominal vehicle; b) The influence of suspension parameters on critical speed; c) the influence of wheel tread conicity on critical speed; d) the influence of wheelset and truck frame mass on critical speed, and e) the influence of consist length and arrangement on critical speed.

The results obtained are discussed below.

Table 2-2. Baseline Parameters for a Ten Vehicle Consist.

Symbol	Value	Unit
m_c	25000	Kg
m_t	5000	Kg
m_w	2000	Kg
mJ	250	Kg
I_{cx}	5.625×10^5	kg. m^2
I_{cz}	6.625×10^5	kg. m^2
I_{tx}	1740	kg. m^2
I_{tz}	7630	kg. m^2
I_{wx}	1500	kg. m^2
I_{wy}	140	kg. m^2
I_{wz}	1500	kg. m^2
k_{sz}	2.936×10^6	N/m
Csz	3.930×10^4	N.m.s/rad
k_{px}	6.800×10^6	N/m
k_{py}	3.920×10^6	N/m
k_{pz}	5.756×10^5	N/m
C_{px}	2.500×10^4	N.s/m
C_{py}	2.500×10^4	N.s/m

Symbol	Value	Unit
k_{cz}	0.0	N.m/rad
C_{jtf}	2.40×10^5	N.m.s/rad
C_{jtm}	2.40×10^5	N.m.s/rad
C_{cx}	0.0	N.m.s/rad
C_{cz}	0.0	N.m.s/rad
f_{11}	6.550×10^6	N/wheel
f_{12}	2.396×10^4	N.m/wheel
f_{22}	0.0	$N.m^2$/wheel
f_{33}	8.150×10^6	N/wheel
λ	0.025	
Δ	0.025	
Γ	0.025	
δ_0	0.0	
W_A	1.5×10^5 (8.7510^4)	N/wheel
a	0.7175	m
b	0.95	m
p	0.95	m
S_f	10.8 (8.75)	m

Table 2-2. contd. Baseline Parameters for a Ten Vehicle Consist.

C_{pz}	3.920×10^4	N.s/m
K_{sy}	3.570×10^5	N/m
C_{sy}	7.845×10^4	N.s/m
k_{jtf}	1.760×10^5	N.m/rad
k_{jtm}	1.760×10^5	N.m/rad
K_{cx}	0.0	N.m/rad
C_{srf}	0.0	N.S/m
C_{srr}	0.0	N.S/m
r_o	0.45	m

S_r	10.8 (8.75)	m
d_f	1.25	m
d_r	1.25	m
h_3	0.365	m
h_4	0.365	m
h_f, h_r	0.36	m
c_f, c_r	0.36	m
T_f, T_r	5.00	m
a_{tf}, a_{tr}	1.25	m

2.5.1. Nature Of The Eigen Solution

The parameters presented in Table 2-2, give a critical speed of 311 km/hr for the ten vehicle consist. The natural frequency of the least damped mode at this speed is 1.567 Hz. This is well below the wheelset kinematic frequency (3.83 Hz) but closer to the truck kinematic frequency (1.9 Hz). The least damped or unstable mode obtained here resembles the car body hunting mode seen in conventional vehicles. The eigenvector is characterized by large lateral motions of the wheelsets, truck frames, and the articulation joints. The eigenvector consists of a magnitude and a phase. The largest element is normalized to a magnitude of one and a phase of zero. All other elements are referenced to the largest element. Since the number of elements is large, a graphical representation of select components of the eigenvector is presented in Figure 2-12. Only linear displacements are plotted. The y-location of each of the elements in the plot is obtained by multiplying the magnitude of the element by the cosine of its phase angle. Hence, the largest element, in this case the tenth truck, is located at y=1. In the front of the train set, the wheelsets, trucks and car body move in-phase. The middle portion shows out-of-phase motions between the trucks and the articulation joints with in-phase motions again at the rear of the train set. The wheelsets follow closely the behavior of the trucks. Though not obvious in Figure 2-12, the elements of the eigenvector show that the magnitude of wheelset, truck and joint motions grow progressively as one approaches the rear of the consist except for the motion of the last truck. The largest motions for the joints occur at the rear end of the train with the exception of the last articulation joint. The mode shape is affected by a number of parameters including wheel conicity.

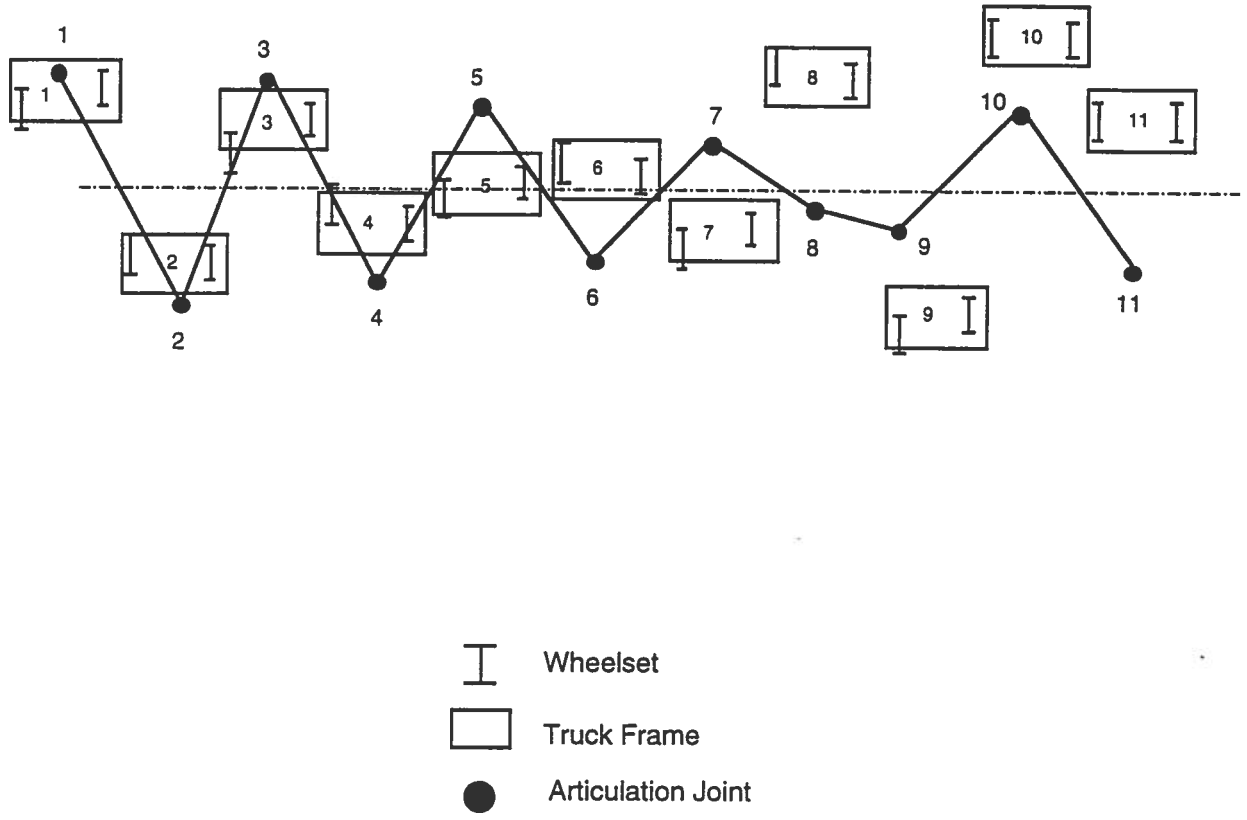

Figure 2-12. Mode Shape for the Least Damped Mode (Nominal Parameters).

2.5.2 Influence of Suspension Parameters

2.5.2.1 Influence Of The Car Body-Truck Connections

The secondary lateral and vertical damping and the secondary yaw stiffness are known to have a significant influence on the stability of a conventional vehicle. In the case of the articulated train models, the secondary suspension elements of interest are the lateral suspension between the articulation joint and the truck, the roll suspension between the car body and the truck and yaw suspensions between the male and female joints and the truck.

Figures 2-13 to 2-16 show the influence of these suspension parameters on the stability of the baseline vehicle. Figure 2-13 shows the influence of the secondary lateral stiffness. A decrease in the nominal lateral stiffness results in a slight increase in critical speed with a maximum value being reached at approximately 2.57e4 N/m, a further decrease leading to a reduction in critical speed. This indicates that an optimum value for the secondary lateral stiffness may exist, the value of which probably depends on the other suspension parameters of the consist. Increase in value past the nominal results in a decrease in critical speed. The influence of lateral damping (Figure 2-14) is more pronounced than that of the stiffness. A decrease in damping increases the critical speed.

The secondary yaw suspension is known to have a strong influence on the stability behavior of conventional vehicles and seems to influence articulated vehicles similarly. Figure 2-15 shows the influence of the secondary yaw stiffness on the critical speed. Increase in yaw stiffness increases the critical speed. Zero stiffness lowers the frequency of the least damped mode but only lowers the critical speed slightly. The yaw dampers also play a strong role in the lateral stability of the articulated train model. Figure 2-16 shows that removal of the yaw dampers reduces the critical speed of the nominal vehicle but an increase in yaw damping increases the critical speed to a point past which the speed starts to decrease. This again indicates an optimum value for the damping that may depend on suspension parameters of the consist. For the case where both the stiffness

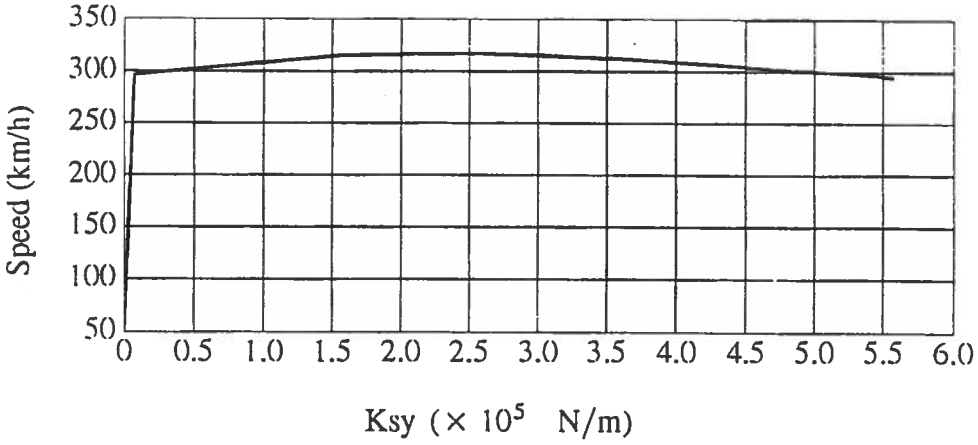

Figure 2-13. Critical Speed Versus Joint-Truck Lateral Stiffness.

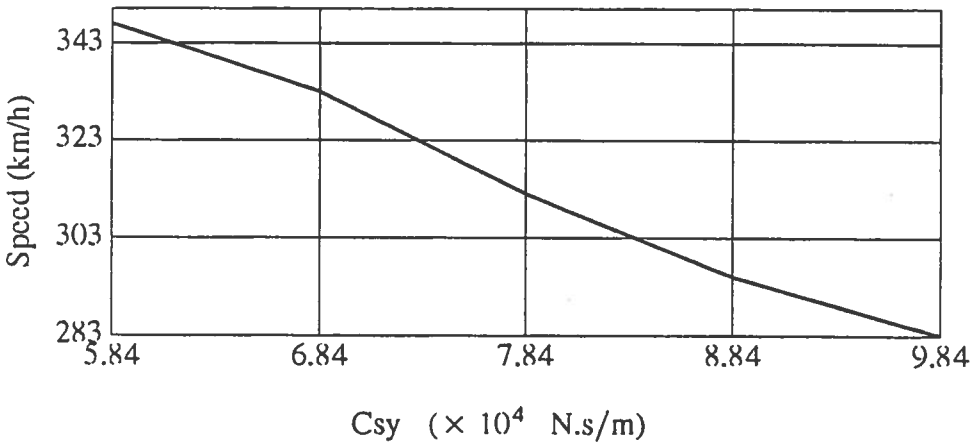

Figure 2-14. Critical Speed Versus Joint-to-Truck Lateral Damping.

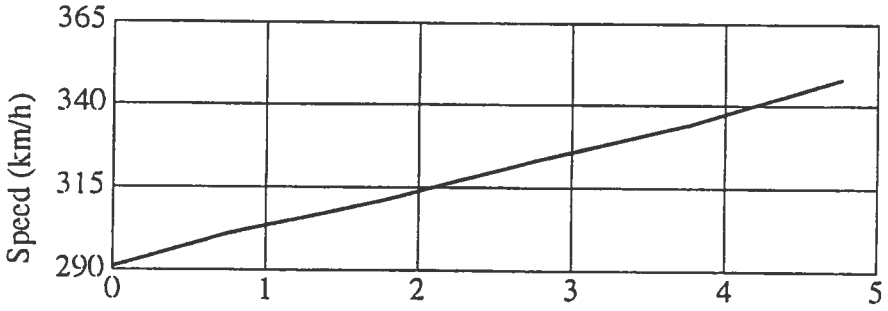

Figure 2-15. Critical Speed Versus Car-to-Truck Yaw Stiffness.

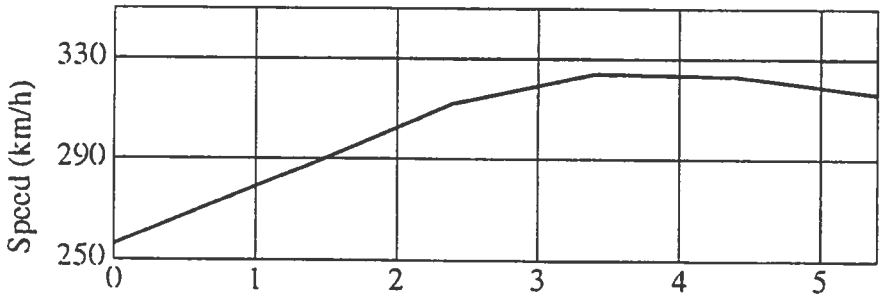

Figure 2-16. Critical Speed Versus Car-to-Truck Yaw Damping.

damping were removed from the model is not shown here. However the influence on critical speed is more pronounced with the removal of the damping playing a bigger role. The critical speed in this case is 241 km/hr as opposed to 291 km/hr for the zero stiffness and 256 km/hr for the zero damping case.

2.5.2.2 Influence Of The Inter-Car Connection -- Yaw And Roll Dampers

Some articulated passenger train sets have inter-body connections to reduce inter-car roll and yaw. The inter-car roll and yaw damping and stiffness between two consecutive car bodies have some influence on the lateral stability. Results are shown in Figures 2-17 and 2-18. Increasing the yaw stiffness has an adverse affect on system stability. Yaw damping has the opposite effect with an increase in yaw damping increasing the critical speed. An increase in the yaw damping adversely affects the critical speed. The influence of inter-car roll damping is minimal.

2.5.3 Influence of Sprung and Unsprung Mass

The unsprung mass has a strong influence on the lateral stability of the consist. Reducing the weight of wheelset from 2000 kg to 1000 kg increases the critical speed significantly. For the ten car consist, this results in an increase in speed from 310 km/hr to about 378 km/hr. Similarly, reducing the weight of the truck frame increases the critical speed .

2.5.4 Influence Of Conicity

Figure 2-19 shows the effect of conicity on critical speed. As expected, the equivalent conicity strongly affects the lateral stability. For conventional vehicles it is well known that in general, decreasing conicity increases bogie hunting stability, with the speed versus conicity curves typically approximating quadratic hyperbolae, and with maximum achievable critical velocities occurring at the lowest conicities. The body hunting modes are similarly affected by decreasing conicity with the accompanying effect that more damping is needed to control body hunting at lower conicities. However, it has been found for steered vehicles that this is not necessarily the

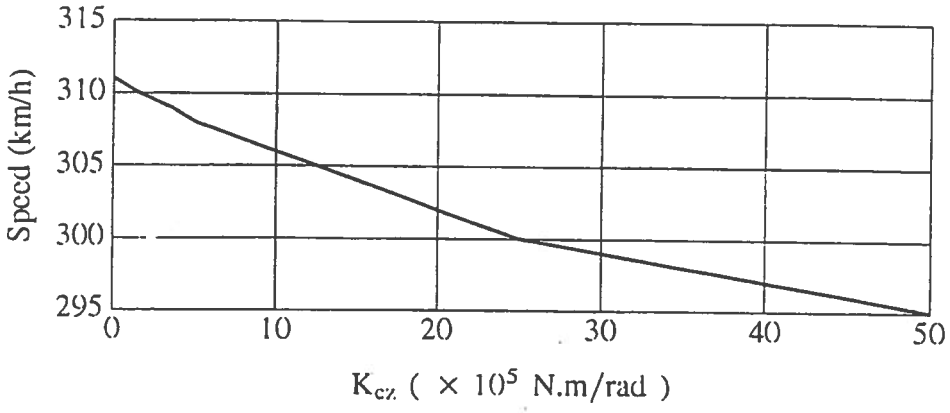

Figure 2-17. Critical Speed Versus Car-to-Car Roll Stiffness.

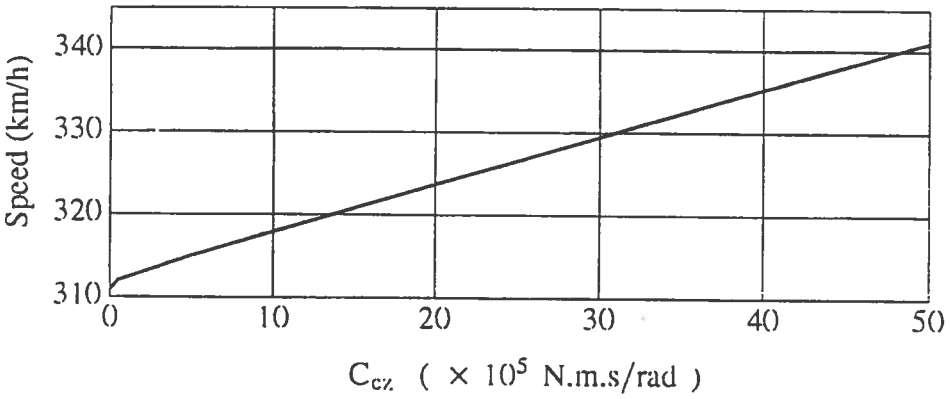

Figure 2-18. Critical Speed Versus Car-to-Car Yaw Damping.

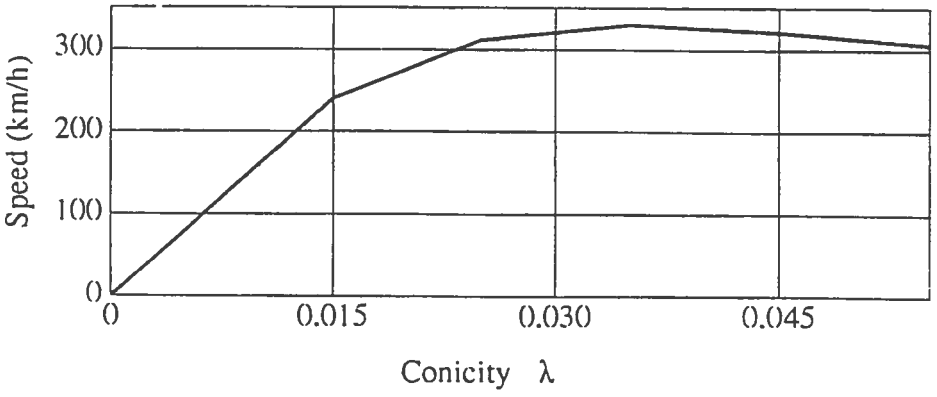

Figure 2-19. Critical Speed Versus Conicity.

case [10]. Steered axle trucks can exhibit low conicity instabilities, *i.e.* areas of instabilities at the low conicity end of the spectrum. This has been termed in the literature as the "Weinstock Effect" [10].

During the course of this study, it was found that articulated vehicles may share similar characteristics. Lower conicities below the nominal value result in lower critical speeds. The critical speed is higher above the nominal value, increasing with conicity until a value of 0.035. Above this value, the critical speed decreases. Table 2-3 shows some of the results. An inspection of the eigenvectors shows that at the low conicities, the consist executes a wave-like motion with the small motions occurring at the front and the larger motions occurring at the end of the train. Again, the eigenvector is dominated by the lateral motions of the components with very small angular motions. The mode shape showing this eigenvector is given in Figure 2-20 and is plotted the same way as described earlier. The modal behavior is similar to the car body hunting modes seen in conventional vehicles. Increasing conicity results in large truck lateral motions as the modal frequency gets closer to the free truck hunting frequency. At and past conicities of 0.045, the modal frequency coincides with the free truck kinematic frequency resulting in fully developed truck hunting for one truck in the consist. In this type of mode, the motion is dominated by large wheelset and truck lateral and yaw motions and smaller articulation joint motions at the 11th truck. All other motions are very small. This eigenvector is shown in Figure 2-21.

2.5.5 Influence Of Primary Suspension

Variations in the parameter values of lateral stiffness and damping in the primary and secondary suspensions affect the lateral stability of the consist. Figures 2-22 and 2-23 show the influence of the primary suspension parameters on the critical speed. The lateral primary suspension, for the nominal parameters chosen for this model, has an influence on vehicle behavior that has been known previously. There exists, for this set of parameters, a range of optimum values of the primary lateral stiffness, below and above which the critical speed of the

Table 2-3. Influence of Conicity on Stability

Conicity	0.015	0.025	0.035	0.045	0.055
Critical Speed	240 km/hr	311 km/hr	330 km/hr	321 km/hr	306 km/hr
Largest Element of Eigenvector	Lateral of 10th Articulation Joint	Lateral of 10th Truck Frame	Lateral of 9th Truck Frame	Front Wheelset Lateral of 11th Truck Frame	Front Wheelset Lateral of 11th Truck Frame
Natural Frequency of Least Damped Mode	1.02 Hz	1.57 Hz	1.92 Hz	2.46 Hz	2.67 Hz

consist is lowered (Figure 2-22). The influence of the primary lateral damping as well as the longitudinal stiffness and damping is shown in Figures 2-23 to 2-25.

2.5.6 Influence of Number of Cars in Consist

The influence of the number of car bodies in the consist on the lateral stability of the consist was studied using the five car and ten car versions of Model II. It was observed that the critical speeds of the two consists were almost the same at any given conicity. Thus the influence of the number of cars was found to be negligible indicating that it may be possible to study these consists using lower order models. Other studies conducted to study the influence of combinations of conventional and articulated vehicles connected together showed that the arangement of the cars in the consist can have a significant affect on consist stability. This needs to be explored further.

2.6 Summary

This chapter has discussed the development of computer models for predicting the lateral stability of articulated vehicles. A number of different models pertaining to different number of bodies in the consist and different truck arrangements were developed. A set of parameters representing a baseline consist consisting of ten cars and giving a critical speed of approximately 310 km/hr were also assembled. Parameter studies were conducted mainly to assess the influence of car-to-car and car-to-truck suspension parameters on consist stability. The studies show the results of the model are sensitive to the parameter values chosen. In addition, for the parameters chosen here, optimum values of suspension characteristics exist that produce the highest critical speeds. It is especially noted that consist stability is sensitive to the yaw damping between the trucks and the car body, the conicity of the wheel profile, and the primary suspension. For the parameters chosen, this arrangement of ten cars in a consist exhibited low conicity instabilities similar to those seen in steered trucks. This behavior may be parameter dependent and should be looked at further. Results were found to be fairly insensitive to the inter-body yaw and roll connections.

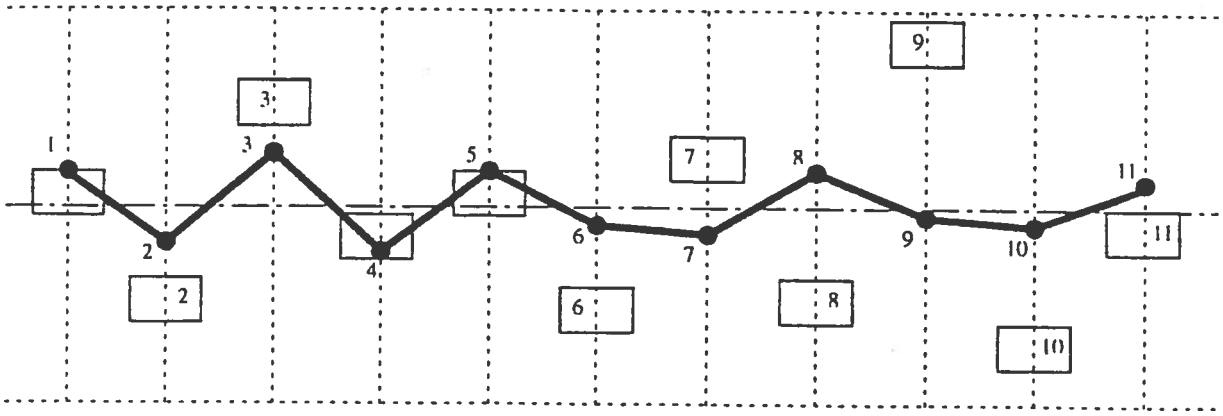

Figure 2-20. Mode Shape for the Least Damped Mode (Conicity=0.055).

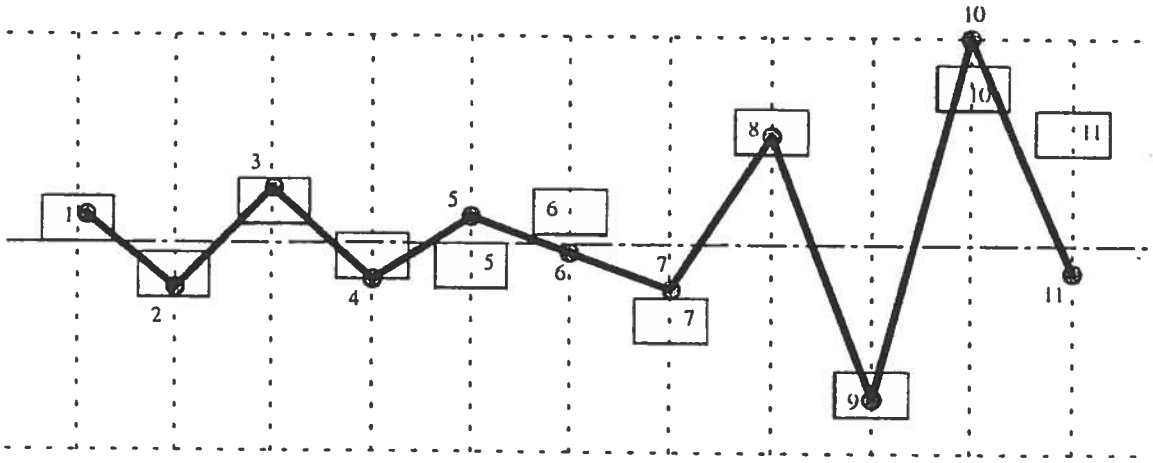

Figure 2-21. Mode Shape for the Least Damped Mode (Conicity=0.015).

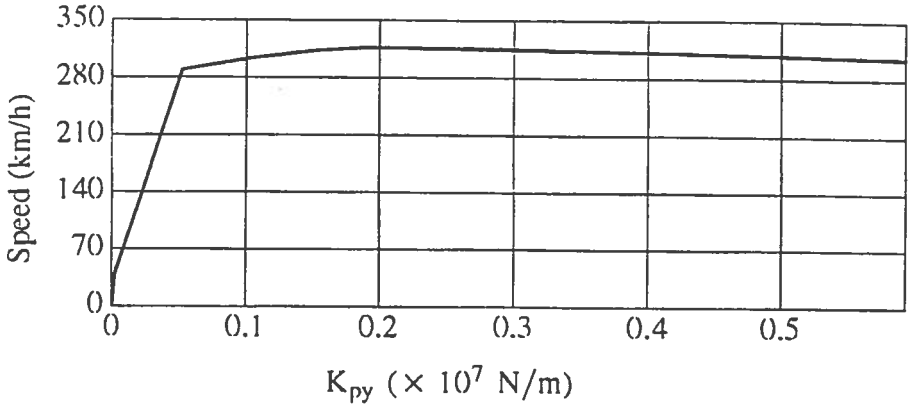

Figure 2-22. Critical Speed Versus Lateral Primary Stiffness.

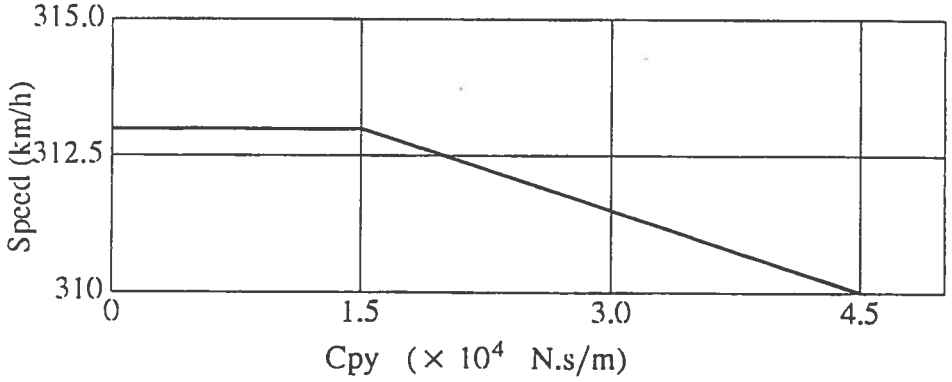

Figure 2-23. Critical Speed Versus Lateral Primary Damping.

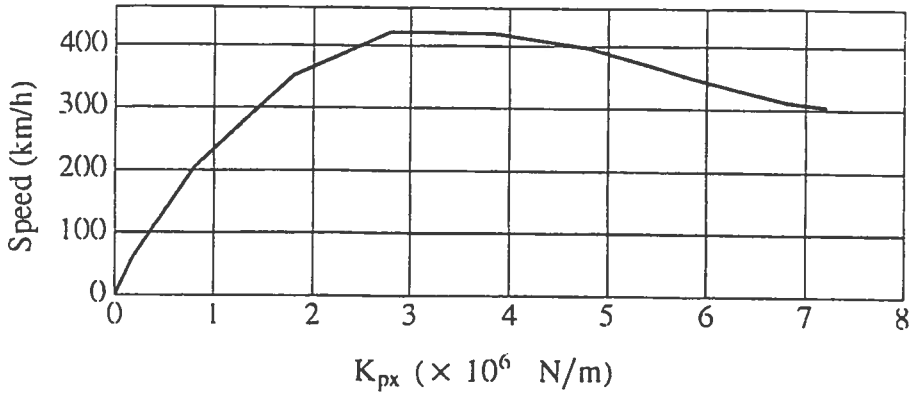

Figure 2-24. Critical Speed Versus Longitudinal Primary Stiffness.

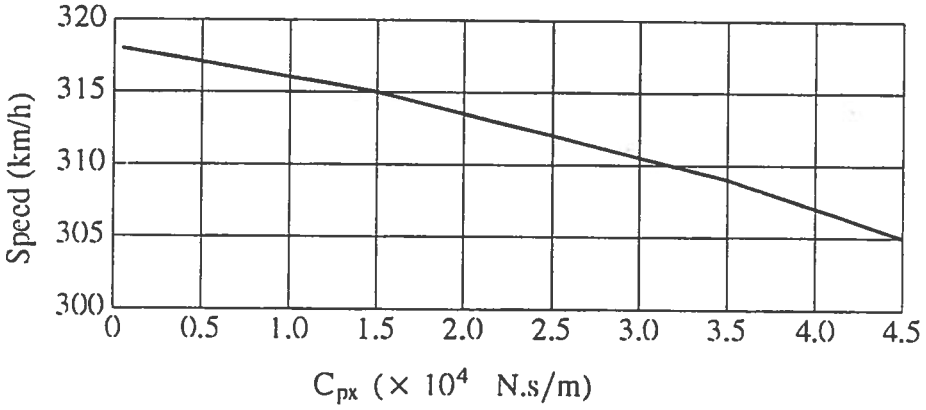

Figure 2-25. Critical Speed Versus Longitudinal Primary Damping.

3.0. VERTICAL RESPONSE OF ARTICULATED TRAIN SETS

3.1. Introduction

This chapter describes the development of a vertical forced response model of an articulated-vehicle train set to discrete and randomly distributed vertical track alignment irregularities. The response of the train set model to random track inputs is also presented. The model is capable of handling 2,3,4,5, and 10 car bodies coupled together. It has a conventional truck arrangement at the front and rear of the consist and shared trucks in the middle. The results presented are only for the vertical dynamic performance of the consist to randomly distributed rail irregularities. The computer programs pertaining to this model are described in [6].

3.2.Vertical Forced Response Model Development

3.2.1 Description Of Vertical Forced Response Model

The model for pitch and bounce motions of an articulated-vehicle train set has an identical arrangement of elements to that for the lateral stability model discussed earlier. Schematics of this model, showing the geometry of the configuration have been shown in Figures 2-1 and 2-2. The generalized coordinates considered in the model are:

1. Bounce and pitch motions of each truck frame.

2. The vertical motions of each articulation joint.

The articulation joint is modeled as a purely kinematic constraint. The joint permits relative pitching motions between the car bodies, but constrains the bounce and pitch motions of the cars. The suspension elements considered are:

1. Vertical primary suspensions between the wheelsets and the trucks. Each element is modeled as a spring and damper in parallel.
2. Vertical secondary suspensions between the car body and the truck frame. Also included are vertical secondary suspensions between the articulation joints and the trucks.

It is assumed that the wheelsets stay in contact with and move along the track. Therefore wheelset motions are the same as track vertical motions. Wheel bounce is not considered. The kinematic quantities are assumed to be small and all suspension elements are assumed to have linear characteristics.

The mathematical model has 3(n+1) degrees of freedom and consists of n articulated vehicles and n+1 trucks. The inputs to the model are the vertical track displacements. The variables z_j, z_t, and Φ_t represent the vertical displacement of the articulation joint, the vertical displacement of the center of gravity of a truck, and the angular displacement of the truck respectively.

3.2.2 Car Body Equations

The relationship between the vertical coordinates of joints and the vertical and pitch motions of the i^{th} car body cg is given by :

$$\ddot{z}_{cgi} = \frac{S_{ri}}{S_{ri}+S_{fi}}(\ddot{z}_{ji} - \ddot{z}_{ji+1}) + \ddot{z}_{ji+1}$$

$$\ddot{\Phi}_i = \frac{\ddot{z}_{ji} - \ddot{z}_{ji+1}}{S_{ri}+S_{fi}} \qquad (3\text{-}1)$$

$$L_i = S_{ri} + S_{fi}$$

and that for the i-1 car body by:

$$\ddot{z}_{cgi-1} = \frac{S_{ri-1}}{S_{ri-1} + S_{fi-1}}(\ddot{z}_{ji-1} - \ddot{z}_{ji}) + \ddot{z}_{ji}$$
$$\ddot{\Phi}_{i-1} = \frac{\ddot{z}_{ji-1} - \ddot{z}_{ji}}{S_{ri-1} + S_{fi-1}} \qquad (3\text{-}2)$$
$$L_{i-1} = S_{ri-1} + S_{fi-1}$$

Thus, the motions of each car body, consisting of translation and rotation of the center of gravity, can be replaced by the vertical displacements of articulated joints on both sides. Applying Lagrange's form of D'Alembert's Principle:

$$\sum_{i=1}^{n}(\vec{F}_i - m_i\vec{a}_i) \bullet \frac{\partial \vec{R}_i}{\partial q_j} + \sum_{i=1}^{m}(\vec{M}_i - \dot{\vec{H}}_i) \bullet \frac{\partial \vec{\omega}_i}{\partial \dot{q}_j} = 0$$
$$j = 1..k$$

(3-3)

one can find the equations of motion associated with the generalized coordinate z_{ji}.

The generalized inertia force associated with the ith car body and the coordinate z_{ji} is:

$$Q_{z_i}{}^{*} = \frac{S_{ri} m_{Ci}}{S_{ri} + S_{fi}}\left[\frac{S_{ri}}{S_{ri} + S_{fi}}(\ddot{z}_{ji} - \ddot{z}_{ji+1}) + \ddot{z}_{ji+1}\right] - \frac{I_{CYi}}{(S_{ri} + S_{fi})^2}(\ddot{z}_{ji} - \ddot{z}_{ji+1})$$

(3-4)

and that associated with the i-1 car body and the coordinate z_{ji} is

$$Q_{z_{i-1}}{}^{*} = \frac{S_{ri-1} m_{Ci-1}}{S_{ri-1} + S_{fi-1}} \left[\frac{S_{ri-1}}{S_{ri-1} + S_{fi-1}} (\ddot{z}_{ji-1} - \ddot{z}_{ji}) + \ddot{z}_{ji} \right] - \frac{I_{CYi-1}}{(S_{ri-1} + S_{fi-1})^2} (\ddot{z}_{ji-1} - \ddot{z}_{ji})$$

(3-5)

Hence the net generalized inertia force associated with the generalized coordinate z_{ji} is:

$$Q^{*}{}_{ToT_{z_i}} = Q^{*}{}_{z_i} + Q^{*}{}_{z_{i-1}} \tag{3-6}$$

The free-body diagram in Figure 3-1 shows the external forces and moments acting on the i-1, i and i+1 bodies. The internal forces and moments are neglected as they do no work. The generalized force associated with the i[th] body and the generalized coordinate z_{ji} is

$$\begin{aligned} Q_{z_i} = {} & \frac{F_{ri} S_{ri}}{S_{ri} + S_{fi}} + \frac{F_{fi+1} S_{ri}}{S_{ri} + S_{fi}} - \frac{F_{fi+1} c_{ri}}{S_{ri} + S_{fi}} + \frac{F_{ri} c_{fi}}{S_{ri} + S_{fi}} + F_{si} \\ & - \frac{F_{ri} c_{fi-1}}{S_{ri-1} + S_{fi-1}} + \frac{M_{ci}}{S_{ri} + S_{fi}} + \frac{M_{ci+1}}{S_{ri} + S_{fi}} + \frac{M_{ci}}{S_{ri-1} + S_{fi-1}} - \frac{M_{ci-1}}{S_{ri-1} + S_{fi-1}} \end{aligned} \tag{3-7}$$

where:

Forces

$$\begin{aligned} F_{si} &= k_{si}(z_{cgi} + S_{fi}\Phi_i - z_{ti}) + C_{si}(\dot{z}_{cgi} + S_{fi}\dot{\Phi}_i - \dot{z}_{ti}) \\ F_{ri} &= 2 * k_{szri}(z_{cgi} + c_{fi}\Phi_i - z_{ti} + a_{tri}\Phi_{ti}) \\ &\quad + 2 * Csz_{ri}(\dot{z}_{cgi} + c_{fi}\dot{\Phi}_i - \dot{z}_{ti} + a_{tri}\dot{\Phi}_{ti}) \\ F_{fi+1} &= 2 * k_{szfi+1}(z_{cgi} - c_{ri}\Phi_i - z_{ti+1} - a_{tf\,i+1}\Phi_{ti+1}) + \\ &\quad 2 * C_{szfi}(\dot{z}_{cgi} - c_{ri}\dot{\Phi}_i - \dot{z}_{ti+1} + a_{tf\,i+1}\dot{\Phi}_{ti+1}) \\ F_{si+1} &= k_{si+1}(z_{cgi} - S_{ri}\Phi_i - z_{ti+1}) + C_{si}(\dot{z}_{cgi} - S_{ri}\dot{\Phi}_i - \dot{z}_{ti+1}) \end{aligned}$$

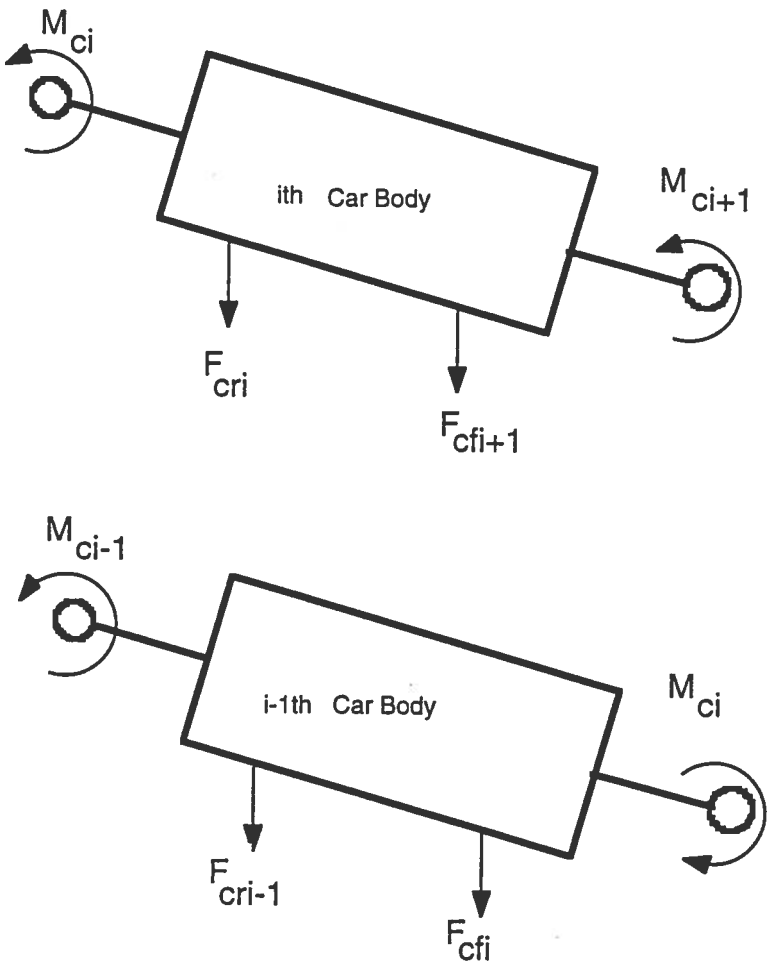

a) Car Bodies 1 and i-1

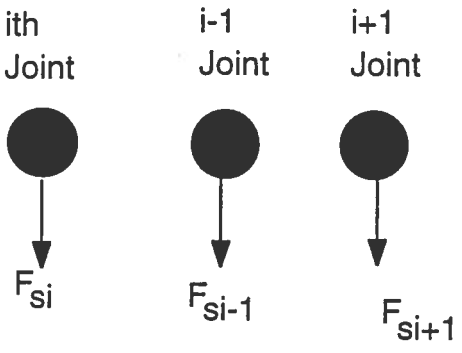

b) Articulation Joints

Figure 3-1. Free-body Diagrams of Car bodies and Articulation Joints Showing Working Forces and Moments.

Moments

$$M_{ci} = k_{cyi}(\Phi_i - \Phi_{i-1}) + C_{cyi}(\dot{\Phi}_i - \dot{\Phi}_{i-1})$$
$$M_{ci+1} = k_{cyi+1}(\Phi_i - \Phi_{i+1}) + C_{cyi+1}(\dot{\Phi}_i - \dot{\Phi}_{i+1}) \quad (3\text{-}8)$$
$$M_{ci-1} = k_{cyi-1}(\Phi_{i-1} - \Phi_{i-2}) + C_{cyi-1}(\dot{\Phi}_{i-1} - \dot{\Phi}_{i-2})$$

The equations of motion pertaining to the generalized coordinate z_{ji} can now be easily obtained.These are:

$$\frac{S_{ri}m_{Ci}}{S_{ri}+S_{fi}}\left[\frac{S_{ri}}{S_{ri}+S_{fi}}(\ddot{z}_{ji}-\ddot{z}_{ji+1})+\ddot{z}_{ji+1}\right]-\frac{I_{CYi}}{(S_{ri}+S_{fi})^2}(\ddot{z}_{ji}-\ddot{z}_{ji+1})$$
$$+\frac{S_{ri-1}m_{Ci-1}}{S_{ri-1}+S_{fi-1}}\left[\frac{S_{ri-1}}{S_{ri-1}+S_{fi-1}}(\ddot{z}_{ji-1}-\ddot{z}_{ji})+\ddot{z}_{ji}\right]-\frac{I_{CYi-1}}{(S_{ri-1}+S_{fi-1})^2}(\ddot{z}_{ji-1}-\ddot{z}_{ji})$$
$$=\frac{F_{ri}S_{ri}}{S_{ri}+S_{fi}}+\frac{F_{fi+1}S_{ri}}{S_{ri}+S_{fi}}-\frac{F_{fi+1}c_{ri}}{S_{ri}+S_{fi}}+\frac{F_{ri}c_{fi}}{S_{ri}+S_{fi}}+F_{si} \quad (3.9)$$
$$-\frac{F_{ri}c_{fi-1}}{S_{ri-1}+S_{fi-1}}+\frac{M_{ci}}{S_{ri}+S_{fi}}+\frac{M_{ci+1}}{S_{ri}+S_{fi}}+\frac{M_{ci}}{S_{ri-1}+S_{fi-1}}-\frac{M_{ci-1}}{S_{ri-1}+S_{fi-1}}$$

3.2.3 Truck Equations

The free-body diagram of the ith truck is shown in Figure 3-2. The forces applied to truck i arise from the primary suspension, the secondary suspension, and the suspension between the articulation joint and the truck. The equations of motion for truck in bounce and pitch are:

$$m_{ti}\ddot{z}_{ti} = F_{si} + F_{fi} + F_{ri} - F_{pzfi} - F_{pzri}$$
$$I_{tyi}\ddot{\Phi}_{ti} = F_{pzri}d_{ri} + F_{fi}a_{tfi} - F_{ri}a_{tri} - F_{pzfi}d_{fi} \quad (3\text{-}10)$$

where

$$
\begin{aligned}
F_{si} &= k_{szi}(z_{ji} - z_{ti}) + C_{szi}(\dot{z}_{ji} - \dot{z}_{ti}) \\
F_{ri} &= k_{szri}(z_{cgi} + c_{fi}\Phi_i - z_{ti} + a_{tr_i}\Phi_{ti}) \\
&\quad + C_{szri}(\dot{z}_{cgi} + c_{fi}\dot{\Phi}_i - \dot{z}_{ti} + a_{tr_i}\dot{\Phi}_{ti}) \\
F_{fi} &= k_{szfi}(z_{cgi-1} - c_{ri-1}\Phi_{i-1} - z_{ti} - a_{tf_i}\Phi_{ti}) \\
&\quad + C_{szfi}(\dot{z}_{cgi-1} - c_{ri-1}\dot{\Phi}_{i-1} - \dot{z}_{ti} + a_{tf_i}\dot{\Phi}_{ti}) \\
F_{pzfi} &= k_{pzfi}(z_{ti} + d_{fi}\Phi_{ti} - z_{fi}) + C_{pzfi}(\dot{z}_{ti} + d_{fi}\dot{\Phi}_{ti} - \dot{z}_{fi}) \\
F_{pzri} &= k_{pzri}(z_{ti} - d_{ri}\Phi_{ti} - z_{ri}) + C_{pzfi}(\dot{z}_{ti} - d_{ri}\dot{\Phi}_{ti} - \dot{z}_{ri})
\end{aligned}
\tag{3-11}
$$

Substituting Equations 3-11 into 3-10 yields the general form of the equations of motion for the truck shown below.

Bounce Equation

$$
\begin{aligned}
m_{ti}\ddot{z}_{ti} &= k_{si}(z_{ji} - z_{ti}) + C_{si}(\dot{z}_{ji} - \dot{z}_{ti}) \\
&\quad + k_{fi}(z_{cgi} - c_{ri}\Phi_i - z_{ti} - atf_i\Phi_{ti}) + C_{fi}(\dot{z}_{cgi} - c_{ri}\dot{\Phi}_i - \dot{z}_{ti} + atf_i\dot{\Phi}_{ti}) \\
&\quad + k_{ri}(z_{cgi} + c_{fi}\Phi_i - z_{ti} + atr_i\Phi_{ti}) + C_{ri}(\dot{z}_{cgi} + c_{fi}\dot{\Phi}_i - \dot{z}_{ti} + atr_i\dot{\Phi}_{ti}) \\
&\quad - k_{pzfi}(z_{ti} + d_{fi}\Phi_{ti} - z_{fi}) + C_{pzfi}(\dot{z}_{ti} + d_{fi}\dot{\Phi}_{ti} - \dot{z}_{fi}) \\
&\quad - k_{pzri}(z_{ti} - d_{ri}\Phi_{ti} - z_{ri}) + C_{pzfi}(\dot{z}_{ti} - d_{ri}\dot{\Phi}_{ti} - \dot{z}_{ri})
\end{aligned}
$$

Pitch Equation

$$
\begin{aligned}
I_{tyi}\ddot{\Phi}_{ti} &= (k_{pzri}(z_{ti} - d_{ri}\Phi_{ti} - z_{ri}) + C_{pzfi}(\dot{z}_{ti} - d_{ri}\dot{\Phi}_{ti} - \dot{z}_{ri}))d_{ri} \\
&\quad + ((k_{fi}(z_{cgi} - c_{ri}\Phi_i - z_{ti} - atf_i\Phi_{ti}) + C_{fi}(\dot{z}_{cgi} - c_{ri}\dot{\Phi}_i - \dot{z}_{ti} + atf_i\dot{\Phi}_{ti}))a_{fi} \\
&\quad - ((k_{ri}(z_{cgi} + c_{fi}\Phi_i - z_{ti} + atr_i\Phi_{ti}) + C_{ri}(\dot{z}_{cgi} + c_{fi}\dot{\Phi}_i - \dot{z}_{ti} + atr_i\dot{\Phi}_{ti}))a_{ri} \\
&\quad - ((k_{pzfi}(z_{ti} + d_{fi}\Phi_{ti} - z_{fi}) + C_{pzfi}(\dot{z}_{ti} + d_{fi}\dot{\Phi}_{ti} - \dot{z}_{fi}))d_{fi}
\end{aligned}
\tag{3-12}
$$

The full model equations are obtained recursively using the above equations.

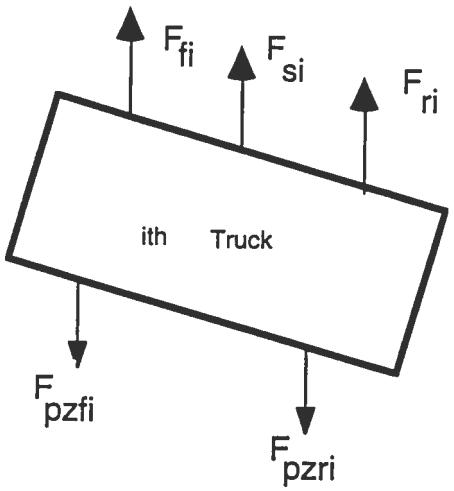

Figure 3-2. Free-body Diagram of the ith Truck

The dynamic behavior of the system can be analyzed in the frequency or the time domain. In the vertical forced response analysis, the inputs to the vehicle are the vertical track alignment irregularities or defects. These irregularities or defects can be described in the form of a power spectral density or a time history. The equations of motion derived for an n-body system can be written in matrix form from Equations (3-9) and (3-12) as:

$$M\ddot{z} + C\dot{z} + Kz = D\dot{z}_d + Ez_d \tag{3-13}$$

Where M, C, and K are mass, damping, and stiffness matrices and $z^T = [z_{j1}, z_{j2}, \ldots, z_{jn+1}, z_{t1}, z_{t2}, \ldots, z_{tn+1}, \Phi_{t1}, \Phi_{t2}, \ldots, \Phi_{tn+1}]$ is the state variable vector, the elements of which are the vertical coordinates of the articulation joints and the vertical and pitch coordinates of the trucks. The matrices D and E are the 3(n+1) x 3(n+1) velocity and displacement input matrices of vertical track irregularities and $z_d^T = [0, 0, \ldots, 0, 0, z_{f1}, z_{r1}, \ldots, z_{f(n+1)}, z_{r(n+1)}]$ is the 3(n+1)x1 input vector which is discussed below in detail.

3.2.4 Model Inputs

The displacements, z_{fi} and z_{ri} from the track and their velocity terms enter into the mathematical model of articulated vehicle train set as the inputs through the primary suspensions. z_{fi} and z_{ri}, represent the vertical displacements of front and rear wheelsets of truck i, and are the average of the vertical displacements of left and right wheels of each wheelset.

The elements of each row of the 3 (n+1) x 1 input matrix, $z_h = D\dot{z}_d + Ez_d$, are given below:

$$
\begin{aligned}
&z_h(i) = 0.0 && \text{i=1 to n+1} \\
&z_h(i) = C_{pfi}\dot{z}_{fi} + K_{pfi}z_{fi} + C_{pri}\dot{z}_{ri} + K_{pri}z_{ri} && \text{i=(n+2) to 2(n+1)} \\
&z_h(i) = \left(C_{pfi}\dot{z}_{fi} + K_{pfi}z_{fi}\right)d_{fi} - \left(C_{pri}\dot{z}_{ri} + K_{pri}z_{ri}\right)d_{ri} && \text{i=(2n+3) to 3(n+1)}
\end{aligned}
\qquad (3\text{-}14)
$$

3.2.4.1 Time Delays and Averaging

Inputs to the model enter the equations through the vertical displacements of the wheel end of the vertical primary suspension. The inputs to the second wheel of the i^{th} truck are assumed to be the same as those seen by the lead wheelset except that there is a time delay present. If the front wheelset of lead truck reaches one of the track points at the time t, the rear one reaches the same point at the time t+ t_r with a time delay t_r. In this case, if $z_{f1}(t) = z_1(V, t)$ where V is the forward speed, then $z_{r1}(t) = z_{f1}(t - t_r)$. The time delays between the i-1 truck and the i^{th} truck can be written as:

$$
\begin{aligned}
t_{fi} &= t_{fi-1} + (d_{fi-1} + S_{fi-1} + S_{ri-1} - d_{fi})/V \\
t_{ri} &= t_{fi} + (d_{fi} + d_{ri})/V
\end{aligned}
\qquad \text{i=2 to 11}
$$

The Laplace Transformation of input vector z can be written as:

$$Z_d(s) = DT(s)Z_f(s) \qquad (3\text{-}15)$$

where:

$$Z(s)=\begin{Bmatrix}0\\0\\.\\.\\0\\Z_{f1}(s)\\Z_{r1}(s)\\.\\.\\Z_{fn+1}(s)\\Z_{m+1}(s)\end{Bmatrix} \qquad DT(s)=\begin{Bmatrix}0\\0\\.\\.\\0\\1\\\exp(-st_{r1})\\.\\.\\\exp(-st_{fn+1})\\\exp(-st_{m+1})\end{Bmatrix}$$

Taking the Laplace transformation on both sides of Equation (3-13) and introducing Equation (3-15), we have:

$$\begin{aligned}Z(s)(Ms^2+Cs+K) &= (Ds+E)Z_d(s)\\ &= (Ds+E)DT(s)Z_{f1}(s)\end{aligned} \tag{3-16}$$

Replacing s with jω where ω is the frequency produces the 3(n+1)x1 complex matrix $[D(j\omega)+E]DT(j\omega)$. This matrix can be expressed by two 3(n+1) x1 real matrices, $Z_dR(\omega)$ and $Z_dI(\omega)$, such that:

$$Z_d(j\omega)=[Z_dR(\omega)+jZ_dI(\omega)]Z_{f1}(j\omega) \tag{3-17}$$

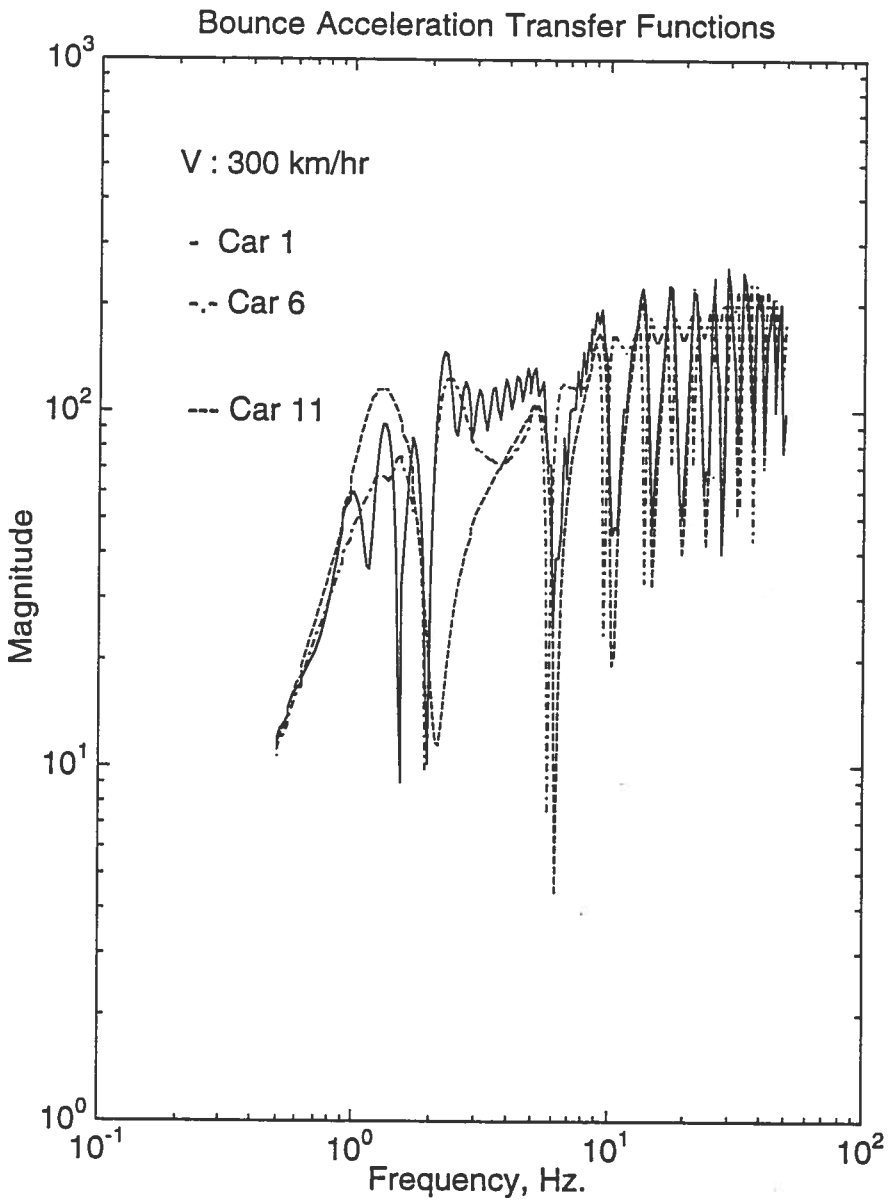

Figure 3-11. Bounce Acceleration Transfer Functions for Cars 1, 6, and 10.

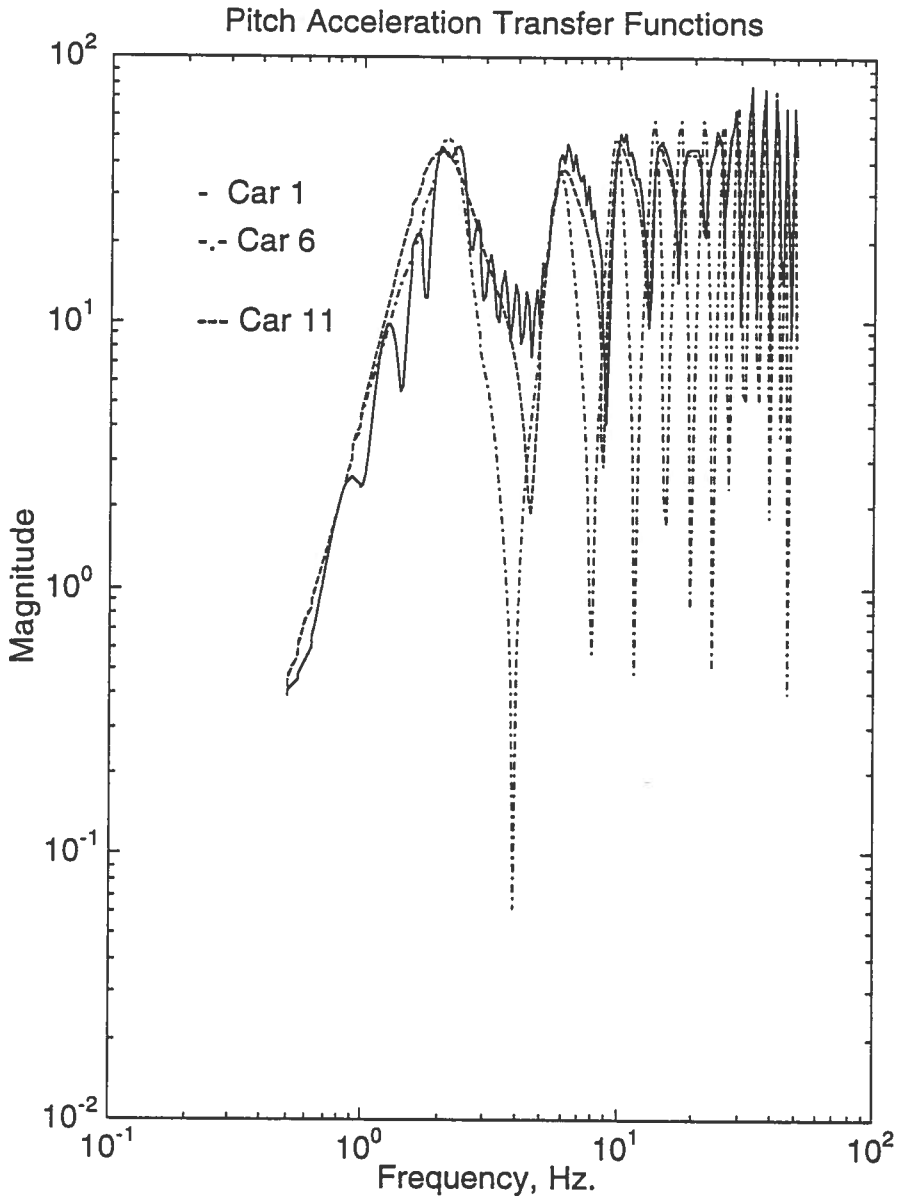

Figure 3-12. Pitch Acceleration Transfer Functions for Cars 1, 6, and 10 (V = 300 km/hr.).

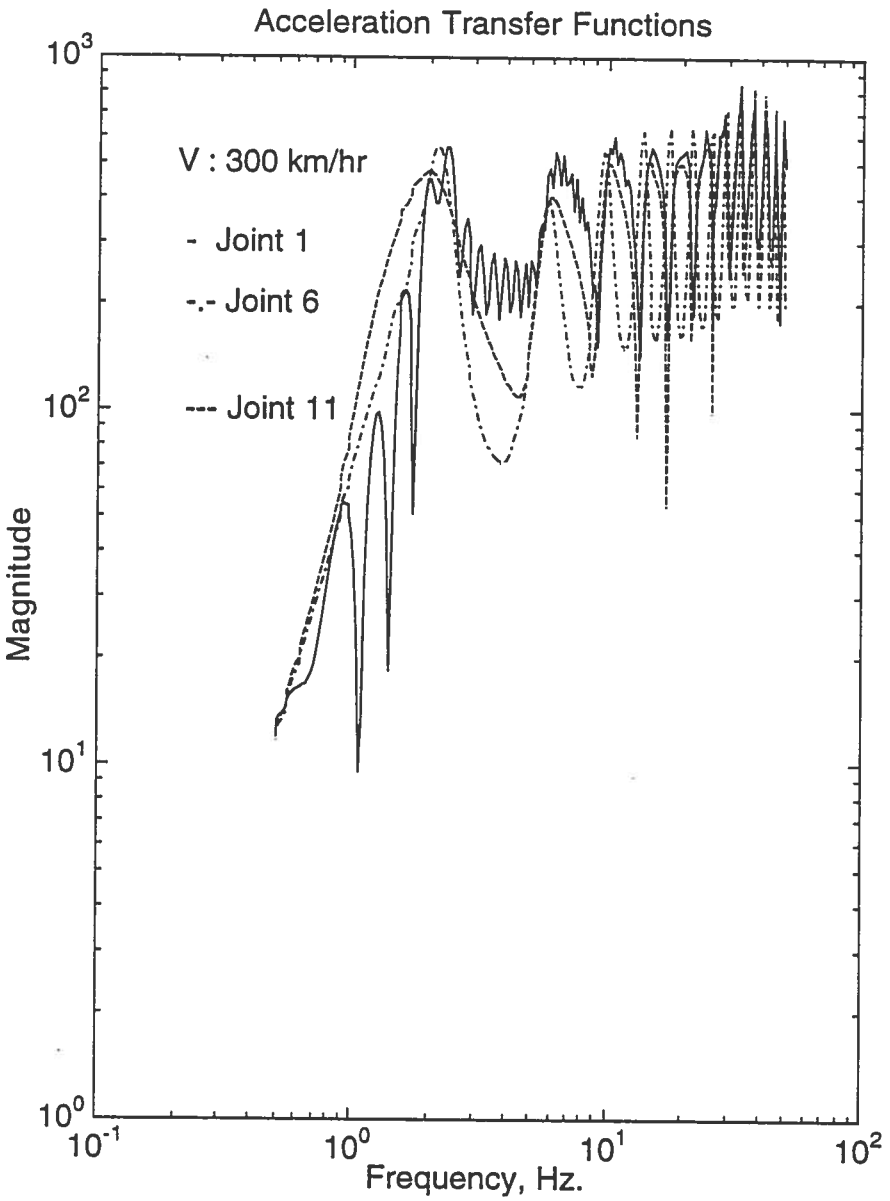

Figure 3-13. Acceleration Transfer Functions for Joints 1, 6, and 11.

The power spectral density (PSD) for a variable is found by multiplying the track input PSD by the square of the transfer function magnitude. A vertical profile PSD for Class 6 track is shown in Figure 3-14 for 300 km/hr. When this is combined with the acceleration transfer functions of Figures 3-11 to 3-13, the PSDs of Figures 3-15 to 3-18 are obtained. Most of the energy is concentrated at the peaks resulting from the system natural frequencies. The acceleration levels generally increase with speed (Figure 3-17) and the movements in dropout frequencies concentrate energy levels at different frequencies. This is especially apparent in going from 280 to 300 km/hr. The change is not as pronounced over the range 300 to 320 km/hr because of the distribution of the modal frequencies at the lower end of the spectrum.

The RMS acceleration levels for the car bodies and Joints 1, 6, and 11 calculated over the frequency range of 0-50 Hz. are shown in Figures 3-19 to 3-21. The plots show an increase in RMS acceleration with speed as well as with location in the consist. The response at the end of the consist is the largest. For ride quality evaluation, the acceleration levels in the car body are of the greatest concern. For this purpose, RMS acceleration levels in gs computed in the one-third octave bands are shown in Figures 3-22 and 3-23. These are for locations at the cg and the front and rear joints for Cars 1, and 10. The joint positions correspond to positions fore and aft for the car body considered. The acceleration values are plotted against ISO reduced comfort level boundaries for a 1 hour exposure[9]. The concentration of energy at the natural frequencies is apparent from the plots and for the joint locations, the values exceed the comfort level limits.

Figures 3-24 and 3-25 show the same plots but with vertical damping and stiffness reduced by an order of magnitude. The influence of this change is to shift the larger response to the higher frequency levels.

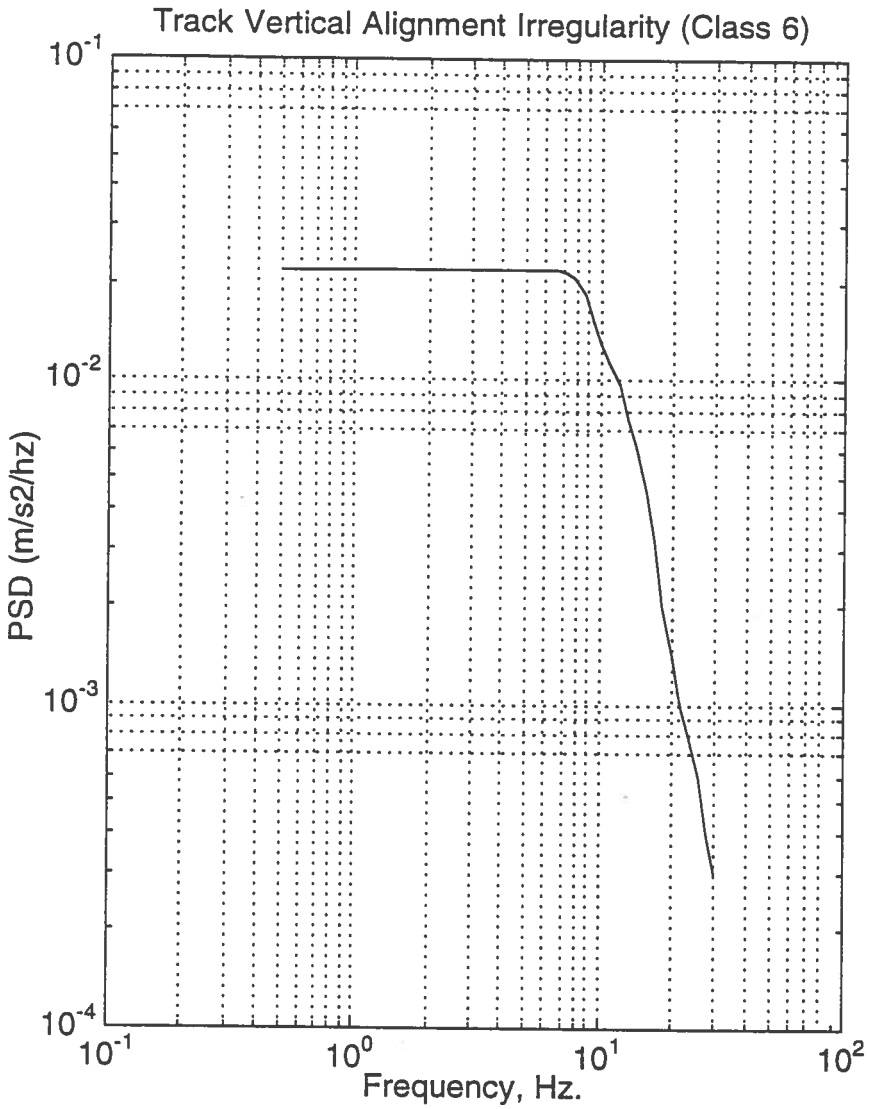

Figure 3-14. PSD for Class 6 Track at 300 km/hr.

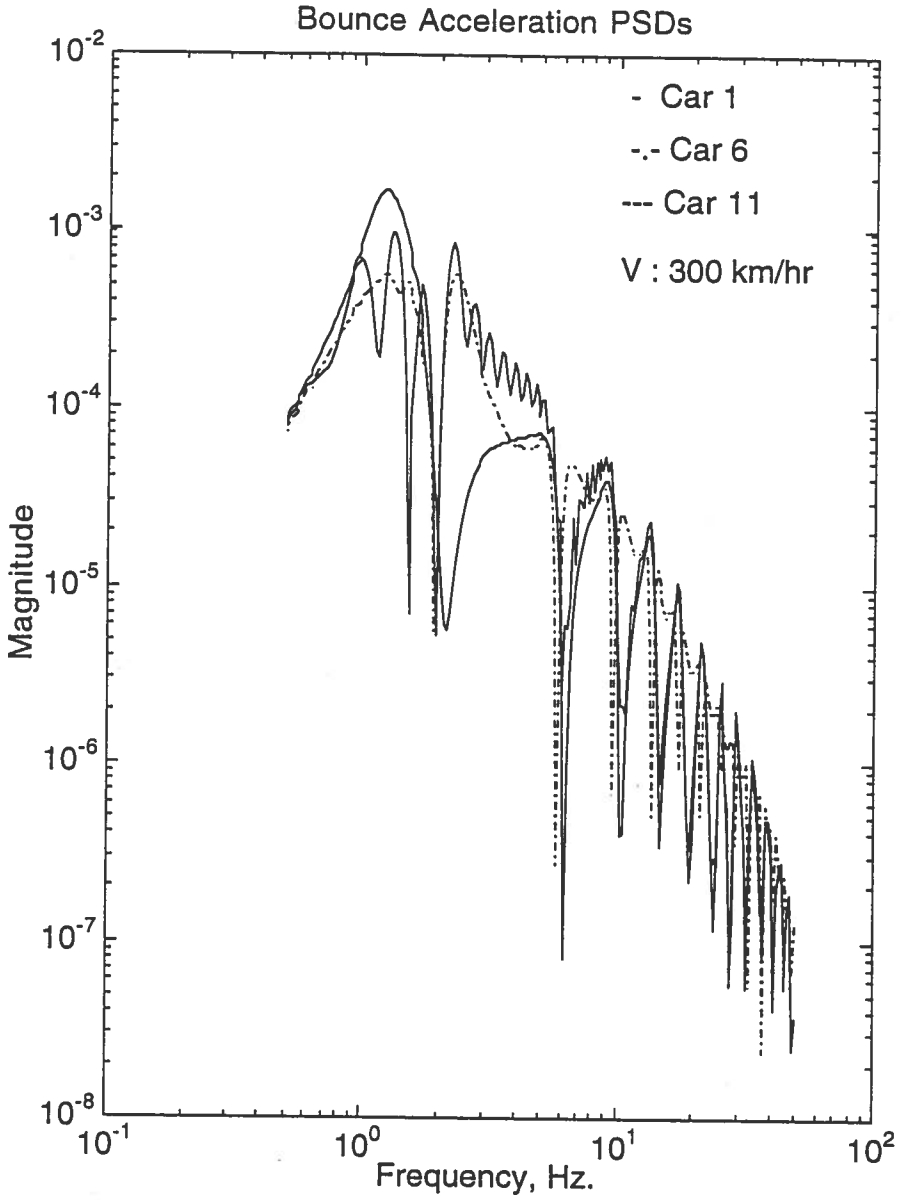

Figure 3-15. Bounce Acceleration PSDs for Cars 1, 6, and 10.

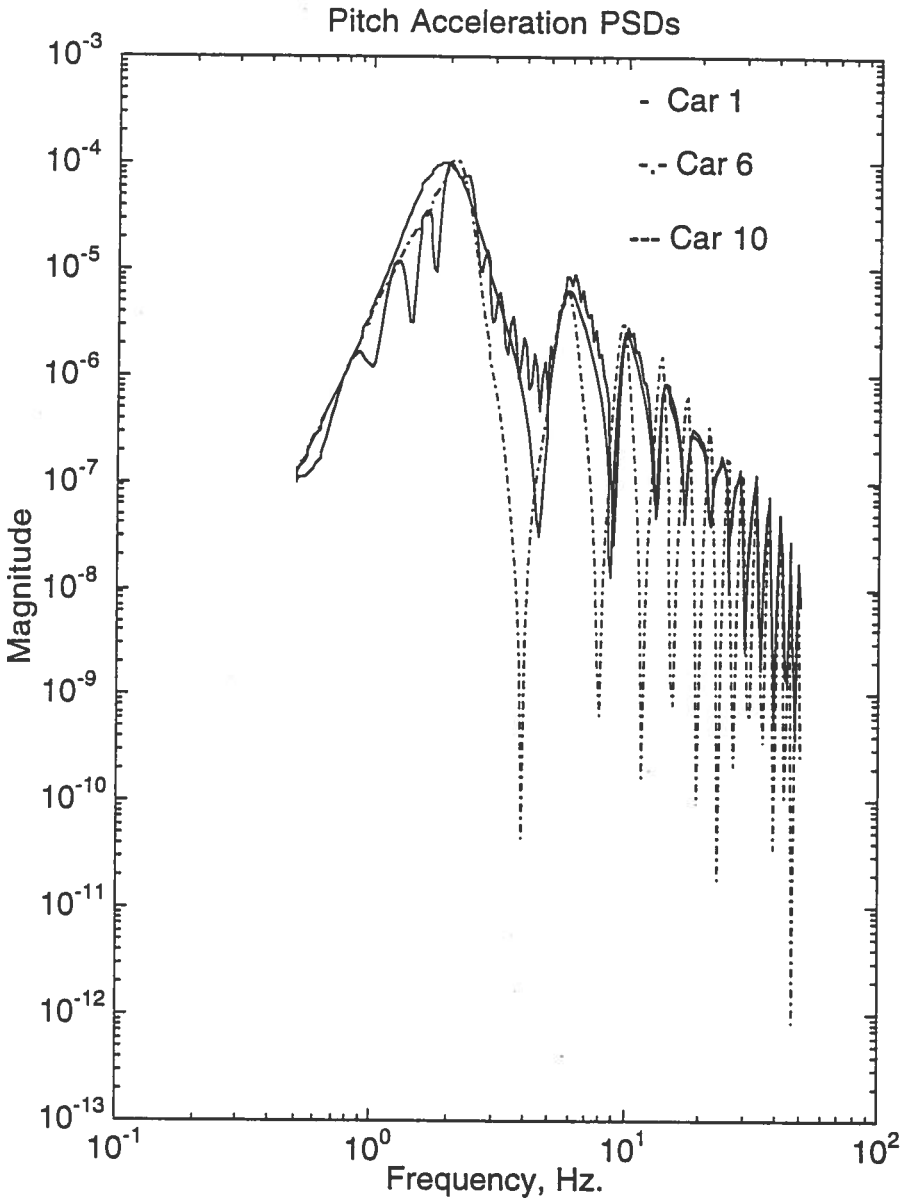

Figure 3-16 Pitch Acceleration PSDs for Cars 1, 6, and 10.

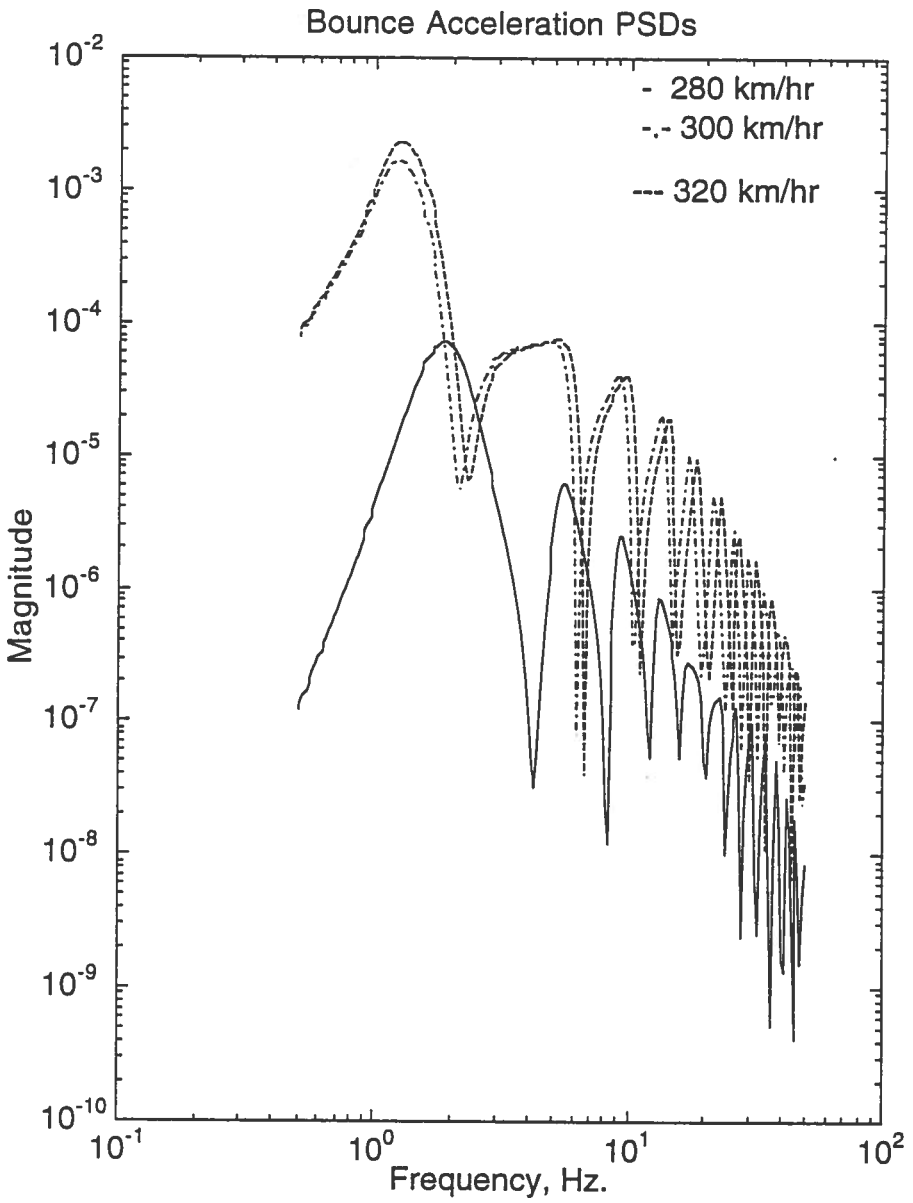

Figure 3-17. Bounce Acceleration PSDs for Car 10 as a Function of Speed.

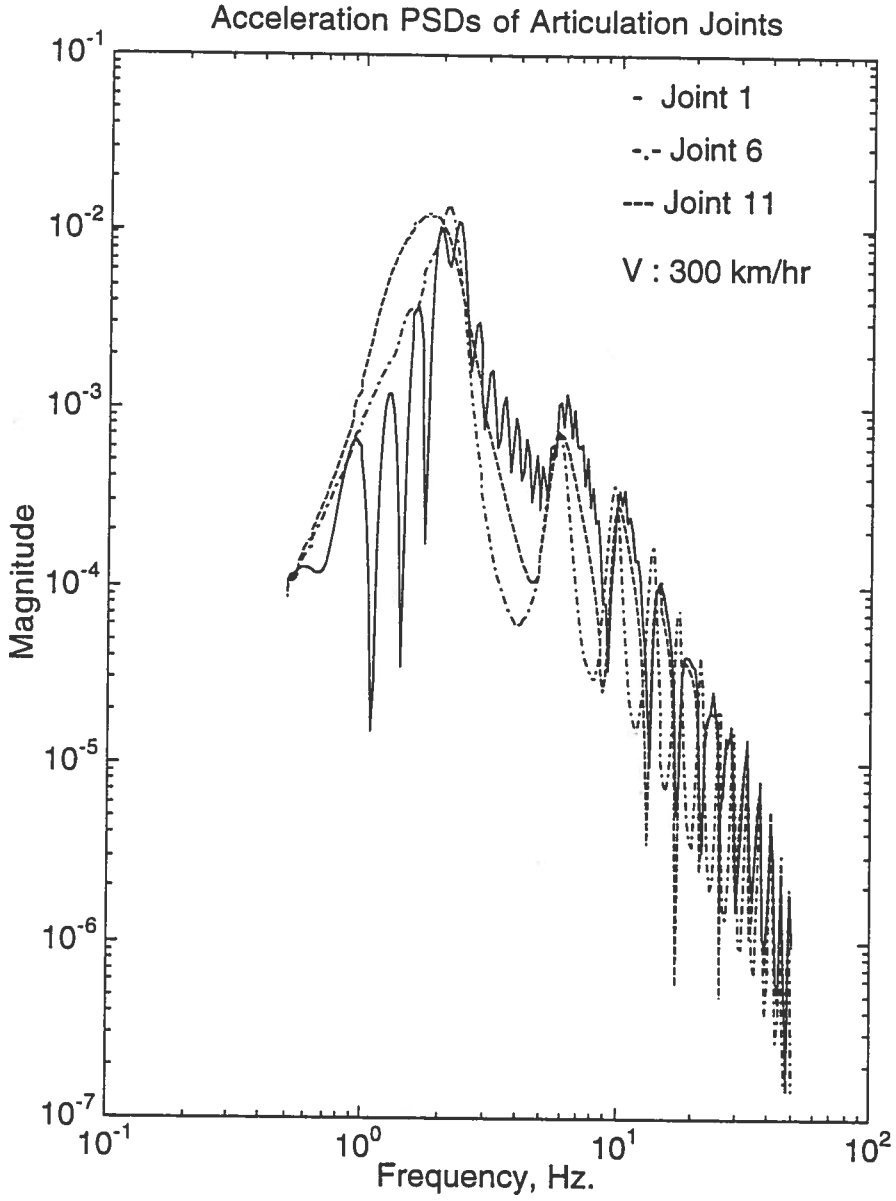

Figure 3-18. Acceleration PSDs for Joints 1, 6, and 11.

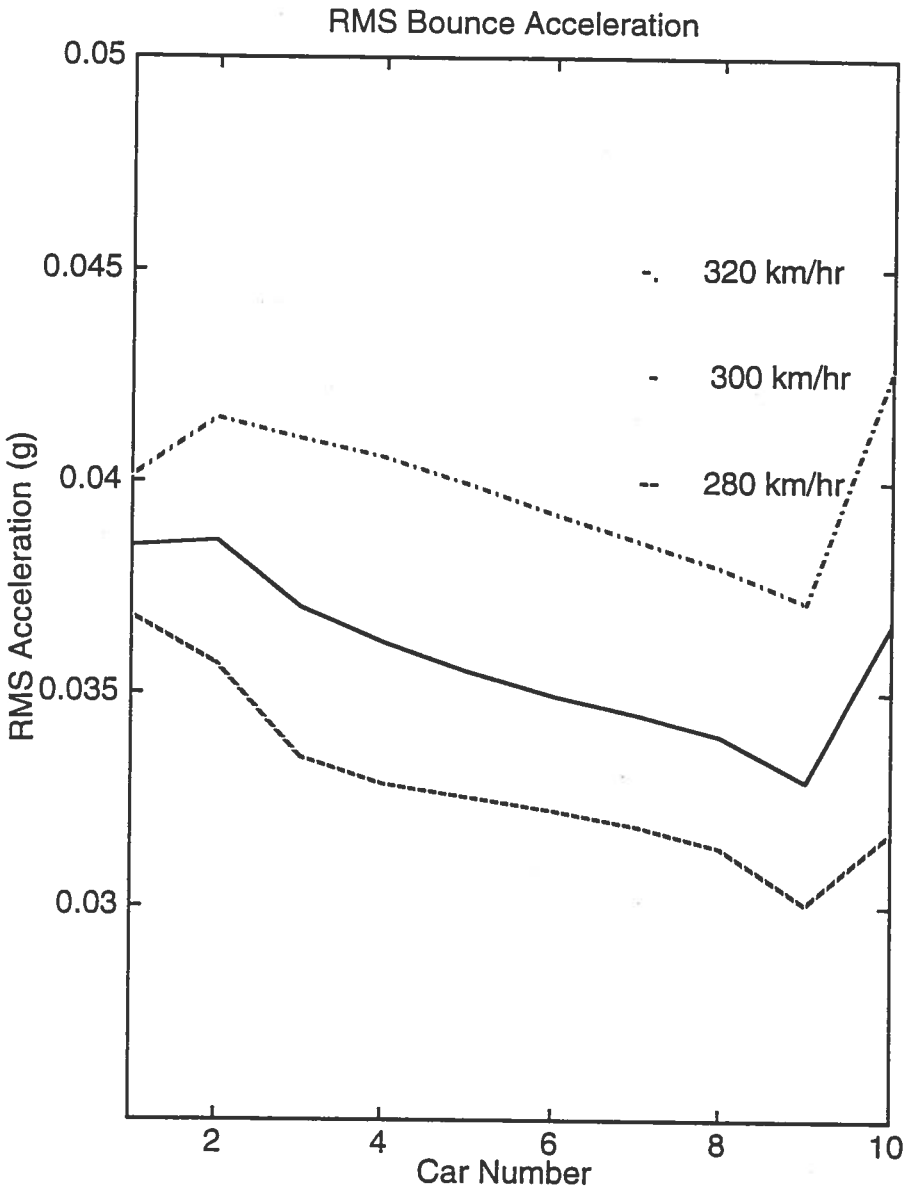

Figure 3-19. RMS Bounce Acceleration of Consist at Different Speeds (0-50 Hz.).

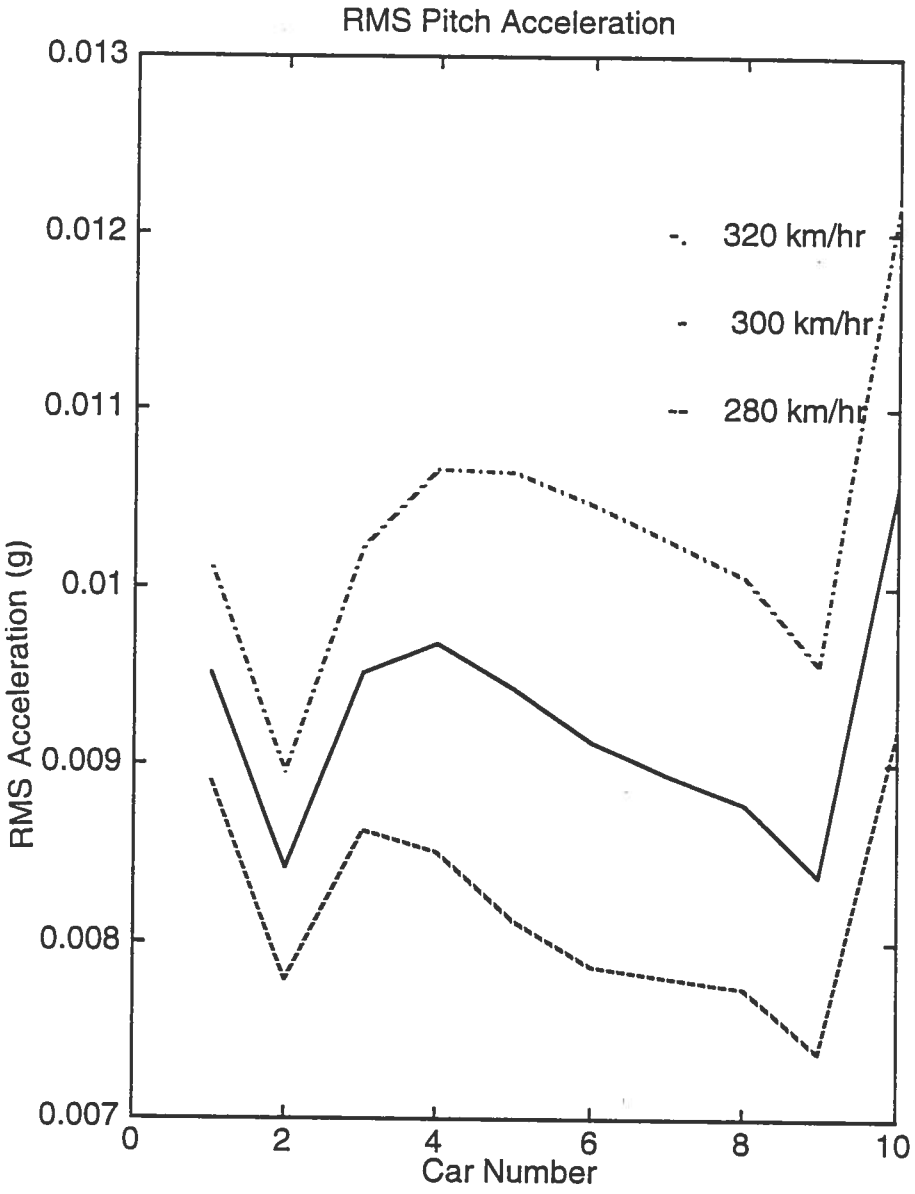

Figure 3-20. RMS Pitch Acceleration.of Consist at Different Speeds (0 -50 Hz).

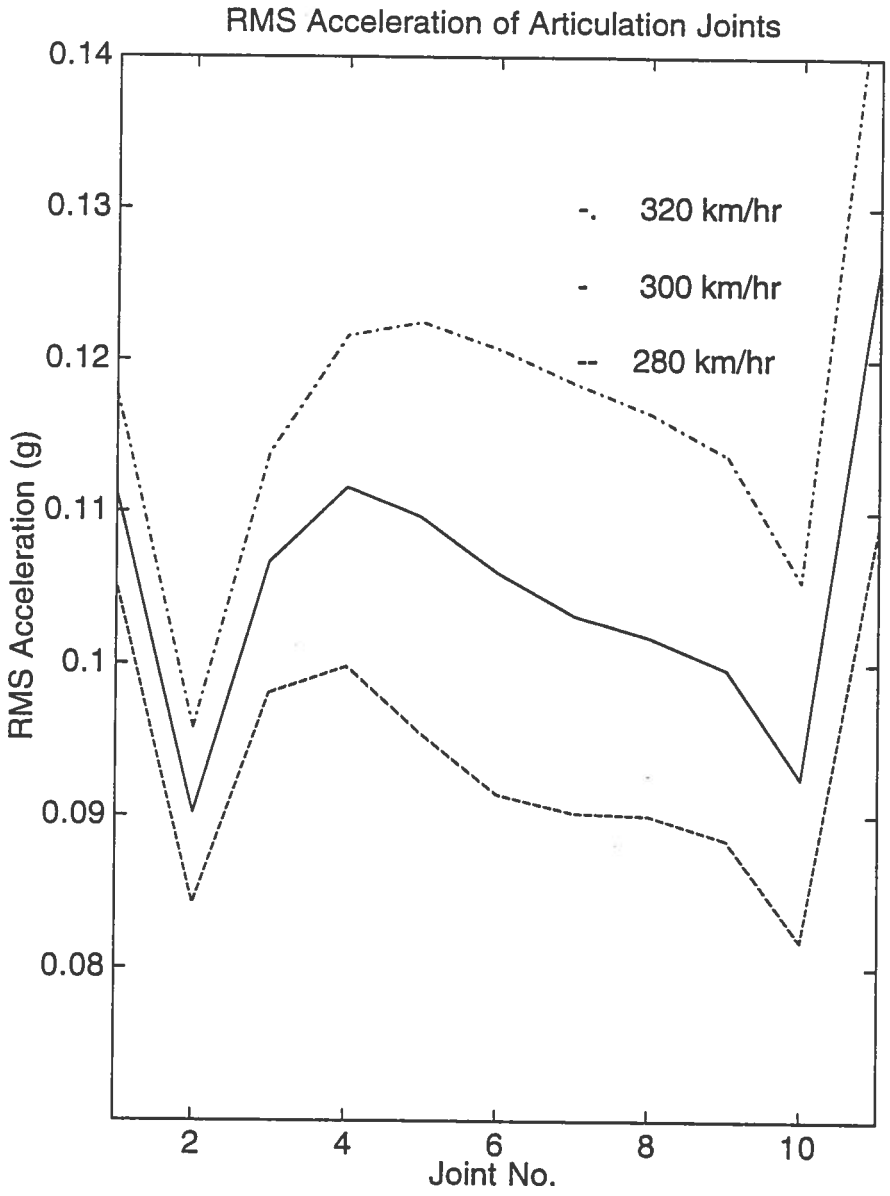

Figure 3-21. RMS Acceleration of Consist Joints at Different Speeds (0-50 Hz).

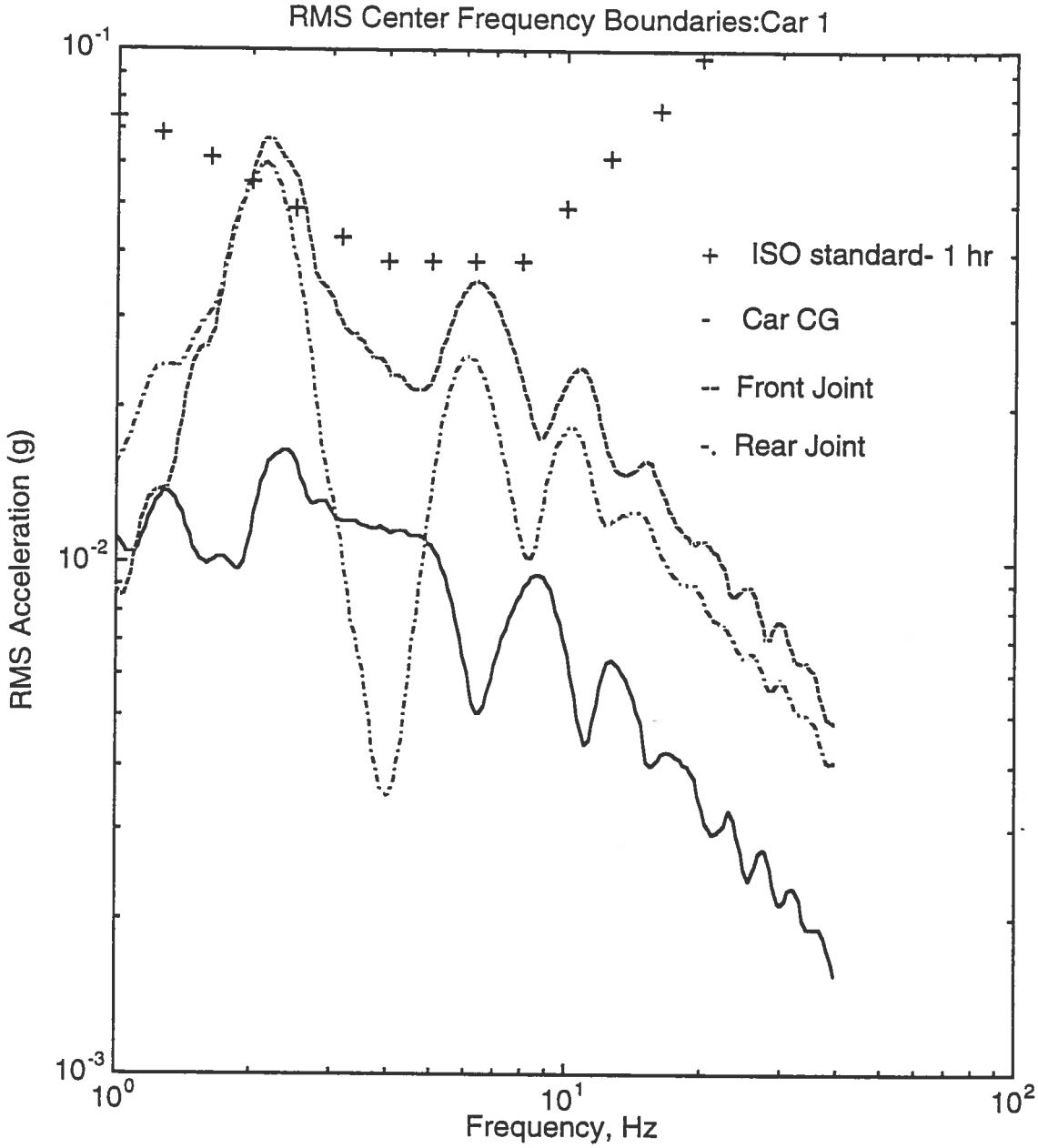

Figure 3-22: RMS of Center Frequency Boundaries for Car 1 Bounce and Joint Motions Compared With ISO Standard 1 Hour Exposure Limits (V=300 km/hr).

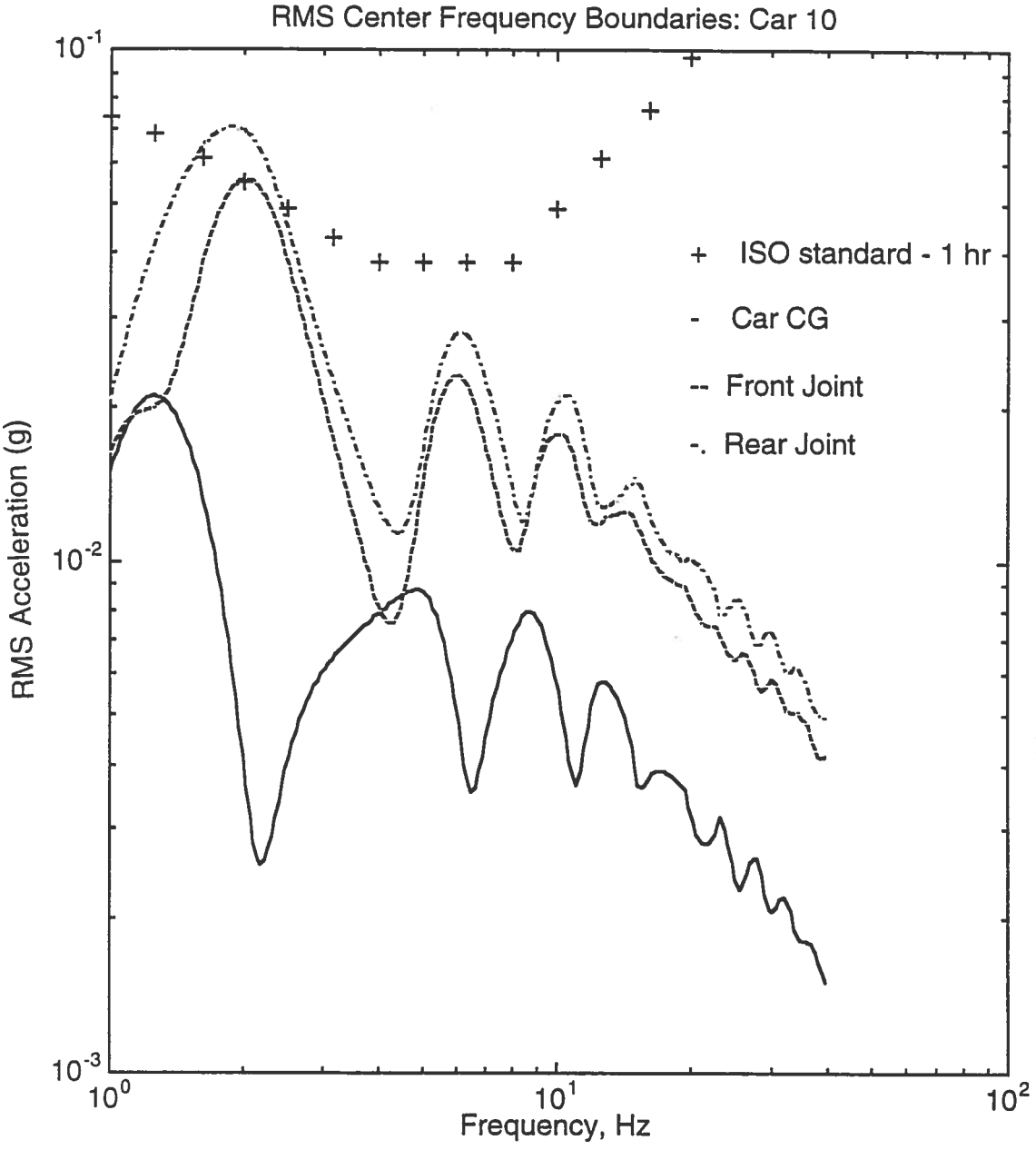

Figure 3-23. RMS of Center Frequency Boundaries for Car 10 Bounce and Joint Motions Compared With ISO Standards 1 Hour Exposure Limits (V=300 km/hr.).

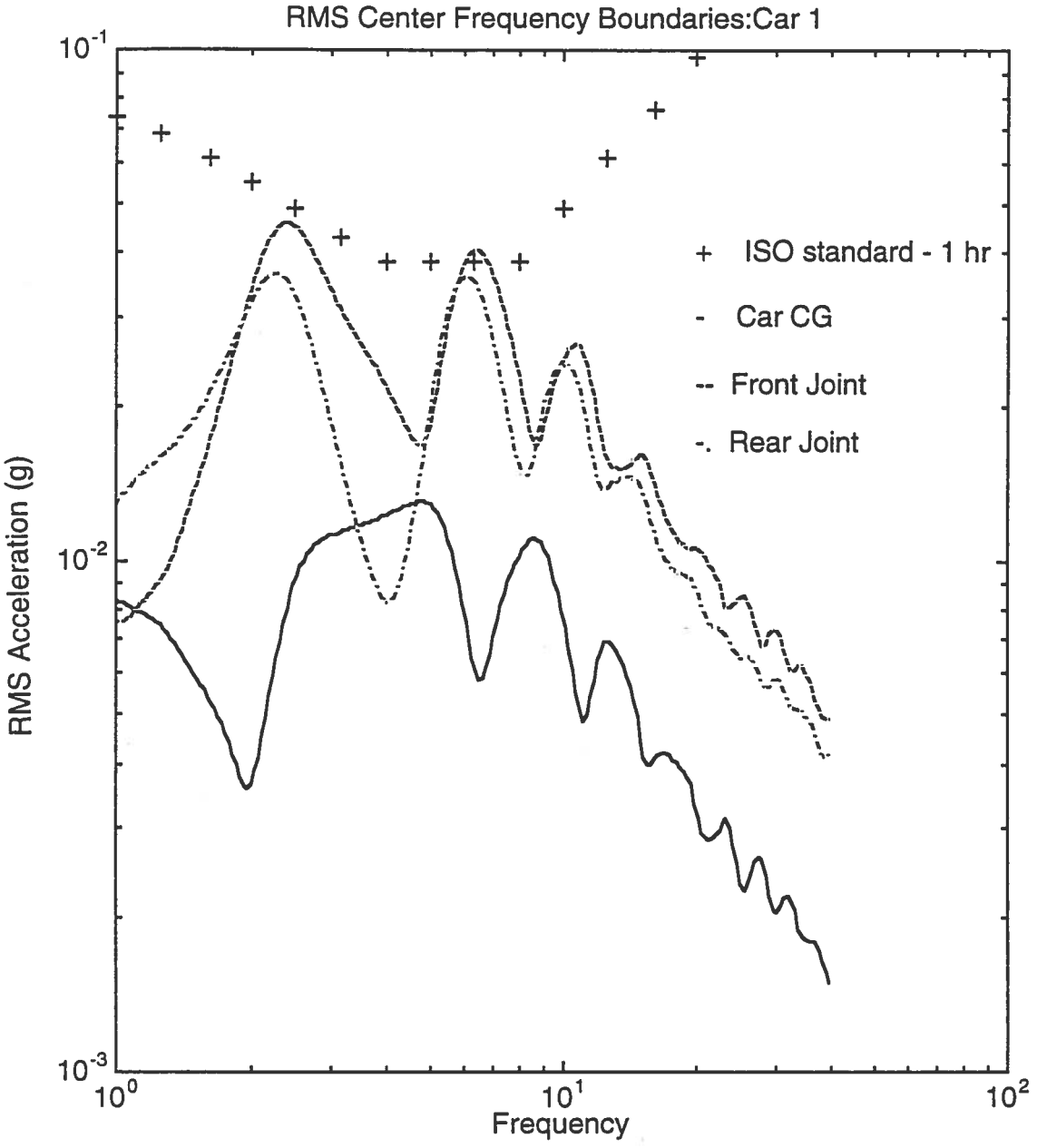

Figure 3-24. RMS of Center Frequency Boundaries for Car 1 Bounce and Joint Motions Compared With ISO Standards 1Hour Exposure Limits for Reduced Secondary Vertical Stiffness and Damping (V=300 km/hr.).

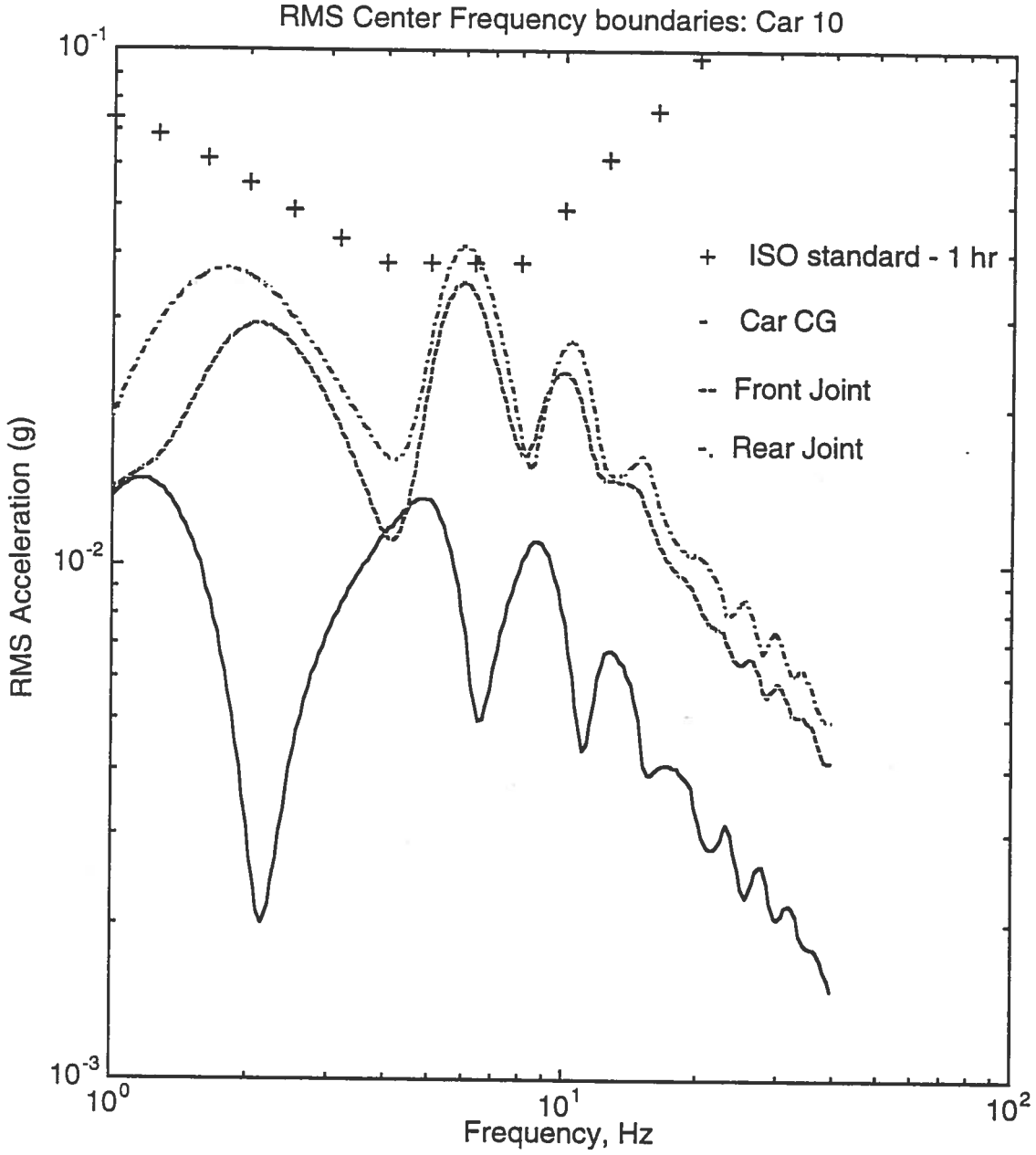

Figure 3-25. RMS of Center Frequency Boundaries for Car 10 Bounce and Joint Motions Compared With ISO Standards 1 Hour Exposure Limits for Reduced Secondary Vertical Stiffness and Damping (V=300 km/hr.).

3.4 Summary

This chapter has presented the development of a linear bounce and pitch model of an articulated train set. The model was developed for both discrete and random rail vertical alignment irregularities. Vertical forced response of a ten vehicle consist to Class 6 vertical track irregularities was obtained by solving linear dynamic equations of motion. The set of baseline parameters developed for the lateral stability model were used in this analysis. The results for selected vehicles in the consist were presented in the form of transfer functions, power spectra, and acceleration RMS at a speed of 300 km/hr.

The following observations were made:

1. The vehicle has a number of lightly damped modes with natural frequencies in the range of 1.2 to 2.1 Hz. These modes correspond to the pitch and bounce motions of specific cars in the consist.
2. The response of the individual cars is more pronounced at the rear of the train than at the front. This has implication for ride quality for this type of train set.
3. The results are parameter dependent. Hence before any specific decisions are made regarding this type of vehicular arrangement, it is important that accurate data be obtained for the particular design.
4. With the development of computer programs to analyze the vertical response of an articulated train set to both discrete and distributed rail disturbances, a new capability has been added to the FRA's ability to assess the dynamic performance of high speed rail vehicles.

4.0 SUMMARY AND CONCLUSIONS

A number of simulation models have been developed to compute the lateral stability and vertical pitch and bounce response of articulated train sets on tangent track. Simulation tools for the curving behavior of articulated train sets have also been developed but have not been reported in this document. These models include the essential features of articulated train sets such as shared trucks and suspension characteristics such as car-to-car connections and car-to-truck yaw dampers. The modeling assumptions made simplify the analysis so that linear analysis tools can be applied. Outputs from the lateral stability models include critical speeds of the train sets, mode shapes, natural frequencies, and damping ratios. The bounce and pitch model outputs include transfer functions and power spectra for various classes of track as well as time histories of the response to discrete disturbances in the track.

In the course of this work, an effort has been made to put together a parameter set of a generic articulated train set. This has been done through an extensive literature review. Information on suspension parameters and inertial parameters of the conventional elements is readily available. However information about the articulation connections is hard to find as is information about center of mass locations of the various elements. Hence it has been necessary in some instances to assume values for them.

For the lateral stability study, a set of parameters representing a baseline consist consisting of ten vehicles and giving a critical speed of approximately 300 km/hr were assembled. A limited set of parameter studies were then conducted to assess the influence of various parameters on consist stability. Mainly suspension parameters were chosen for the study. The studies show that consist stability is sensitive to the yaw damping between the trucks and the car body, the conicity of the wheel profile, and the primary suspension. Other parameters affect the stability but to a lesser degree. A decrease in yaw damping adversely affects the critical speed. A stiffer primary suspension increases the critical speed to a point past which the speed may begin to drop. The results were found to be fairly insensitive to the inter body yaw and roll connections. The most

surprising result of the study was the presence of a low conicity instability for the articulated train set. The results show that an increase in wheelset conicity increases the critical speed of the train set until it reaches an optimum value. Past this optimum value, the critical speed begins to drop. This affect may be a function of the parameters chosen and should be studied further. In looking at modal behavior of the consist, it was observed that the instability is in the form of whole consist modes, in some cases a wave-like motion, especially at the low conicities. The influence of the number of car bodies in a consist was also explored. Dropping consist size from ten to five did not change the critical speed significantly. However, arrangement of the trucks in the consist affected the results significantly. The dynamic behavior of a consist consisting of two conventional cars at the ends and the ten articulated vehicle consist in the middle was studied. This was done to simulate an actual arrangement where powered cars are arranged at the ends of the consist. The behavior was found to be quite different from that of the ten car consist by itself.

For the bounce and pitch response, the ten car consist on Class 6 track was studied. In this case the response was computed to vertical track alignment irregularities. Displacement and acceleration transfer functions, along with acceleration PSDs of the different elements of the consist were computed. The results showed the presence of a number of lightly damped modes with natural frequencies in the range of 1.2 to 2.1 Hz. These modes corresponded to the pitch and bounce motions of specific cars in the consist. The response of the individual cars was more pronounced at the rear of the train than at the front. This has implications for ride quality for this type of train set. The results were found to be parameter dependent. Hence before any specific decisions are made regarding this type of vehicular arrangement, it is important that accurate data be obtained for the particular design.

With the development of computer programs to analyze the vertical response of an articulated train set to both discrete and distributed rail disturbances, a new capability has been added to the FRA's ability to assess the dynamic performance of high speed rail vehicles. This is however a first step in developing a comprehensive tool kit to address the safety related issues that may arise with such train sets.

Suggestions for future work include a study of the curving behavior of such train sets using the linear model developed in the course of this work. In addition, the limited study conducted during the course of this work indicated that the arrangement of vehicles in the consist can have a significant effect on the stability of the consist. This refers to having a mix of conventional vehicles coupled with articulated vehicles as is the case with the TGV or the new Japanese STAR21 experimental train [12]. This needs to be explored further. The issues that are important refer to the coupling between the vehicles and how it is to be modeled. The linear models developed constitute a first step in developing modeling capability for HSR articulated train sets. These models provide good qualitative information. However, to study the safety related behavior of such train sets it is necessary to develop non-linear models. Issues such as wheel climb and wheel lift in response to discrete and random track disturbances etc. can only be adequately studied if non-linear time domain models are used. In addition the suspension characteristics used in train sets such as the TGV-Atlantique have non-linear characteristics and therefore must be included in the simulation tools. It is therefore recommended that further efforts be devoted to the development of non-linear time domain models to study the safety related behavior of HSR articulated train sets. These models should include viable representations of non-linear wheel rail geometry, creep forces, and non-linear suspension elements. They should also encompass the three regimes of vehicle dynamic behavior, i.e. lateral dynamics, vertical dynamics, and curving.

5.0. REFERENCES

1. *Proceedings of the International Conference on Speedup Technology for Railway and Maglev Vehicles*, Japanese Society of Mechanical Engineers, Yokohama, Nov. 1993.

2. Elkins, J. A., and Eikoff, B. M., *Advances in Non-Linear Wheel-Rail Force Prediction Methods and Their Validation*, ASME Journal of Dynamic Systems, Measurement, and Control, Vol. 104, pp. 133-142, 1982.

3. Wormley, D. N., Hedrick, J. K., and Nagurka, M. K., *Analysis of Rail Transit Vehicle Dynamic Curving Performance*, Final Report to UMTA, PB85-112845, June, 1984.

4. Law, E.H., Frank, H., and I. Haque, *Nonlinear Steady-State Curving of Locomotives Equipped with Three Axle Trucks*, ASME Paper No. 86.-WA/RT-9, December, 1986.

5. Haque, I., Chengyu Liu, and Guong Zhu, *A User's Manual Of A Linear Steady State Curving Computer Program For An Articulated Train set*, Report submitted to Volpe National Transportation Center, May 1995.

6. Haque, I., Chengyu Liu, and Guong Zhu, *A Brief User's Manual Of A Lateral Stability Analysis Computer Program For An Articulated Train set*, Report submitted to Volpe National Transportation Center, May, 1995.

7. Pars, L. A., *A Treatise on Analytical Dynamics*, Heinemann, London, 1965

8. Haque, I., Chengyu Liu, and Guong Zhu, A *Users' Manual Of A Frequency Response Computer Program For A Pitch And Bounce Model Of An Articulated Train set*, Report submitted to Volpe National Transportation Center, May, 1995.

9. Law, E. H., Haque, I., and Cooperrider, N.K., *Railway Vehicle Dynamics Course Notes* , Short Course delivered to AAR, Pueblo, Colorado, September, 1993.

10. Smith, R. E., and Anderson, R. J., *Characteristics of Forced Steered Trucks*, Vehicle System Dynamics, 1985.

11. White, R.C., Limbert, D.A., Hedrick, J.K., and Cooperrider, N.K.,*Guideway Suspension Trade-offs in Rail Vehicle Systems*, Arizona State University Engineering Research Center Report, ERC-R-78035, Jan. 1978.

12. Takao, T, Taguchi, H., Tuge, M.,Terai, J., *Dynamic Characteristics of the STAR21 Experimental Train,* Proceedings of the International Conference on Speedup Technology for Railway and Maglev Vehicles, Japanese Society of Mechanical Engineers, Yokohama, Nov. 1993.

Equation (3-13) then becomes:

$$Z(j\omega)[(-M\omega^2 + K) + C\omega j] = [Z_d R(\omega) + Z_d I(\omega) j] Z_{f1}(j\omega) \tag{3-18}$$

The inverse of complex matrix $[(-M\omega^2 + K) + C\omega j]$ can be expressed by two real matrices, DR and DI ,i.e.

$$[(-\mathrm{M}\omega^2 + \mathrm{K}) + \mathrm{C}\omega\mathrm{j}]^{-1} = \mathrm{DR} + \mathrm{DIj} \tag{3-19}$$

where j is the complex quantity $\sqrt{-1}$. The transfer function of the model can be written as follows:

$$H(j\omega)_{fi} = \frac{Z(j\omega)}{Z_{fi}(j\omega)}$$

$$= [DR.Z_d R(\omega) - DI.Z_d I(\omega) + [DR.Z_d R(\omega) - DI.Z_d I(\omega)]j \tag{3-20}$$

The displacement output PSD can then be calculated from the input PSD as follows:

$$PSD_z = |H(j\omega)_{fi}|^2 PSD_{z_{fi}} \tag{3-21}$$

where PSD_z represents the PSD of the output and $PSD_{z_{fi}}$ represents the PSD of the rail vertical alignment.

White et al. [11] used a model of track vertical profile given below. The PSD of the vertical profile in spatial form is:

$$PSD_z = \frac{A_y \Omega_c^2}{(\Omega^2 + \Omega_r^2)(\Omega^2 + \Omega_c^2)} \tag{3-22}$$

In temporal form, for a constant speed V,

$$PSD_z = \frac{(C_1 \omega_c)^2}{(\omega^2 + \omega_r^2)(\omega^2 + \omega_c^2)} \tag{3-23}$$

where $C_1 = (A_Y V)^{1/2}$, $\omega = \Omega V$, and values of A_y, W_c and W_r are given in Table3-1. These coefficients are appropriate for use in the above equations for track classes 4, 5, and 6. If the rail vertical irregularity is discrete, Equations 3-12 can be numerically integrated in state variable form using standard numerical integration packages to solve for the vehicle response. Three mathematical functions have been widely used to represent the various discrete irregularities encountered on the rail roadbed [9]. The first of these is a rectified sine wave. The function given by the equations:

$$\begin{aligned} z_{fi} &= 0 && t \le 0, t > t_p \\ z_{fi} &= h_r\left(\left|\cos\frac{\pi t}{t_p}\right| - 1\right) && 0 < t \le t_p \end{aligned} \tag{3-25}$$

is frequently used to describe the vertical and lateral alignment variation of one rail at a rail joint. Here h_r is the amplitude, t is the time, and t_p is the pulse width.

Table 3-1 Track PSD model Parameters [11]

Class of Track	4	5	6
A_y (m)	2.39 x10^{-5}	9.35 x10^{-6}	1.50 x10^{-5}
Ω_c(rad/m)	0.825	0.825	0.825
Ω_r(rad/m)	2.06 x 10^{-2}	2.06 x 10^{-2}	2.06 x 10^{-2}

A second related function is the cosine section given by the equations:

$$z_{fi} = 0 \qquad t \le 0, t > t_p$$
$$z_{fi} = 0.5h_c(\cos\frac{2\pi t}{t_p} - 1) \qquad 0 < t \le t_p \tag{3-26}$$

This function is widely used to describe irregularities in the vertical profile that are commonly found when the roadbed subgrade or ballast is weak. The third common input form is the sinusoid section

$$z_{fi} = 0 \qquad t \le 0, t > t_p$$
$$z_{fi} = h_s \sin\frac{\pi t}{2t_p} \qquad 0 < t \le t_p \tag{3-27}$$

which is used to describe the effects of grade crossings or other short spans on the vertical profile and the presence of crossovers in the alignment of the roadbed.

3.3 Results

3.3.1 Computer Program

The above equations were used to develop two computer programs. The programs simulate consists of 2, 3, 4, 5, and 10 articulated vehicles. The computer programs developed in FORTRAN have been reported in [7]. The primary program outputs for the frequency response analysis are the displacement and acceleration transfer functions, and acceleration PSDs of articulation joints, and similar outputs for the truck degrees of freedom. The time domain model provides as outputs, the states of the components of the consist.

3.3.2. Transfer Function Dropouts

For a conventional single car model with two trucks, the transfer function magnitudes suddenly 'drop out' and the phase abruptly shifts 180 deg at certain frequencies [9]. This filtering effect occurs at frequencies where the truck wheel base or the distance between trucks corresponds to an odd number of half track wavelengths. The case for the articulated train is a bit more complicated as there are a large number of wheelsets, trucks, and car bodies. However data suggests that dropouts in articulated vehicles occur in much the same way as they do in conventional vehicles. The dropout frequencies correspond to wheelset spacing and truck spacing in a given car. The car body bounce transfer function exhibits 'dropouts' at the spatial frequencies:

$$f = \frac{nV}{2(d_f + d_r)}, \qquad n = 1,3,5,...$$
$$f = \frac{nV}{2(S_f + S_r)}, \qquad n = 1,3,5,.. \tag{3-28}$$

and the pitch transfer function exhibits similar dropouts at:

$$f = \frac{nV}{2(d_f + d_r)}, n = 1,3,5,...$$
$$f = \frac{nV}{2(S_f + S_r)}, n = 2,4,6,.. \quad (3\text{-}29)$$

3.3.2 Parameter Study

The objectives of the parameter study was to demonstrate the features of the frequency domain model and to explore articulated train behavior. Models of articulated trains have not been presented before in the open literature. This study serves to explain what may be expected of such vehicular arrangements. The model used in this study is a ten vehicle consist with a conventional truck arrangement in the front and shared trucks in the middle. This model consists of 33 degrees of freedom. These are shown in Table 3-2. The set of representative baseline parameter values given in Table 2-2 was used to determine the response. All cars were assumed to have the same suspension characteristics. The track input PSD used in the study is for Class 6 track. A frequency domain analysis is performed.

The consist is assumed to be traveling at a forward speed of 300 km/hr which is just below the critical speed for lateral stability for the consist. It should be emphasized that the numerical results presented here are true only for the set of parameters used and generally should not be extrapolated to infer the behavior of other articulated train set designs. However they are probably quite representative qualitatively of articulated train behavior. The following results are presented:

1. Modal characteristics of the consist.
2. Acceleration and Displacement Transfer Functions.
3. Acceleration PSDs.
4. RMS. values of acceleration in g's over the 0-50 Hz frequency range.

Table 3-2. DOFs of a 10 Articulated Vehicle Model For Vertical Forced Response.

Degree of freedom	Symbol
Vertical displacement of articulation joint i, i=1, 11	z_{ji}
Vertical displacement of truck i, i =1, 11	z_{ti}
Pitch displacement of truck i, i =1,11	Φ_{t1}

5. ISO one-third-octave RMS. accelerations at 300 km/hr and the ISO reduced comfort boundary for one hour exposure.

3.3.2.1. Modal Characteristics

The 33 degree of freedom system results in sixty six eigenvalues and eigenvectors. Of these, some of the modes are over damped while others are oscillatory. The results show the presence of a number of lightly damped modes with damping ratios ranging from 0.155 to 0.26 and closely spaced natural frequencies between 1.2 and 2.1 Hz. These modes correspond mainly to the car body pitch and bounce motions and these motions are most pronounced at the front, rear, and middle of the consist. The presence of these closely spaced frequencies indicates the possibility of strong interaction between modes such as the beat phenomena. Other under damped modes with higher damping ratios and natural frequencies between 3 and 5 Hz. are also present. They correspond to the truck bounce and pitch modes. Table 3-3 shows some of the frequencies and damping values obtained. The truck modes are not included because they are heavily damped. Figures 3.3, 3.4, and 3.5 show some of the mode shapes. These have been plotted to show both the phase and the magnitude. In the figures, the circles represent the articulation joints and the lines the car bodies. Table 3-4 shows the dropout frequencies for the pitch and bounce modes of the cars. These frequencies have been calculated using Equations 3-28 and 3-29.

Table 3-3. Frequencies and Damping Ratios of the Lightly Damped Modes.

Frequency, Hz	Damping Ratio	Largest Element of Eigenvector
1.192	0.1555	2nd Articulation Joint
1.2	0.1652	2nd Articulation Joint
1.235	0.1576	6th Articulation Joint
1.292	0.1624	6th Articulation Joint
1.292	0.1728	Front Articulation Joint
1.37	0.1624	Front Articulation Joint
1.5	0.1943	Front Articulation Joint
1.635	0.1752	Rear Articulation Joint
1.91	0.1967	Front Articulation Joint
1.915	0.1967	Rear Articulation Joint
2.0	0.1864	Rear Articulation Joint
2.1	0.1783	6th Articulation Joint

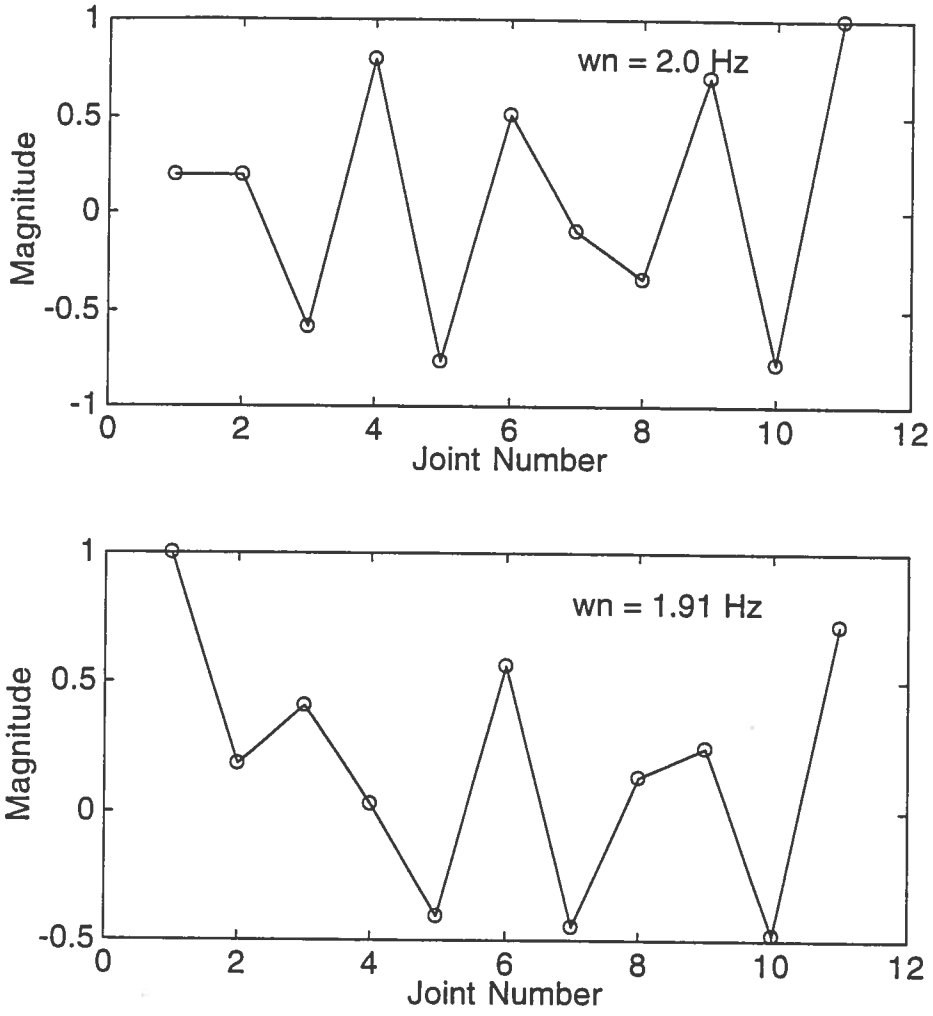

Figure 3-3. Modes Shapes for Select Natural Frequencies, ω_n = 1.91 Hz. and 2.0 Hz.

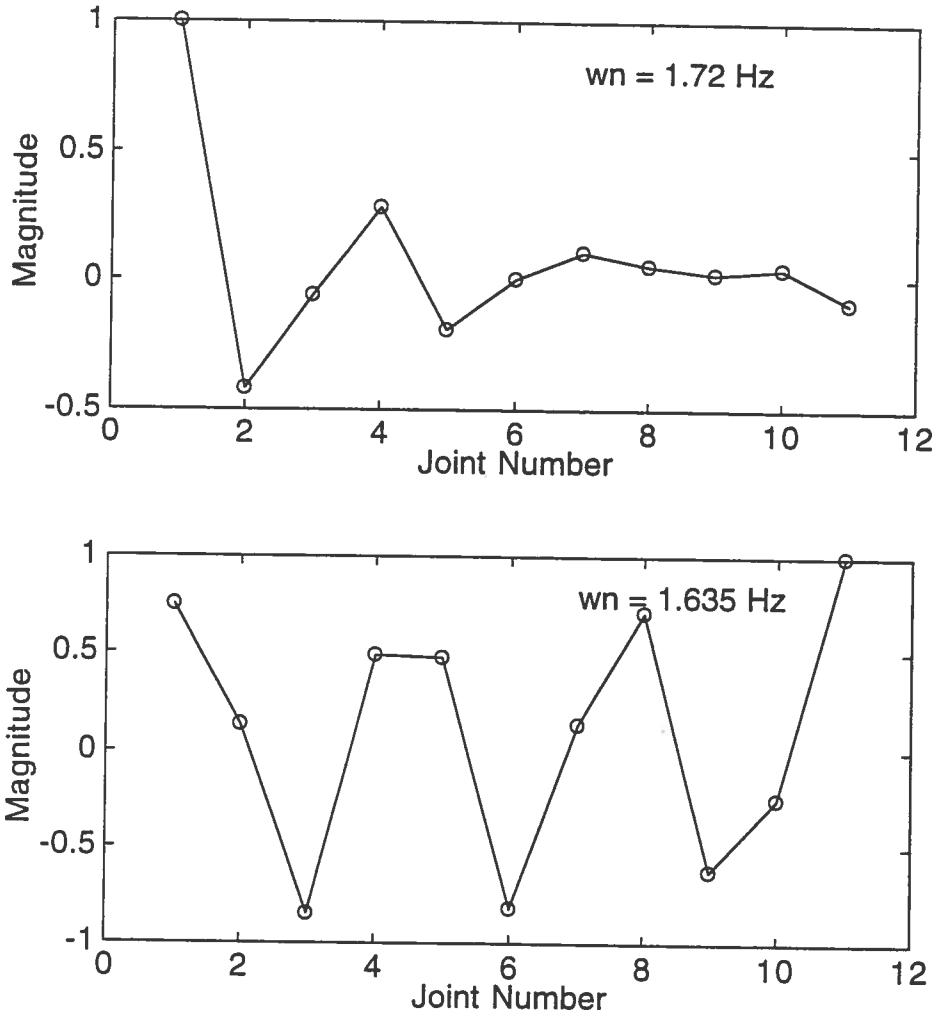

Figure 3-4. Modes Shapes for Select Natural Frequencies, ω_n = 1.635 Hz. and 1.72Hz.

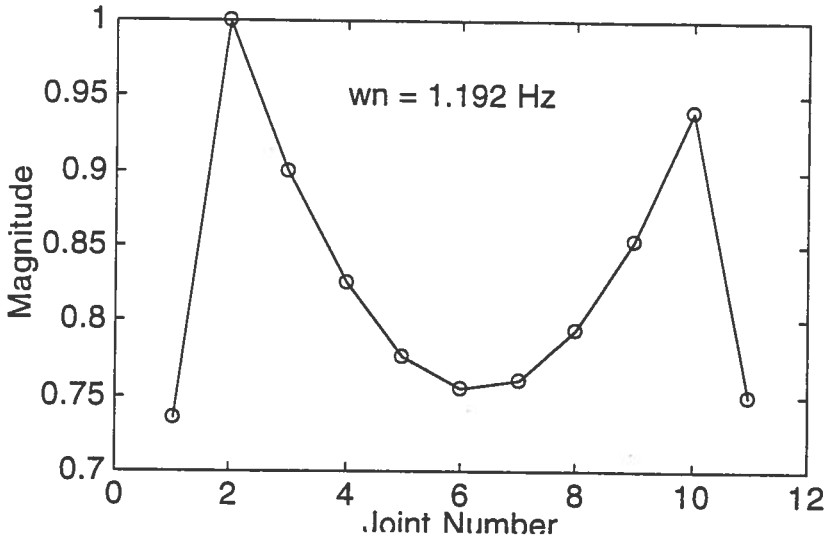

Figure 3-5. Modes Shape for Select Natural Frequencies, ω_n = 1.192 Hz.

3.3.2.2 Transfer Functions

Figures 3-6 and 3-7 show the bounce and pitch displacement transfer functions for the first, sixth, and tenth cars. Figure 3-8 shows the transfer functions for the first, sixth and eleventh articulation joints. Figure 3-9 shows the influence of speed on the transfer function for Joint 11 which is the last joint in the consist. These transfer functions represent the ratio of vehicle displacements to the track input at the front wheel. Since the articulation joints represent the connection points to the trucks, their transfer functions include the effects of bounce and pitch. The following observations are made:

1. The natural frequencies span 1.2 to 2.1 Hz approximately. They correspond to the bounce and pitch motions of the vehicles. These frequencies represent modes of behavior where the pitch or bounce of a given car is accentuated. Because of the articulated interconnections between the cars, different cars have different frequencies at which their behavior will be accentuated. Some of the natural frequencies are not apparent in the

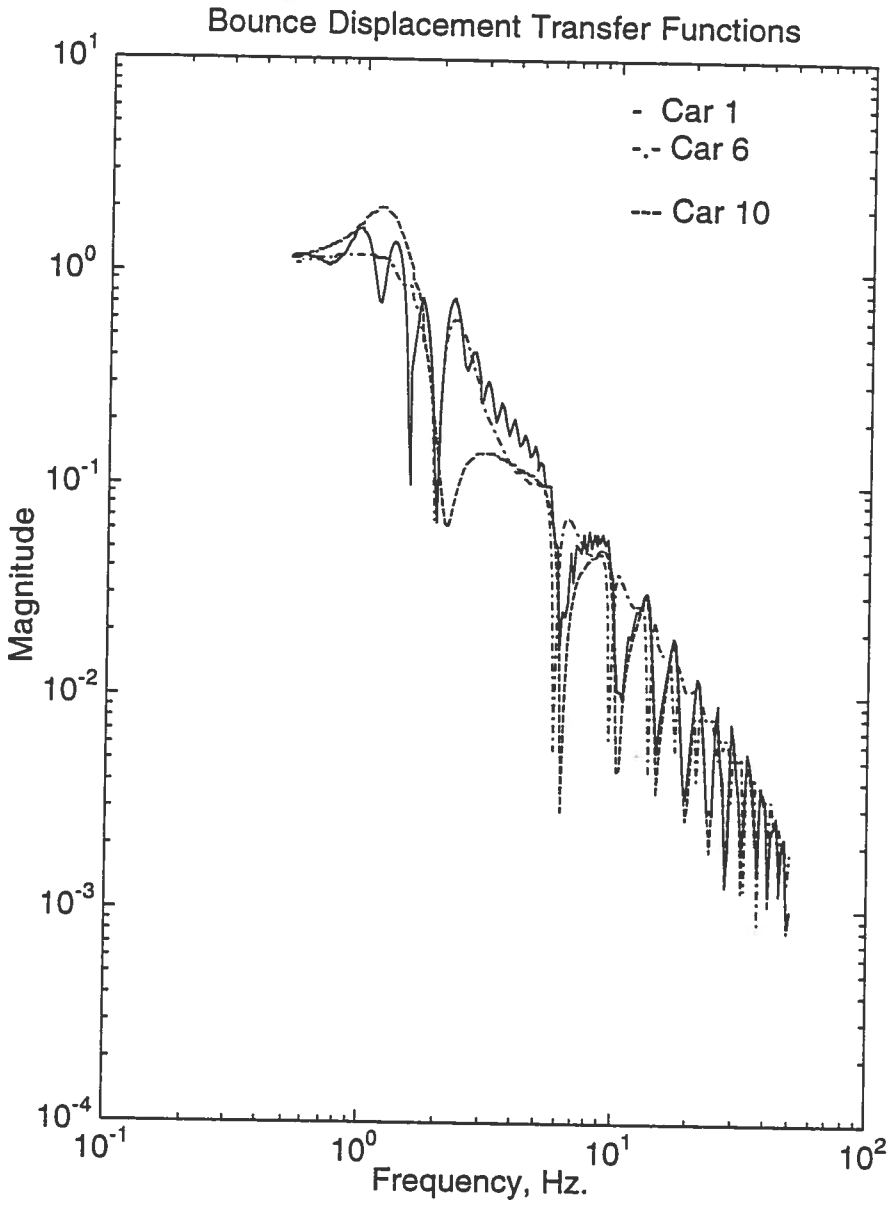

Figure 3-6. Car body Bounce Transfer Functions for Car 1, Car 6, and Car 10

(V=300 km/hr)

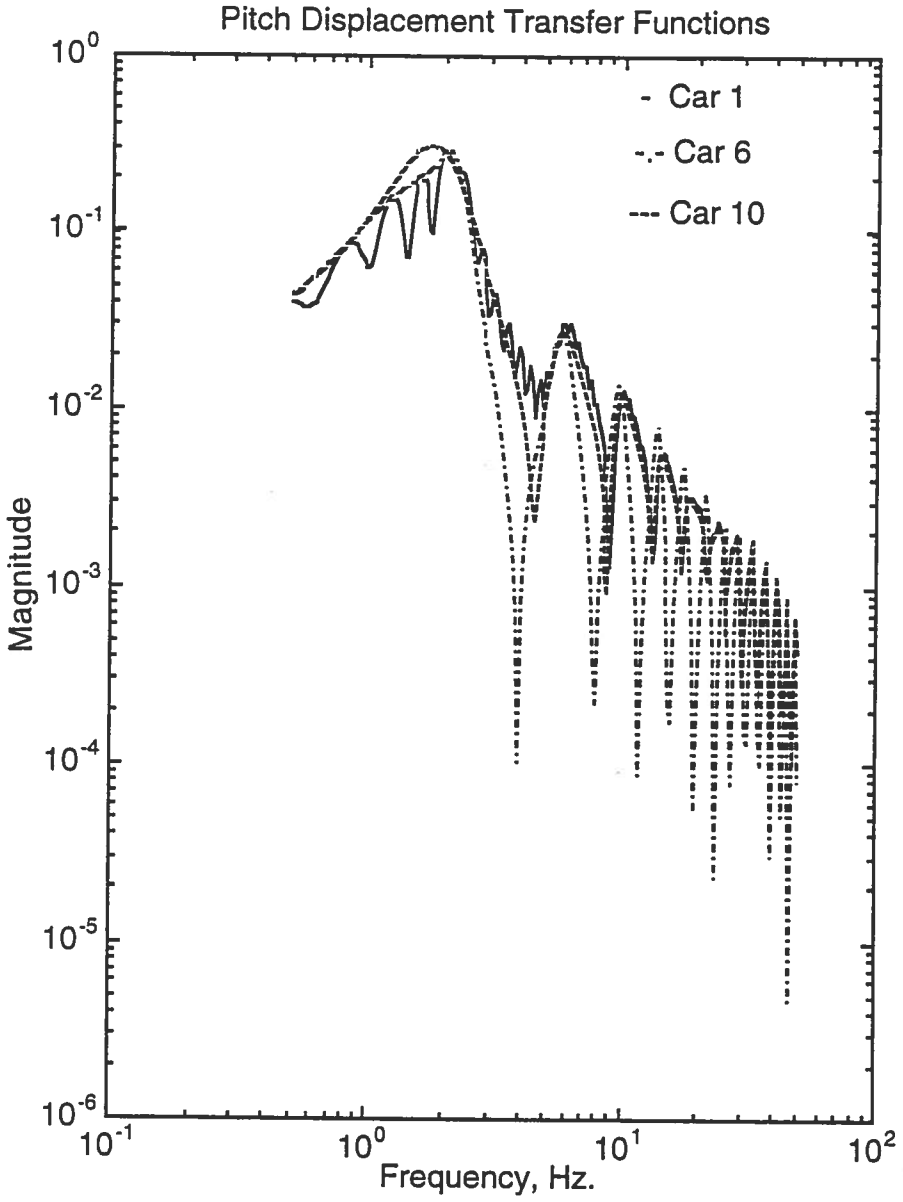

Figure 3-7. Car Body Pitch Transfer Functions for Car 1, Car 6, and Car 10

(V=300 km/hr)

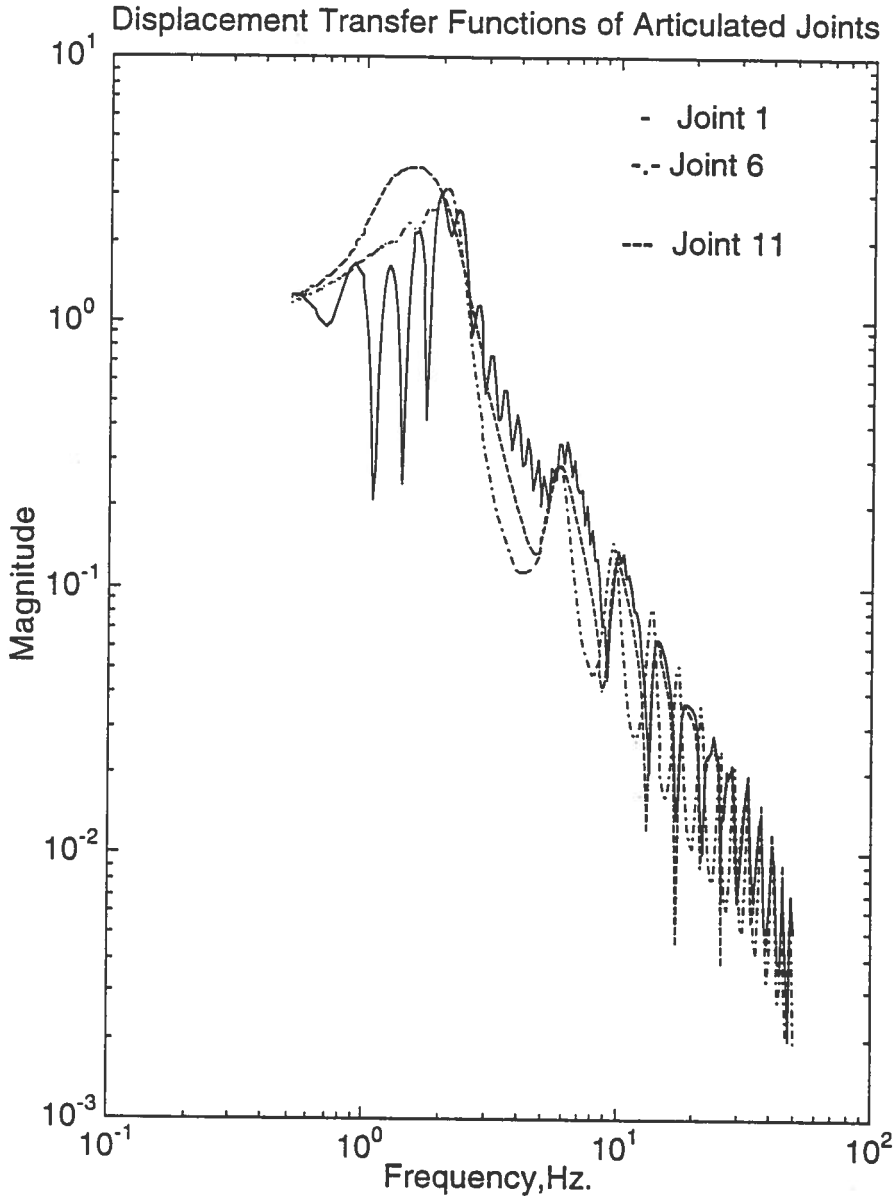

Figure 3-8. Transfer Functions for Joints 1, 6, and 10 (V=300 km/hr).

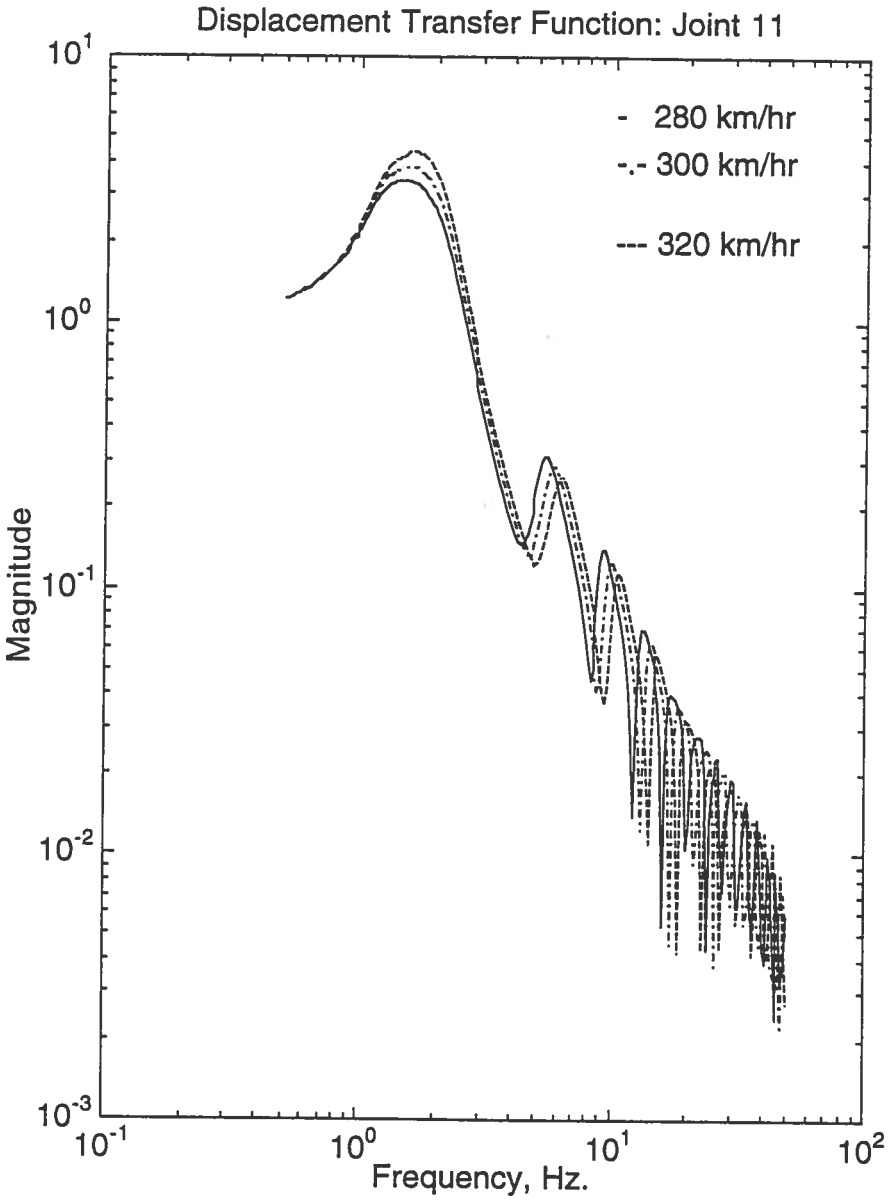

Figure 3-9. Transfer Functions for Joint 11 at Different Speeds

(V=280 km/hr, 300 km/hr, 320 km/hr).

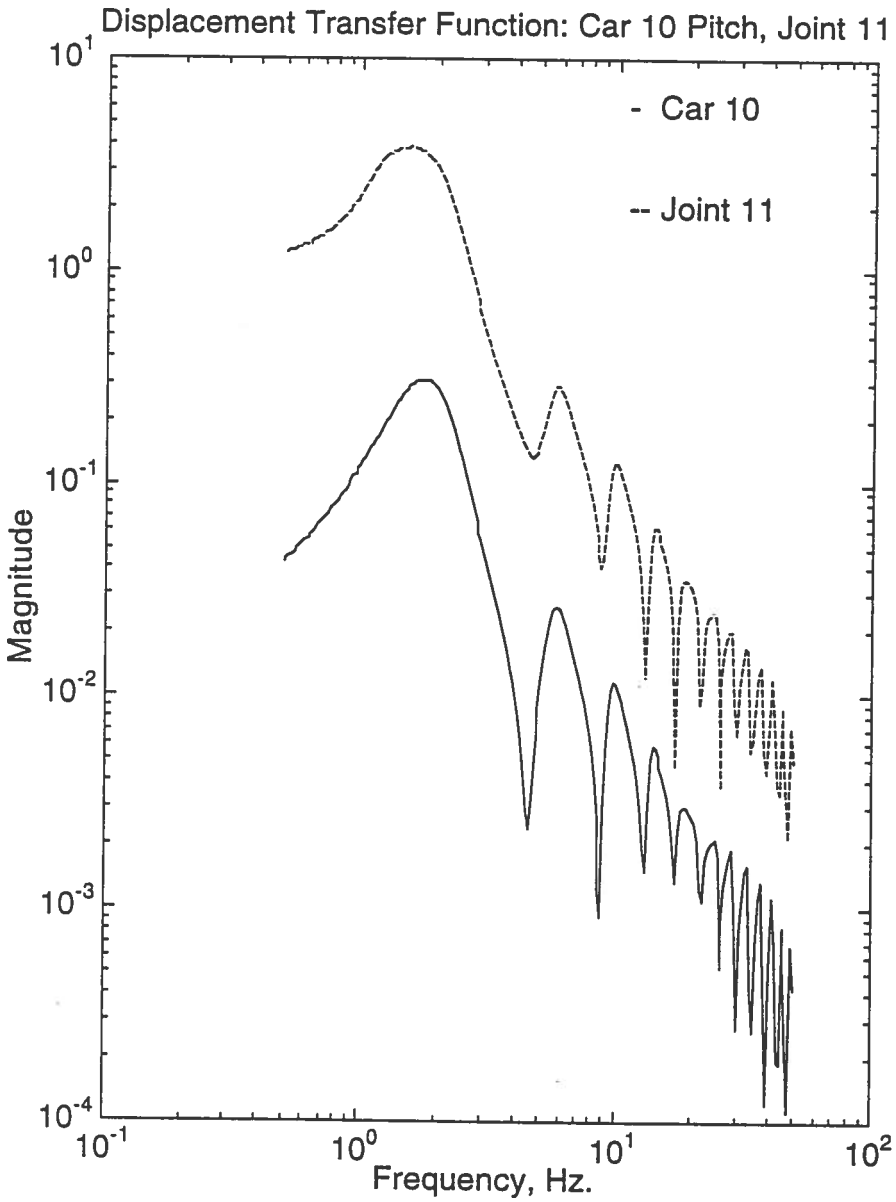

Figure 3-10. Transfer Functions for Car 10 Pitch Motion and Joint 11 (V=300 km/hr).

plots due to the dropouts. This masking effect of the dropouts makes it difficult to identify the natural frequencies from the transfer functions alone.

2. Dropouts occur as predicted. These dropouts are functions of the wheel base and the truck center distance. The frequencies at which they occur for Cars 1 and 10 are different than for the other cars in the consist. This is because of the arrangement of trucks in the front of the consist. For the car bounce functions, the dropouts are odd multiples of the frequencies corresponding to the truck wheel base and truck spacing. Dropouts for the car pitch correspond to the odd multiples of truck wheel base and even multiples of the truck spacing. These frequencies are shown in Table 3-4.

3. Response at the joints is typically greater than the bounce and pitch taken separately. In addition, the combination of bounce and pitch attenuates the dropouts somewhat, although the dropouts corresponding to the pitch motion are still easily identifiable (Figure 3-10).

4. The influence of speed is to shift the transfer functions. The amplitude of the transfer function at the resonant frequency is also increased (Figure 3-8).

5. The response at the end of the train set is stronger than at the middle. Car 10 has the largest response of the three cars at the natural frequency of around 1.3 Hz. In addition, Joint 11, the last joint at the end of the train has the highest transfer function amplitude at the resonant frequency in the vicinity of 1.9 Hz.

Figures 3-11 to 3-13 show the acceleration transfer functions. The same observations are made as earlier except that more power is now concentrated at the higher frequencies.

Table 3-4. Dropout Frequencies for First, Sixth, and Tenth Car Bounce and Pitch Transfer Functions, V=300 km/hr.

Car Number	n	Bounce, Hz	Pitch, Hz
1, 10	1	16.66, 2.13	16.66
	2		4.26
	3	49.98, 6.39	49.98
	4		8.52
	5	10.65	
	6		12.78
6	1	16.66, 1.93	16.66
	2		3.86
	3	49.98, 5.79	49.98
	4		7.72
	5	9.65	
	6		11.58